THE 3RD INTERNATIONAL WORKSHOP ON INNOVATIVE SIMULATION FOR HEALTH CARE

SEPTEMBER 10-12 2014

BORDEAUX, FRANCE

EDITED BY

AGOSTINO BRUZZONE

MARCO FRASCIO

FRANCESCO LONGO

YURY MERKURYEV

VERA NOVAK

PRINTED IN RENDE (CS), ITALY, SEPTEMBER 2014

ISBN 978-88-97999-37-9 (Paperback)
ISBN 978-88-97999-43-0 (PDF)

ISBN 978-88-97999-37-9 (Paperback)
ISBN 978-88-97999-43-0 (PDF)

THE 3RD INTERNATIONAL WORKSHOP ON INNOVATIVE SIMULATION FOR HEALTH CARE

SEPTEMBER 10-12 2014, BORDEAUX, FRANCE

ORGANIZED BY

DIME – UNIVERSITY OF GENOA

LIOPHANT SIMULATION

SIMULATION TEAM

IMCS – INTERNATIONAL MEDITERRANEAN & LATIN AMERICAN COUNCIL OF SIMULATION

DIMEG, UNIVERSITY OF CALABRIA

MSC-LES, MODELING & SIMULATION CENTER, LABORATORY OF ENTERPRISE SOLUTIONS

MODELING AND SIMULATION CENTER OF EXCELLENCE (MSCOE)

LATVIAN SIMULATION CENTER – RIGA TECHNICAL UNIVERSITY

LOGISIM

LSIS – LABORATOIRE DES SCIENCES DE L'INFORMATION ET DES SYSTEMES

MIMOS – MOVIMENTO ITALIANO MODELLAZIONE E SIMULAZIONE

MITIM PERUGIA CENTER – UNIVERSITY OF PERUGIA

BRASILIAN SIMULATION CENTER, LAMCE-COPPE-UFRJ

MITIM - MCLEOD INSTITUTE OF TECHNOLOGY AND INTEROPERABLE MODELING AND SIMULATION – GENOA CENTER

M&SNET - MCLEOD MODELING AND SIMULATION NETWORK

LATVIAN SIMULATION SOCIETY

ECOLE SUPERIEURE D'INGENIERIE EN SCIENCES APPLIQUEES

FACULTAD DE CIENCIAS EXACTAS. INGEGNERIA Y AGRIMENSURA

UNIVERSITY OF LA LAGUNA

CIFASIS: CONICET-UNR-UPCAM

INSTICC - INSTITUTE FOR SYSTEMS AND TECHNOLOGIES OF INFORMATION, CONTROL AND COMMUNICATION

NATIONAL RUSSIAN SIMULATION SOCIETY

CEA - IFAC

LOCAL SPONSORS

UNIVERSITY OF BORDEAUX

IMS LAB

AQUITAINE REGION

I3M 2014 INDUSTRIAL SPONSORS

CAL-TEK SRL

LIOTECH LTD

MAST SRL

SIM-4-FUTURE

I3M 2014 MEDIA PARTNERS

INDERSCIENCE PUBLISHERS – INTERNATIONAL JOURNAL OF SIMULATION AND PROCESS MODELING

INDERSCIENCE PUBLISHERS – INTERNATIONAL JOURNAL OF CRITICAL INFRASTRUCTURES

INDERSCIENCE PUBLISHERS – INTERNATIONAL JOURNAL OF ENGINEERING SYSTEMS MODELLING AND SIMULATION

INDERSCIENCE PUBLISHERS – INTERNATIONAL JOURNAL OF SERVICE AND COMPUTING ORIENTED MANUFACTURING

IGI GLOBAL – INTERNATIONAL JOURNAL OF PRIVACY AND HEALTH INFORMATION MANAGEMENT

HALLDALE MEDIA GROUP: MILITARY SIMULATION AND TRAINING MAGAZINE

HALLDALE MEDIA GROUP: THE JOURNAL FOR HEALTHCARE EDUCATION, SIMULATION AND TRAINING

EUROMERCI

EDITORS

AGOSTINO BRUZZONE
MITIM-DIME, UNIVERSITY OF GENOA, ITALY
agostino@itim.unige.it

MARCO FRASCIO
UNIVERSITY OF GENOA, ITALY
mfrascio@unige.it

FRANCESCO LONGO
DIMEG, UNIVERSITY OF CALABRIA, ITALY
f.longo@unical.it

YURI MERKURYEV
RIGA TECHNICAL UNIVERSITY, LATVIA
merkur@itl.rtu.lv

VERA NOVAK
BETH ISRAEL DEACONESS MEDICAL CENTER, HARVARD MEDICAL SCHOOL, USA
vnovak@bidmc.harvard.edu

INTERNATIONAL MULTIDISCIPLINARY MODELING & SIMULATION MULTICONFERENCE, I3M 2014

GENERAL CO-CHAIRS

AGOSTINO BRUZZONE, *MITIM-DIME, UNIVERSITY OF GENOA, ITALY*
YURI MERKURYEV, *RIGA TECHNICAL UNIVERSITY, LATVIA*

PROGRAM CO-CHAIRS

FRANCESCO LONGO, *DIMEG, UNIVERSITY OF CALABRIA, ITALY*
EMILIO JIMENEZ, *UNIVERSITY OF LA RIOJA, SPAIN*

THE 3RD INTERNATIONAL WORKSHOP ON INNOVATIVE SIMULATION FOR HEALTH CARE, IWISH 2014

GENERAL CO-CHAIRS

MARCO FRASCIO, *UNIVERSITY OF GENOA*, *ITALY*
VERA NOVAK, *BETH ISRAEL DEACONESS MEDICAL CENTER, HARVARD MEDICAL SCHOOL, USA*

IWISH 2014 INTERNATIONAL PROGRAM COMMITTEE

MAJA ATANASIJEVIC-KUNC, *UNIVERSITY OF LJUBLJANA, SLOVENIA*
WERNER BACKFRIEDER, UNIVERSITY OF APPLIED SCIENCES, UPPER AUSTRIA
JERRY BATZEL, *UNIVERSITY OF GRAZ, AUSTRIA*
FELIX BREITENECKER, *TU VIENNA, AUSTRIA*
AGOSTINO BRUZZONE, UNIVERSITY OF GENOA, ITALY
EDUARDO CABRERA, UNIVERSIDAD AUTONOMA DE BARCELONA, SPAIN
GIANLUCA DE LEO, *OLD DOMINIUM UNIVERSITY, USA*
RAFAEL DIAZ, VMASC VIRGINIA MODELING, ANALYSIS AND SIMULATION CENTER, VIRGINIA, *USA*
GOTTFRIED ENDEL, *ASSOCIATION OF AUSTRIAN SOCIAL SECURITY, AUSTRIA*
GIONATA FRAGOMENI, *UNIVERSITY MAGNA GRAECIA, ITALY*
MARCO FRASCIO, UNIVERSITY OF GENOA, ITALY
NANDU GOSWAMI, *MEDICAL UNIVERSITY OF GRAZ, AUSTRIA*
AMIR HUSSAIN, UNIVERSITY OF STIRLING, SCOTLAND, UK
WITOLD JACAK, UNIVERSITY OF APPLIED SCIENCES, UPPER AUSTRIA
KORINA KATSALIAKI, *INTERNATIONAL HELLENIC UNIVERSITY, GREECE*
FRANCESCO LONGO, *UNIVERSITY OF CALABRIA, ITALY*
MARINA MASSEI, *UNIVERSITY OF GENOA, ITALY*
NAVONIL MUSTAFEE, *UNIVERSITY OF EXETER, UK*
MUAZ NIAZI, BAHRIA *UNIVERSITY OF ISLAMABAD, PAKISTAN*
LETIZIA NICOLETTI, *UNIVERSITY OF CALABRIA, ITALY*
VERA NOVAK, *HARVARD MEDICAL SCHOOL, USA*
METTE OLUFSEN, *NORTH CAROLINA STATE UNIVERSITY, USA*
STEPHAN ONGGO, *UNIVERSITY OF LANCASTER, UK*
NIKI POPPER, *DWH SIMULATION SERVICES VIENNA, AUSTRIA*
PAOLO PROIETTI, *MIMOS, ITALY*
JOSEPH ROSEN, *THAYER SCHOOL OF ENGINEERING AT DARMOUTH, USA*
ALBERTO TREMORI, *SIMULATION TEAM, ITALY*
GERALD ZWETTLER, *UPPER UNIV. OF APPLIED SCIENCE, AUSTRIA*

TRACKS AND WORKSHOP CHAIRS

APPLICATION OF SIMULATION FOR HEALTHCARE SUPPLY CHAINS
CHAIR : NAVONIL MUSTAFEE, UNIVERSITY OF EXETER, UK; KORINA KATSALIAKI, INTERNATIONAL HELLENIC UNIVERSITY, GREECE

HEALTHCARE AND PUBLIC HEALTH M&S
CHAIRS: RAFAEL DIAZ, VMASC VIRGINIA MODELING, ANALYSIS AND SIMULATION CENTER, VIRGINIA, USA; EDUARDO CABRERA, UNIVERSIDAD AUTONOMA DE BARCELONA, SPAIN

MODELING AND SIMULATION FOR COGNITIVE COMPUTATION
CHAIRS: MUAZ NIAZI, BAHRIA UNIVERSITY OF ISLAMABAD, PAKISTAN; AMIR HUSSAIN UNIVERSITY OF STIRLING, SCOTLAND, UK

STUDYING BIOMECHANICAL PROBLEMS FOR CARDIOTHORACIC AND CARDIOVASCULAR CLINICAL PROBLEMS: MODELS, DESIGNING TOOLS, SIMULATION ENVIRONMENTS AND CRITICAL CONDITION PREDICTION FOR SURGICAL INTERVENTIONS.
CHAIR: GIONATA FRAGOMENI, UNIVERSITY MAGNA GRAECIA, CATANZARO, ITALY

PATIENT SPECIFIC MODELING OF THE CARDIOVASCULAR-RESPIRATORY SYSTEM: INTERDISCIPLINARY APPROACHES TO THEORY AND PRACTICE
CHAIRS: JERRY BATZEL, UNIVERSITY OF GRAZ, AUSTRIA; NANDU GOSWAMI, MEDICAL UNIVERSITY OF GRAZ, AUSTRIA; METTE OLUFSEN, NORTH CAROLINA STATE UNIVERSITY, USA

MATHEMATICAL MODELING AND HEALTH TECHNOLOGY ASSESSMENT
CHAIRS: NIKI POPPER, DWH SIMULATION SERVICES VIENNA, AUSTRIA; FELIX BREITENECKER, VIENNA UNIV. OF TECHNOLOGY, AUSTRIA; GOTTFRIED ENDEL, MAIN ASSOCIATION OF AUSTRIAN SOCIAL SECURITY INSTITUTIONS, AUSTRIA

MODELLING AND SIMULATION IN PHYSIOLOGY AND MEDICINE (COMMON TRACK IWISH-EMSS)
CHAIRS: MAJA ATANASIJEVIC-KUNC, UNIV. LJUBLJANA, SLOVENIA; FELIX BREITENECKER, VIENNA UIV. OF TECHNOLOGY, AUSTRIA

SIMULATION AND MODELING IN COMPUTER AIDED THERAPY
CHAIRS: WERNER BACKFRIEDER, UNIVERSITY OF APPLIED SCIENCES, UPPER AUSTRIA, AUSTRIA; WITOLD JACAK, UNIVERSITY OF APPLIED SCIENCES, UPPER AUSTRIA, AUSTRIA

CHAIRS' MESSAGE

The third "International Workshop on Innovative Simulation for Healthcare" (IWISH), part of the I3M Multiconference, intends to highlight the emerging power of Modelling & Simulation and related methodologies in the field of Healthcare.

People working in the healthcare sector are embracing new technologies quite quickly nowadays, driven by the rapid rise of new devices (including mobile technologies) and attracted by the one-to-one relationship between the specialist and the patient. A digital patient is being born and Modeling & Simulation as well as Information Technology (IT) are continuously changing the way in which diseases are diagnosed and treated thanks to a continuous improvement in personnel training, to new decision support systems and to a better management of the information flow among all the actors involved. Modeling & Simulation as well as new technologies are of primary importance and necessary to investigate the mechanisms and causes of illnesses and to improve the corresponding treatment, including the development of new treatment methods. In this sense, IWISH is the opportunity to share and find together solutions to problems, searching for new Modeling & Simulation applications that should lead to an improvement in patient's care. This is not ambitious: if anything, the opposite!

As additional aspects, we would like to express our gratitude to the IWISH International Program Committee, reviewers and authors; they did a great job in collecting outstanding papers that will be indexed by SCOPUS (now all the IWISH proceedings starting from the first edition in 2012 are indexed by SCOPUS).

This year, the IWISH Workshop Organisation Committee and the Conference co-chairs welcome you in Bordeaux, with the hope that papers' presentation, as well as knowledge sharing between all the I3M attendees will be capable of creating a step forwards in Healthcare over the next years.

Marco Frascio
University of Genoa
Italy

Vera Novak
Harvard Medical School,
USA

ACKNOWLEDGEMENTS

The IWISH 2014 International Program Committee (IPC) has selected the papers for the Conference among many submissions; therefore, based on this effort, a very successful event is expected. The IWISH 2014 IPC would like to thank all the authors as well as the reviewers for their invaluable work.
A special thank goes to all the organizations, institutions and societies that have supported and technically sponsored the event.

I3M 2014 INTERNAL STAFF

AGOSTINO G. BRUZZONE, *MISS-DIPTEM, UNIVERSITY OF GENOA, ITALY*
MATTEO AGRESTA, *SIMULATION TEAM, ITALY*
CHRISTIAN BARTOLUCCI, *SIMULATION TEAM, ITALY*
ALESSANDRO CHIURCO, *DIMEG, UNIVERSITY OF CALABRIA, ITALY*
FRANCESCO LONGO, *DIMEG, UNIVERSITY OF CALABRIA, ITALY*
MARINA MASSEI, *LIOPHANT SIMULATION, ITALY*
MARZIA MATTIA, *DIMEG, UNIVERSITY OF CALABRIA, ITALY*
LETIZIA NICOLETTI, *CAL-TEK SRL*
ANTONIO PADOVANO, *DIMEG, UNIVERSITY OF CALABRIA, ITALY*
EDOARDO PICCO, *SIMULATION TEAM, ITALY*
GUGLIELMO POGGIO, *SIMULATION TEAM, ITALY*
ALBERTO TREMORI, *SIMULATION TEAM, ITALY*

I3M 2014 LOCAL ORGANIZATION COMMITTEE

GREGORY ZACHAREWICZ, *UNIVERSITY OF BORDEAUX, FRANCE*
THECLE ALIX, *UNIVERSITY OF BORDEAUX, FRANCE*
JEAN CHRISTOPHE DESCHAMPS, *UNIVERSITY OF BORDEAUX, FRANCE*
JULIEN FRANCOIS, *UNIVERSITY OF BORDEAUX, FRANCE*
BRUNO VALLESPIR, *UNIVERSITY OF BORDEAUX, FRANCE*

This International Workshop is part of the I3M Multiconference: the Congress leading **Simulation around the World and Along the Years**

Index

BUILDING THE DIGITAL PATIENT: CONSIDERATIONS FOR THE NEXT DECADE

C. Donald Combs, Ph.D.
Vice President and Dean, School of Health Professions
Eastern Virginia Medical School
Norfolk, Virginia USA
combscd@evms.edu

ABSTRACT
Advancing medical practice to the level of personalized patient care is not a fanciful notion. Nor is it improbable or exaggerated. It is a credible end-state for medical M&S in the mid-term (10-15 years) future. Thus, the purpose of this paper is to provide an overview of the research and infrastructure that is needed to advance personalized patient care using the digital human and its ability to represent accurately the human physiome and diseaseome in real time for patient care, education, research and development. At the core of this endeavor to facilitating personalized healthcare is the primary beneficiary--the patient. The research agenda outlined in this paper is a call to action to ensure and compel the full development of a robust digital patient to enable personalized healthcare and, in the aggregate, more effective programs in research and in population health management.

Keywords: digital patient, physiome, personalized healthcare, research agenda, simulation

1. INTRODUCTION

The impact of new technologies during the past fifteen years has been extraordinary. It is difficult to remember that the now ubiquitous emails, web pages, text messages, I devices (pods, phones, and pads), tweets, blogs, and apps have a very brief history, widely used only in the past decade. One measure of this impact is the increasing demand for communication and information distribution: there are approximately 6 billion subscribers using some form of cellular device globally. So-called smart technologies are replete with advanced capabilities that enable the creation, imitation, and projection of virtual environments and simulated real-world experiences in most domains of everyday life.

Medical applications engaging these technologies are also experiencing exponential growth. Often the applications are developed within the confines of the discipline of modeling and simulation (M&S). In fact, medical M&S hosts the broadest spectrum of such usage, including fundamental aspects of healthcare such as human anatomy and physiology, human behavior, human systems to elaborate training and education exercises with computerized manikins and virtual operating rooms. Significantly, these advanced capabilities can even replicate aspects of a virtual human physiome to include anatomical, physiological, and behavioral attributes. Also underway is the *diseaseome* project, which maps disorders and diseases of an organism, viewed as a whole, with special reference to genetic features. The potential result of these combined capabilities can provide positive affects for the future of patient care. For example, a holistic, detailed simulation of a patient (*a digital patient*) can move diagnosis and treatment plans for that patient away from norm-driven options to patient-specific care, that is, true personalized care. Because medical M&S technology is inter-disciplinary (combining life and physical sciences, engineering, and medical expertise) and it is being executed at various levels for various purposes (at research and development institutions worldwide), there exists the substantial challenge of integrating these independent, yet complementary efforts to exploit their full potential. This is especially true with regard to the digital patient, wherein there is the necessity to assimilate the developed and developing components of the human physiome and diseaseome to advance patient care, medical practice, research and development, and education and training. In Europe, a substantial effort to develop a roadmap for the integration of data and models into a usable platform has been made through the Discipulus project and its evolving focus on the Virtual Physiological Human (VPH) and, ultimately, the Digital Patient.

Advancing medical practice to the level of personalized patient care is not a fanciful notion. Nor is it improbable or exaggerated. It is a credible end-state for medical M&S in the mid-term (10-15 years) future. Thus, the purpose of this paper is to provide an overview of the research and infrastructure that is needed to advance personalized patient care using the digital human and its ability to represent accurately the human physiome and diseaseome in real time for patient care, education, research and development. At the core of this endeavor to facilitating personalized healthcare is the primary beneficiary--the patient. The research agenda outlined in this paper is a call to action to ensure and compel the full development of a robust digital patient to enable personalized healthcare and, in the aggregate, more

effective programs in research and in population health management.

2. BACKGROUND

The dramatic growth in data about the human body and the human in social context combined with the progress in informatics, and modeling and simulation present an opportunity to realize a thirty-year old vision for a virtual human. This virtual human, however, will be far more sophisticated than the initial vision in that it will be capable of serving as a platform for research, education, patient care, drug and device testing. It will also be capable of accurately representing individuals and populations over time for purposes of screening, prevention, treatment, and analysis.

In the late-1980's, the U.S. National Library of Medicine established the Visible Human Project and, over the following decade, created male and female data sets designed to serve as a reference for the study of human anatomy, to serve as a set of common public domain data for testing medical imaging algorithms, and to serve as a test bed and model for the construction of network accessible image libraries. The Visible Human data sets have been applied to a wide range of educational, diagnostic, treatment planning, virtual reality, artistic, mathematical, and industrial uses by nearly 2,000 licensees in 48 countries.

In the late 1990', scientists at the U.S. Oak Ridge National Laboratory conceived the notion of a Virtual Human, a simulation of the structure and function of the human body that would integrate smaller models of individual organs, body processes, cells, and even neurons in the brain. The flesh and blood of these models would be floods of data, ranging from digitized anatomical images from the National Library of Medicine's Visible Human Project, to known electrical and mechanical properties of human tissue, to information on gene structure and function emerging from the federal.

In 2000, the International Union of Physiological Sciences Council formalized the Physiome Project. In its description, the IUPS notes that the Physiome Project is trying to put "Humpty Dumpty" back together again in a concerted effort to explain how each component in the body works as part of the integrated whole. Major diseases like cancer and neurological and cardiovascular diseases are complex in nature, involving everything from genes to environment, lifestyle and aging. Integrating knowledge of all these different components into robust, reliable computer models is expected to yield enormous medical advances in the shape of new therapies and diagnostic tools. Dozens of research institutions around the world are contributing to the building of the online computational modeling framework for integrating every level in human biology – one that links genes, proteins, cells and organs to the whole body. Ultimately, the goal of the Physiome Project is to piece together the complete virtual physiological human: a personalized, 3-D model of an individual's unique physiological make-up.

This international effort continues, but has been substantially accelerated by work lead by European Union institutions, both through the DISCIPULUS Project and its successor effort to develop the VPH. This latter effort (the description of which is drawn from the project website) aims to develop a methodological and technological framework that, once established, will enable collaborative investigation of the human body as a single complex system. The collective framework will make it possible to share resources and observations formed by institutions and organizations creating disparate, but integrated computer models of the mechanical, physical and biochemical functions of a living human body.

The Virtual Physiological Human (VPH) is a framework that aims to be descriptive, integrative and predictive:

- Descriptive. The framework should allow observations made in laboratories, hospitals and the field, at a variety of locations situated anywhere in the world, to be collected, catalogued, organized, shared and combined in any possible way.
- Integrative. The framework should enable experts to analyze these observations collaboratively and develop systemic hypotheses that involve the knowledge of multiple scientific disciplines.
- Predictive. The framework should make it possible to interconnect predictive models defined at different scales, with multiple methods and varying levels of detail, into systemic networks that solidify those systemic hypotheses; it should also make it possible to verify their validity by comparison with other clinical or laboratory observations.

The objective is to develop a systemic approach that avoids a reductionist approach and seeks not to subdivide biological systems in any particular way by dimensional scale (body, organ, tissue, cells, molecules), by scientific discipline (biology, physiology, biophysics, biochemistry, molecular biology, bioengineering) or anatomical sub-system (cardiovascular, musculoskeletal, gastrointestinal, etc.).

The Digital Patient is a vision of what a fully developed, usable VPH (with social factors incorporated)

could do in practice—in patient care, in research, in education, in drug and device development, and in population health.

3. USING A COMMON LANGUAGE

As with all interdisciplinary studies it is useful to first provide a common lexicon:

- *complicated and complex systems* – these systems diverge based on the level of understanding of the system; a physics-based model is complicated because it has numerous parts, but it is not complex in that it is predictable. On the other hand, a complex system like the human body might have fewer parts, but is complex because it is difficult to ascertain absolutes in the data. Humans are organic it is therefore not possible to predict the behavior of the human system with absolute certainty.
- *computer and computational models* – a computer model refers to the algorithms and equations used to capture the behavior of the system being modeled; while the computational model is a mathematical model that requires extensive computational resources (*e.g*., computer memory and speed) to study the behavior of a complex system by computer simulation or, more accurately, systems/federations of simulations
- *interoperability and integration* – the technical term interoperability refers to computer systems that can exchange information; integration (of systems) seeks to embed systems into an existing environment
- *live, virtual, constructive simulation* – examples of each in the medical domain are: live – using simulated patients to mimic illness; virtual – synthetic training environments where people employ simulated equipment like the virtual operating room; and constructive – simulated people and simulated equipment augment real-world conditions
- *simulation and simulator* – simulation is a means, a technique, to replace or augment real-world experiences with case studies or guided experiences that represent or replicate substantial aspects of that real-world with an interactive capacity; the simulator is a device that can be used to accomplish this, such as a computerized manikin that can mimic fluid loss
- *digital patient* – an artificial human that includes anatomical, physiological, behavioral and, ultimately social, attributes
- *anatomical model* – models of the human anatomy ranging in complexity from single cell to organ to organ system; single or multiple components (e.g., the femur or the entire skeletal system) with a view to studying form, *what it is*
- *physiological model* – models to understand how the anatomy works in totality; how cells, muscles and organs operate together and interact from the molecular basis to whole integrated behavior of entire body with a view to studying function,
- *behavioral model* – for purposes of this study, this modeling focuses on representing changes in human behavior that result from a wide range of factors such as information, motivation, ability, physical change
- *individualized and personalized patient care* – moving from treating the individual patient based on the norms for his / her symptoms or disease patterns, then prescribing norm-set treatment options to personalized patient care with specified treatment options that are not norm driven but based on the specific effects of selected treatments on an individual human, rather than an "average" human

4. WHY THE DIGITAL PATIENT IS IMPORTANT

Simply stated, human biology is a science of complexity. The typical approach to studying the complex entity that is the human body has been reductionist biology, wherein a scientist looks at specific segments of the body, in essence taking the pieces apart. This has its place in the examination of individual anatomical components, but it falls short when attempting a holistic analysis of the body. Thus, an ideal approach is one that accommodates an integrated, interoperable and necessarily complex and dynamic, examination of human biology coupled with physiological and behavioral components of the individual's experience. And that is what simulation can deliver in the form of the digital patient. Moreover, employing a digital human simulation in patient care can provide the best personal healthcare because it encourages, even requires, that the patient be more aware of consequences and take an active role in his/her own health as opposed to depending solely on guidance gained from hospitals, clinics, and specialists that may, or may not, be implemented appropriately.

Personalized Healthcare – this is the primary goal for the digital patient – personalized healthcare with the

patient actively participating. Among the groups spearheading this discussion is *Intel's Health Strategy & Solutions Group,* which advocates for proactive healthcare models using technology for broadband infrastructure, interoperability, and care in the home. Intel's three-pillar approach, *Care Anywhere*, *Care Networking*, *Care Customization*, requires fully exploiting the capability of smart technology. The ideal situation is to make *care-at-home* the default location for the patient in contrast to clinics and hospitals with their associated challenges and costs. All-too-often these disparate teams address the patient as distinct parts of the body, individual pathologies, and isolated aspects of physiology. The data prove that healthcare is more effective when it is a coordinated effort: 80% of medical errors are the result of communication errors as multi-disciplinary units fail to communicate effectively as a team. The digital patient facilitates a self-care approach coupled with a networking capability that can (because the same information is available to everyone who is involved) avert communication gaps while fostering care customization.

A 2012 study by the National Institute for Medicine found that approximately 75 million Americans have more than one chronic condition. Effective treatments therefore require substantial coordination among multiple specialists and therapies, which increases the potential for miscommunication, misdiagnosis, potentially conflicting interventions, and dangerous drug interactions. The study noted the importance of mobile technologies and electronic health records that offer significant potential to capture and share health data more efficiently. To accomplish this, clinicians and care organizations need to fully adopt these technologies, while encouraging patients to use these tools as personal health information portals that allow them to actively engage in their own care.

To facilitate an active, engaged patient community, other segments of the medical community must subscribe. Three additional areas where the digital patient can significantly affect the future of healthcare are: Practice, Research, and Education.

Practice – the future of health care, in the US and globally, is proving to be fraught with overwhelming challenges. Changing practice to provide holistic, personalized care in an expanding (longer-lived and growing population) and demanding (multiple pathologies and needs per individual patient) environment requires optimizing research, technology, and training. Clinicians must exploit new generation capabilities in diagnostic and therapeutic patient care for the burden of patient need to be met. Medical technology can be leveraged to provide safe and effective personalized patient care through the use of digital patient technology. Gone will be the "normed set of symptoms, normed set of treatments" approach.

Research – for purposes of this discussion, research encompasses using the digital patient platform to conduct medical studies and to develop new devices, tools and medications.

Another significant body of work is in the area of the human diseaseome. One of the most advanced diseaseome projects is a collaborative effort, the Human Disease Network – HDN – housed at the Center for Complex Network Research at the University of Notre Dame, Indiana. This research is in the form of a web-based disease/disorder relationships explorer via an innovative map-oriented network. The team of researchers and engineers use a HDN dataset to facilitate intuitive knowledge discovery by mapping the complexity of disease. The premise of the research is that a network of disorders and disease genes are linked by known-disorder gene associations. The network that has been developed offers a platform to explore in a "single graph-theoretic framework all known phenotype and disease gene associations." Their findings support the notion that there is a common genetic origin of many diseases. This is done via a bi-partite graph of two disjoint sets of nodes, one to correspond to known genetic disorders and one to correspond to known disease genes. A disorder and a gene are connected by a link if a mutation in the gene is implicated by the disorder (data for which was found in OMIM – Online Mendelian Inheritance of Man, reference 18, which includes 1,284 disorders and 1,777 disease genes as of 2005.) The significance of this research is the representation of a genome-wide roadmap for future studies of disease associations via the disease map which details all diseases and the genes associated with different disorders.

Another important research domain wherein the digital patient can be a significant asset is in pharmacology and biologic medicine. There are numerous agencies and institutions, for various reasons, that contribute to the growing body of literature condemning animal research in disease studies, pharmaceutical development, and biologic medicine. The literature details some of the failures of animal research and testing specific to toxicity safety and vaccine development by declaring this research as unreliable and not especially predictive when applied to humans. In short, the literature contends that animals have proven to be inadequate models for human disease research because they are genetically different from humans; therefore, studying diseases in animals can give us inadequate or erroneous information.

Research also entails the development of devices and tools: devices to support the body, such as stents, heart

valves, dental implants, spine and joint implants as well as tools to interrogate the body from the surgical scalpel to ultrasound technology. In 2006 the U.S. registered 46 million such devices and tools engaged in patient care.

The U.S. Food and Drug Administration is responsible for the oversight of the development of these apparati under its Center for Device and Radiological Health. The Center regulates via four evaluation models: animal, bench, computational, and human. Simulation supports this evaluation as it is premised on mathematical modeling. The FDA will soon to publish a guidance document, "Reporting Computational Modeling Studies in Medical Device Regulatory Submissions," as a means of encouraging simulation in medical research. The FDA is also developing the Virtual Physiological Patient (VPP), a library of computer models of the human body at various levels of disease states. Additionally, there is the partnership among device developers, software providers, and medical professionals, the Medical Device Innovation Consortium (MDIC) that serves as a center for disease-specific information gathering. Significantly, the goal of the VPP is to serve as a shared point of reference that will improve both understanding the value and limitations of models. For the FDA and its associate partners in this endeavor, these applications are distinct parts of what could grow into a whole representation.

The FDA commitment is one example of an excellent component of this study – an integrated, inter-operable fully developed digital patient that can serve all aspects of medical development to a more complete, perhaps spanning the whole-body, device assessment and evaluation.

Education **–** there are two essential skill-sets that must be mastered by students: 1) cognitive, to identify human anatomy / pathology; and 2) motor (or psychomotor) to distinguish and diagnose physiology via physical manipulation of the body (with one's hands or with devices). Medical training can be both patient-centric and education-centric with each perspective requiring varying levels of model and/or simulation fidelity. A digital patient can support both: for cognition training very high levels of modeling can facilitate a detailed teaching curriculum can be developed; the training of motor skills can take place with physical models that can support robotics or ultrasound training intent on manipulation skills of the probe. Of course, better education and training leads to better medical practice. The education prospects of the digital human support the means to train and assess learner performance more effectively.

5. CONCLUDING DISCUSSION

This paper shows the potential of the digital patient across all healthcare domains—education, research, product and drug development, and patient care. Integral to realizing this potential is understanding how the digital patient is being pieced together. For purposes of this paper, the state-of-the-art in the development of the virtual human physiome (the necessary precursor to the digital patient) includes three general areas: 1) anatomical, 2) physiological, and 3) behavioral.

This paper has outlined a general research agenda aimed at assimilating these various resources toward completing the digital patient, and then extending that integrated, interoperable capability to further research and development, augment education and training, and advance patient care.

REFERENCES

http://lsmarr.calit2.net/multimedia?vid=PmAj0Gr3cgI [accessed 15 May 2014]

http://physiomeproject.org/about/molecules-to-humankind [accessed 15 May 2014]

http://physiomeproject.org/about/the-virtual-physiological-human [accessed 15 May 2014]

http://www.academia.edu/3470720/The_Commodification_of_Patient_Opinion_the_Digital_Patient_Experience_Economy_in_the_Age_of_Big_Data [accessed 15 May 2014]

http://www.digital-patient.net/files/DP-Roadmap _FINAL _N.pdf [accessed 15 May 2014]

http://www.healthview.com/about.htm [accessed 15 May 2014]

http://www.intel.com/content/dam/www/public/us/en/documents/white-papers/healthcare-reinventing-for-21st-century-paper.pdf [accessed 15 May 2014]

http://www.iom.edu/Reports/2012/Best-Care-at-Lower-Cost-The-Path-to-Continuously-Learning-Health-Care-in-America.aspx [accessed 15 May 2014]

http://www.technologyreview.com/featuredstory/426968/the-patient-of-the-future/ [accessed 15 May 2014]

http://www.vph-institute.org/news/the-definition-of-the-digital-patient-high-on-the-discipulus-roadmap-agenda.html [accessed 15 May 2014]

Hood L, Rowen L., 2013. The human genome project: big science transforms biology and medicine. *Genome Medicine,* 5:79.

Sokolowski, J.A., Banks, C.M. 2011. *Modeling and Simulation in the Medical and Health Sciences.* Hoboken: Wiley.

A LIFETIME INDIVIDUAL SAMPLING MODEL (ISM) FOR HEROIN USE AND TREATMENT EVALUATION IN AUSTRALIA

Nagesh Shukla1[(a)], Van Hoang2[(b)], Marian Shahanan3[(b)], Alison Ritter4[(b)], Vu Lam Cao5[(a)], Pascal Perez6[(a)]

[(a)] SMART Infrastructure Facility, University of Wollongong, NSW, Australia 2522
[(b)] Drug Policy Modelling Program, National Drug and Alcohol Research Centre, University of New South Wales, NSW, Australia 2052

[1]nshukla@uow.edu.au, [2]v.hoang@unsw.edu.au, [3]m.shanahan@unsw.edu.au, [4]a.ritter@unsw.edu.au, [5]vlcao@uow.edu.au, [6]pascal@uow.edu.au

ABSTRACT

Illicit drug use has created an enormous burden at societal, family and personal levels. Every year a significant amount of resources is allocated for treatment and the consequences of illicit drug use in Australia and around the world. Heroin is one of the major forms of illicit drugs that are used illegally. Several independent heroin treatment strategies or interventions exist and state-of-the-art research demonstrates their efficacy and relative cost-effectiveness. However, assessing total potential gains and burden from providing all treatment interventions or varying the mix of heroin treatments has never been attempted. Furthermore, the need to include multiple treatments, multiple important outcomes, and the chaotic nature of drug dependence means cost-effectiveness studies are not able to provide evidence on net benefit of providing heroin treatments over the lifetime. Evaluations of the current mix of treatment provision remain very limited. Thus, this paper will discuss an individual level model which addresses net social benefit over a lifetime, also known as individual sampling model (ISM), that can accommodate the complexity of individuals going in and out of multiple treatments and their corresponding costs and benefits arising from different treatments during the life-course of heroin users in the context of New South Wales (NSW) Australia. This model is intended to serve as an effective tool for economic evaluation and policy making in illicit drug area in Australia.

Keywords: individual sampling model, illicit drug use, net social benefit, cost-effectiveness

1. INTRODUCTION

Governments, non-governmental organizations *(*NGOs) and International Organizations worldwide invest hundreds of billions of dollars in health care projects. Australia spends around 10% of its GDP or AUD 100 billion per year in recent years in health care (WDI, 2012). In area of illicit drug spending, Australian federal and state governments spend about AUD 1.7 billion per annum in prevention, treatment, harm reduction and law enforcement to combat illicit drugs. . Interestingly, the amount of spending and spending mix has remained relatively unchanged since 2000-2001, except there is a notable decrease in harm reduction to 2.1% (Ritter et al., 2013). There is an increasing pressure from both the government and the public to know whether the current spending is optimal or what needs to change to increase the benefits of spending. This is particularly important for complicated policies where there are many external costs and benefits, and as such; there are diverse views about the value of the projects.

Existing research demonstrates efficacy and relative cost-effectiveness for individual heroin treatments, such as pharmacotherapy maintenance. “Cost of illness” studies have estimated the total social burden related to all illicit drugs, and have been important in communicating this burden. But these studies do not provide evidence on the total potential gains from all interventions. And neither of these approaches can be used to value the net benefit, over the lifespan, of providing a system of heroin treatment interventions. There is a pressing need to demonstrate whether the existing combinations of heroin treatment interventions are a good investment for government. For this reason, this study will make a unique and fundamental contribution to the policy debate about investment in treatment mix for heroin dependence.

The aim of this study will be to assess the net social benefit of current heroin treatment strategies, and compare different combinations of treatment alternatives through modelled scenarios. This will lead to better informed policy decisions about the mix and type of treatments.

There are three original aspects to this study: 1. using a cost-benefit analysis (CBA) framework that provides a summative analysis across multiple treatment types; 2. taking a life-course perspective, which accommodates the multiple cycles into and out of treatment in a drug using career; and 3. using preference elicitation methods to quantify the economic burden to the family of the drug user, a neglected area in research to date. These unique elements require substantial

methodological rigor. This study entails the development of a mathematical model that will be parameterised from secondary data sources.

The mathematical model needs to capture recurring events over time as well as reflect alternative trajectories for individuals who use heroin. The chosen model is a micro-simulation model, also referred to as an Individual Sampling Model (ISM). ISM depicts events and outcomes at the level of the individual. The ISM enables 'memory' for each individual of such things as the length of heroin use, past treatments and incarcerations. The model will simulate a life-course with a start age of between 18 and 24 and an end age of 60 or death, with individual paths through mutually exclusive states. The characteristics of individuals at the outset of the model will be based on age, gender, use status, and incarceration and treatment history. The time each person spends in a given state before potentially transitioning to another state will depend on these characteristics. The model will be built for one jurisdiction, NSW. This was a pragmatic decision, made based on data availability (including treatment data, outcome data and costing data) and the inability to represent different models of treatment funding which exist in other jurisdictions in Australia.

There are limitations in using micro simulations. The most important one is that the model is 'data intensive'. To represent the heterogeneity (multiple states, multiple transitions between states, multiple outcomes and costs), a large number of parameter estimations are required. Therefore it needs to be kept as simple as possible, while also representing reality.

2. LITERATURE REVIEW

ISM has been widely used to evaluate health policies and other social and economic policies in many countries. It serves as an effective tool for policy evaluation, decision making and allocation of scarce financial resources. Many large ISM models have been built in Australia and overseas. There are a number of papers that describe the basic framework of the micro simulation model in health policy evaluation (Karnon, 2003, Briggs and Sculpher 1998, Zucchelli et al., 2012, Rutter et al., 2011, Ringel et al., 2010, Harding et al., 2010). Li and O'Donoghue (2013) provide a comprehensive review of micro simulation models up to recently, as well as highlighting some current methodological issues and future research directions.

However, there are very few ISM models that have been built to specifically evaluate illicit drug treatment policies. It is noted that it is important to build an ISM specifically for a country/state due to the differences in health care financing structure, costs and benefits, as well as the substantial difference in the availability of treatment methods.

There are two models in the context of the U.S. First, RAND Marijuana Micro simulation Model models the use of marijuana over the life course in the U.S. The model follows a cohort of 12 year olds representative of the United States population in 2004. This is a key paper in modelling of drug epidemiology over the life course (Paddock et al., 2012). Second, a paper by Zarkin et al., (2005) models the costs and benefits of methadone treatment related to heroin use, treatment for heroin use, criminal activity, labour market participation and health care utilization. This model follows 1,000,000 individuals from 18 to 60 year olds who are representative of the United States population.

Despite taking into account the life-course perspective of illicit drug use, they only evaluate a single treatment method and few states of drug use. In addition, these models make many simplifications about internal and external costs and benefits.

Another health model developed for Australian population is Australian Population and Policy Simulation Model-Health Module (APPSIM). It models the government spending on health care from 2002 to 2050. The model follows 1% of Australian population or 180,000 individuals over time. Individual characteristics such as disability, demographics, household formation, education, earnings, social security and taxation, health and aged care are estimated at any time period in the model (Lymer and Brown, 2012).

A population model, Population Health Model (POHEM), is developed for health care utilisation evolution in Canada. This is a population-based model, which takes into account a set of specific diseases and health risk factors at the individual level)Statistics Canada, 2010).

3. MODEL OVERVIEW

The ISM model for heroin use careers will create a population of individuals who ever used heroin and currently use heroin in the community and in prison. These individuals are distributed in various health/treatment states (eg, abstinence, irregular use, dependent use, various treatment and prison states). There are six model components which are to be conceptually defined, namely, initial population, states, transition matrix, transition probability, outcomes, and resource implications (these will be 'attached' where relevant to being in a given state i.e. treatment, prison, societal costs of crime).

Schematic representation of working of the proposed model is illustrated in Figure 1. The proposed model starts with the initial population of current heroin users and heroin abstainers. This population of individuals are transitioned from one health state to other using predefined (individual based) state transition probabilities. After each state transition, outcomes such as heroin use, crime committed; and resource implications are computed. This process is repeated at each time step (where time step is defined as the length of stay in each state, individually driven) until the end of simulation time period is reached. Each year, a sub-population of new drug initiators is added to the current population to include new drug users. Finally, net social benefit is computed based on the outcomes of the

simulation model. Following section provides more detail on each of the model components.

3.1. Data Sources

The following data sources will be used to establish the initial proportions in each state, individual length of stay and the transition probabilities between states, cost/awards and outcomes estimation:

3.1.1. Australian Treatment Outcome Study (ATOS) Dataset

ATOS is a longitudinal study of entrants to treatment for heroin dependence. The study originally followed up heroin users for 3, 6 and 12 months in three Australian states (New South Wales, South Australia and Victoria), and at 24 and 36 months in NSW. The cohort consisted of entrants to all three major heroin treatment modalities: methadone/buprenorphine maintenance, drug free residential rehabilitation (RR) and detoxification as well as a group not in or not seeking treatment (Darke et al., 2007, Teesson et al., 2007).

3.1.2. MIX study dataset

MIX is a prospective cohort study of people who inject drugs (PWID) conducted in Melbourne, Victoria. Baseline interviews were conducted with 688 people over the period November 2008 – November January 2010. Data collected includes data on demographics, drug use history and market access patterns, treatment history, criminal involvement, and current psychological, social and health states were conducted with information and consent collected at baseline allows linkage to a variety of objective datasets such as the National Death Index and Ambulance Victoria's ADIS system (Horyniak et al., 2013).

3.1.3. National Opioid Pharmacotherapy Statistics Annual Data (NOPSAD)

The NOPSAD collection is an administrative by-product collection which is collated in each jurisdiction and is a census of all people receiving opioid pharmacotherapy maintenance (methadone and buprenorphine) on a typical day in a year and provided to Australian Institute of Health and Welfare (AIHW). Data in the NOPSAD collection relate to a 'specified/snapshot' day, usually in June (AIHW 2013a). On this day the number of clients is counted for the NOPSAD collection permitting the number of clients to be estimated at a single point in time. The snapshot day varies slightly between states and territories, however is usually 30 June.

3.1.4. Alcohol and Other Drug Treatment Services National Minimum Data Set (AODTS-NMDS treatment data)

The AODTS-NMDS captures the number of closed treatment episodes in government funded alcohol and other drug treatment services across Australia. This number does not equate to the total number of people in Australia receiving treatment for alcohol and other drug use. The current collection methodology does not identify when a client receives multiple treatment episodes in the same or different agencies, either concurrently or consecutively (AIHW 2013b website).

3.1.5. Other datasets

Other datasets that will be used in the model development are: Australian National Drug Strategy Household Survey; Drug Use Monitoring Data; NSW Prisoners Health Survey; Bureau of Crime Statistics and Research crime data; Australian Bureau of Statistics data; and National Coronial Information System data.

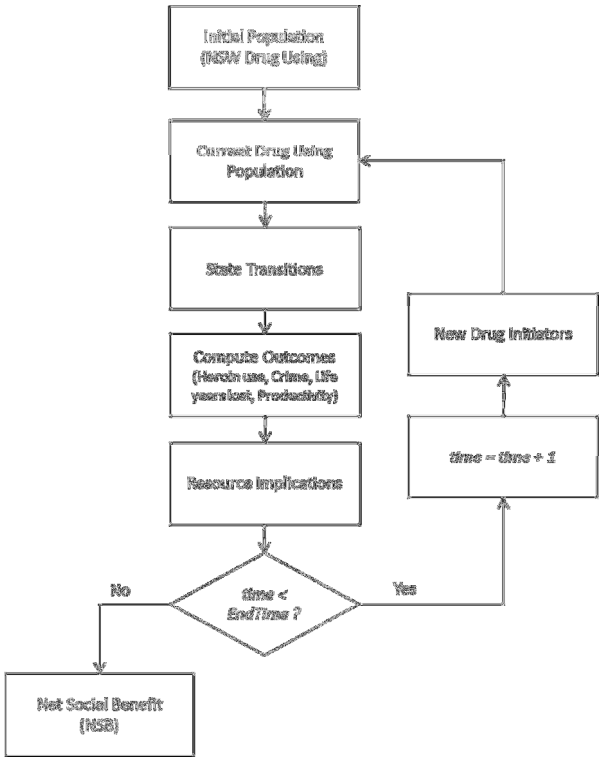

Figure 1: Conceptual working of proposed model

3.2. Model Components

3.2.1. Initial Population

The initial population in the current model is the estimated current NSW heroin using population. This will include those currently abstinent, those in treatment subgroups as well as those currently in the heroin using subgroup. The characteristics of the initial population are age, gender, among others; which will be obtained from various data sources. Once the initial cohort is defined across the various modelling states, there will be subgroup of new initiates which will be introduced every year into the simulation run.

The individual attributes/characteristics are:

- Age: starting with 18 to 60 years spread
- Gender: male or female
- State: current state
- Opioid use history
- Incarceration history
- Treatment history

This initial population is evolved over the lifetime to model and record the transitions from one state to

another which represent discrete events in the ISM simulation model.

3.2.2. States

In the proposed ISM, we have used two types of states – drug using state, and treatment states. For the drug using states (in the absence of treatment) we have selected 3 states - i) abstinence; ii) irregular use; iii) regular/dependent use. For the treatment states, we have included four mutually exclusive states – i) withdrawal from heroin (at this stage not withdrawal from methadone); ii) Residential rehabilitation (RR); iii) Pharmacotherapy maintenance (Opioid Treatment Program (OTP)); and, iv) counselling only.

In addition to these states, we have also considered the three important locations (stages) in the drug using individual's trajectory such as i) in community, ii) in prison; and, iii) death stage. The first two stages are considered in this study to model the cost, benefit and treatment variations in drug using population. Exit from the model occurs if alive at age 60, death from drug related or non-drug related causes. Hence the total number of states is provided in Table 1. It should be noted that we have used only one treatment state in the prison stage. This is due to the fact that we do not have sufficient in-prison treatment data to be able to distinguish transition probabilities between all the different prison treatment states. For this reason, we have simplified prison treatment down to one state.

Table 1: Total number of states when combined with stages

State Name	Stage
Abstinence (S1)	COMMUNITY
Irregular use (S2)	COMMUNITY
No Treatment & Use (S3)	COMMUNITY
Withdrawal (S4)	COMMUNITY
Residential rehabilitation (S5)	COMMUNITY
Pharmacotherapy (OTP) (S6)	COMMUNITY
Counselling Only (S7)	COMMUNITY
Abstinence (S8)	PRISON
No Treatment & Use (S9)	PRISON
Treatment (S10)	PRISON
Drug related (Death) or 60+ years old (S11)	DEATH
Non-Drug related (Death) (S12)	DEATH

The descriptions of each of the model states are:

In community Stage:

Abstinence: individuals in this state are not using heroin but have used heroin at some previous time.

Irregular use: individuals in this state use heroin irregularly, as defined as less than weekly or "weekly or less" (as compared to 'more than weekly but not daily").

Not in Treatment & Use: individuals in this state use heroin regularly and they are not in receipt of any type of treatment

Withdrawal: Withdrawal treatment is concerned with neuro-adapation reversal, involves about 5-7 days care (in inpatient or outpatient setting) and includes medications to manage symptoms, supportive care and case management.

Residential rehabilitation (RR): RR is concerned with behavioural change across all life areas, including relapse prevention, psychological well-being, physical health, nutrition etc. It is provided in residential settings, and an ideal treatment program is 6-9 months long although it will have many who leave in the first week.

Opioid Treatment Program -Pharmacotherapy (OTP): the provision of a legal, safe opioid (either methadone or buprenorphine), dispensed daily or less frequently with take-away doses; requires prescriber and attendance at a pharmacy (primary care or clinic settings).

Counselling Only: Provision of psychological therapy only, on outpatient basis, (weekly or fortnightly) with case management.

In prison Stage:

Abstinence: individuals in this state are not using heroin but have previously used heroin and are incarcerated. We assume that no-one commences heroin use in prison (this is a simplifying assumption).

No Treatment & Use: individuals in this state are incarcerated, use heroin and are not having any type of treatment

Treatment: In prison treatment is mainly happening in the form of pharmacotherapy.

Death Stage:

Drug Related: A drug-related death is one where the cause of death is directly attributable to heroin (overdose, or cardiac arrest etc. caused by heroin use in immediate or long-term).

Non-Drug Related: Death from any causes not directly attributable to heroin: car accident, homicide, cancer, heart attack etc.

In summary, we have selected a set of mutually exclusive states large enough to capture the complexity of the treatment process and low enough to ensure the resulting model is tractable and does not overburden the model with very detailed and specific data requirements.

3.2.3. Transition Time

In this model, we have used an approach which provides heterogeneous 'time to transition' for each individual in the model based on his/her attributes such as age, sex, treatment history, and state. For this, we are using length of stay (LOS) distributions for each state in the ISM stratified by age, sex, history. These distributions are derived from a number of different datasets. As a result, this approach is free from

traditional fixed time steps for individual movements across states as we use continuous function for individual's length of stay determination.

3.2.4. State Transitions

Once individuals in each state finish their assigned LOS in a state, they transition to other state based on transition probability functions. These functions are dependent upon the individual's attributes. In the model, these probabilities will be estimated based on survey dataset or derived from literature. We will use ATOS dataset, MIX dataset, and review of relevant literature to estimate these probability functions. Two types of transition functions in the model are as follows:

1. An equation, empirically derived, that specifies the probability based on individual's characteristics and history of the transition. These will be derived from ATOS, MIX etc data.
2. A probability distribution of the likelihood of transition, based on a known distribution of an event (empirically derived from summary data). Once a distribution function is established, Monte Carlo sampling is used to choose transition probabilities

3.2.5. Costs and Outcomes

As already outlined, the model will run through cycles, and costs and outcomes (also referred to as rewards) are accrued within each cycle.

There will be resources attached to simply being in some states and are referred to as State Awards. For example, while in S4 (withdrawal in the community), there will be a cost per episode of withdrawal; similarly there will be a cost attached to residential rehabilitation (by days in RR); pharmacotherapy (by days in OTP); counselling (by visits); prison (days); treatment in prison (days in OTP). These will be average unit costs (more about this below).

The variation in resource use will be driven by the length of time in a state. There will also be resources attached to some transitions (transition awards) i.e. transitioning into prison would incur the costs of the police and court. For individuals in prison, the social costs of crime, police and courts would only occur once even if a person stayed in prison for several cycles but the cost of being in prison, or being in treatment in prison would be applied as long as the person remained in that state. Another example is the cost of moving from a live to a dead state; as obviously the cost of dying occurs only the one time; not in every subsequent cycle.

Overall, we focus on the main categories of costs and benefits because they account for the main outcomes of heroin treatment. We decide to leave out unimportant costs and benefits because of their insignificance in total costs and benefits and it is time consuming to obtain all those costs and benefits. Total costs include the following components (i) life-years (saved, or lost); (ii) treatment costs; (iii) other health care utilisation (i.e. hospital, emergency department visits, and treatment for specific diseases such as Hepatitis B and C); (iv) crime costs; (v) and economic impact on family burden. Total benefits include: (i) earnings due to returning to work after successful treatments; (ii) cost-savings to the government and society due to successful treatments (e.g. reduction of crime and health care utilization).

Health care costs would be of two types – some which are one-off i.e. an overdose which results in hospitalisation but not death. And others which are ongoing i.e. Hepatitis – here the costs will be low in early years of the disease but with some probability will increase as some proportion of the cohort will develop chronic hepatitis its sequelae.

3.2.6. Net social benefit

Once the costs and benefits have been calculated, the criterion for assessing the overall efficiency of an intervention is the Net Social Benefit (NSB).

$$NSB = \sum_{t=1}^{T} \frac{B_t - C_t}{(1+r)^{t-1}}$$

where B_t are benefits in year *t*, C_t are costs in year *t, r* is the discount rate, and T is the duration in years under consideration. The NSB is the sum of the present value of all benefits minus the sum of the present value of all costs. A policy is potentially worthwhile if NSB is > 0.

The time span of the model is about 40 years. Therefore, it is no doubt that NSB will be sensitive to discount rate. The discount rate reflects cost of capital and risk premium of the project. The cost of capital is the next best alternative use of capital if the project was not implemented. We can use the interest rate of the Australian government bond/or risk-free interest rate, which is about 3-4% per year as a proxy for discount rate. Risk premium is the extra return above risk-free return to compensate for the probability of project failure. However, it is thought that risk-premium in government project is small. It is very hard to precisely estimate a discount rate. Therefore, a base discount rate of 3% will be used to calculate NSB. In addition, a sensitivity analysis will be conducted using a range of discount rates, including 0%, 3%, 5% and 10%.

4. MODEL ARCHITECHTURE

A survey of existing modelling software packages indicated lack of adequate existing software that would enable ISM modelling for heroin users. Therefore, a customised software platform is designed. Figure 2 illustrates the software architecture for the simulation model. Major opensource software tools used in developing the simulation model include; the Java for coding the simulation model components, Java swing for GUI development, and PostgreSQL databases for storing model inputs, intermediate and final outputs. The functions of each are briefly discussed in the following subsections:

Java: The general-purpose, concurrent, object-oriented programming language is used to implement algorithms

managing the creation of the initial population of individuals, individual transitions from one state to another based on transition probabilities, and estimating state and transition awards and outcomes. The Eclipse Integrated Development Environment (IDE) is used as the main development platform. There are three components which have been embedded in Java Eclipse:

Population Generation – creates the initial population for heroin use with age, gender, initial state, opioid use and incarceration history attributes. It also adds new heroin initiating population sub-group which enters the simulation at the start of every year.

State Transition Algorithm – it makes the individuals in the population move from one state to other. Based on individual attributes such as age, gender, state, opioid use and incarceration history, it calculates

a. The length of stay (LOS) that each individual needs to serve in the current state (in community or prison).
b. The probability of transition, for each individual, to transition to next state at the end of LOS.

Cost/Benefit Estimation – computes the benefits and costs which is attached to each individual in the simulation model

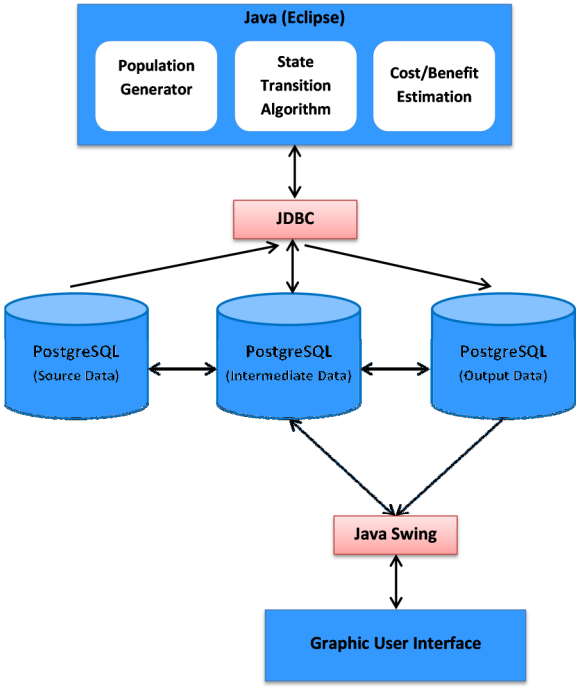

Figure 2: Software architecture of the simulation model

PostgreSQL: an open source object-relational database system, which is used to record (i) inputs to the model; (ii) intermediate data; and, (iii) model outputs. The main database tables are:

Model Configuration – stores all parameters required to run the simulation model such as simulation time period, number of individuals in initial population of heroin users in NSW, and new heroin users per year.

Costs Table – stores all cost data attached with the states (per unit LOS in a state cost) and transitions cost (as per event cost).

Benefits Table – stores all the benefits data attached with states and transitions

Current population table – stores simulated population generated at each year of the simulation.

Intermediate state transition table – stores the state transition trajectory of individuals in the simulation model

Intermediate cost table – stores the accumulated cost of each individual in the simulation model

Intermediate benefit table – stores the accumulated benefits of each individual in the simulation model

Output tables – stores the overall costs, benefits, mortality, and others at the end of the simulation

Java Swing: a pure Java widget toolkit is used to provide a graphic user interface (GUI). As a part of Oracle's Java Foundation Classes (JFC), it provides a native look for GUI and can be used across multi-platforms.

Graphic User Interface (GUI): a user interface that allows policy makers to interact with the model as well as allowing visualization of the model output and intermediate data in form of graphs and tables. Policy makers can plan new "what-if" scenarios, which can then be used for scenario based comparison analysis.

5. WORK IN PROGRESS

This study involves the development of lifetime state transition model of heroin using population in NSW, Australia. The conceptual model for the simulation is developed to identify i) crucial model elements such as states, transitions, costs, and benefits; and, ii) data sources to estimate transition probabilities, costs, benefits.

Thus far, we have built an initial prototype simulation model which creates the initial heroin using population, new heroin initiators, and transitions to different states. We are in the process of feeding the model with validated transition functions, per unit/event costs, and benefits; derived from historical heroin using individual datasets or literature review. Figure 3 illustrates the graphical user interface which is developed to support users to interact with the model to design and run different scenarios.

The final step in the modelling will be to validate whether the model is consistent with heroin user career trajectory. Various key outcomes from the model such as the distribution of participants across states, mortality rate and like these others will be verified with other datasets/sources that were not used to parameterize the model.

6. CONCLUSION

This paper presents a simulation modelling framework and concepts for the development of individual sampling model (micro-simulation) for lifetime simulation of the heroin using population in one Australian jurisdiction, NSW. This study will evaluate the long term (lifetime) cost-effectiveness of a set of

treatment options available for heroin users together with the societal costs and benefits. The proposed methodology involves creating realistic initial population of heroin users, development of state transition algorithm, and estimating costs and benefits from the heroin treatments in a lifetime. This is a work in progress study and the next steps are to i) feed the input datasets to estimate individual state transitions, costs and benefits; and ii) validate and verify the model outputs with other data sources.

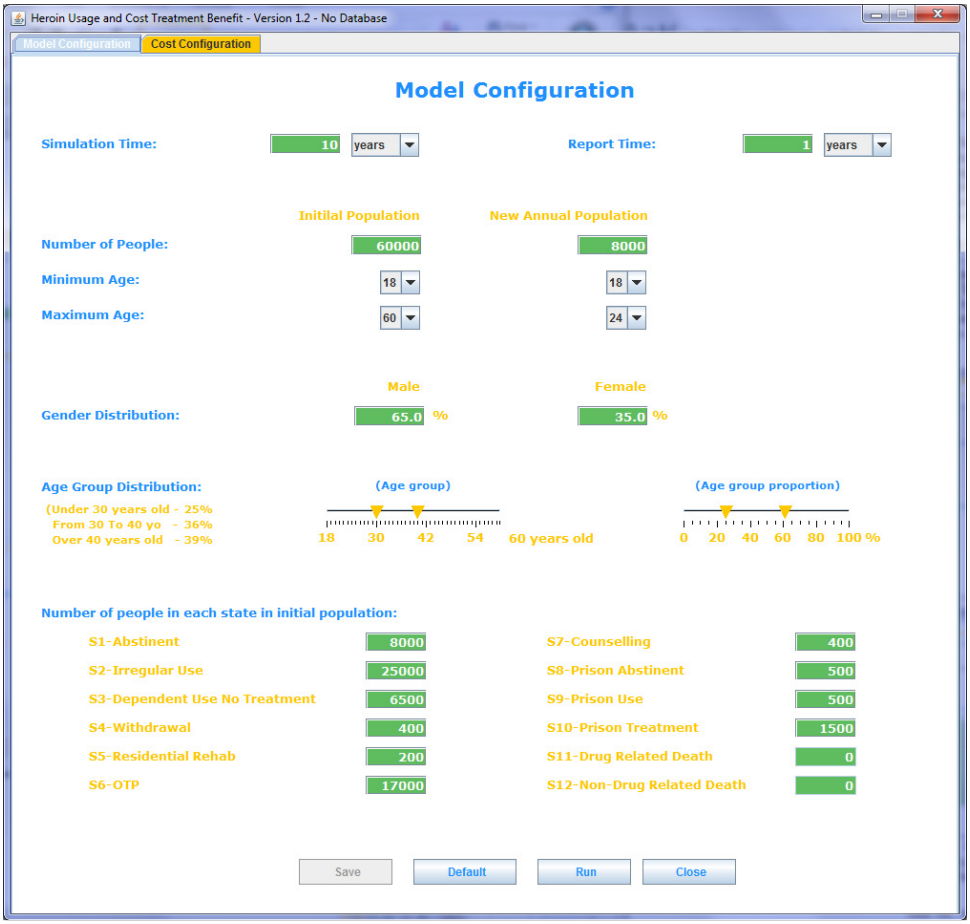

Figure 3: GUI for model interaction and scenario analysis

REFERENCES

AIHW, Australian Institute of Health and Welfare. 2013a. *National Opioid Pharmacotherapy Statistics Annual Data Collection 2012*. Drug treatment series no. 20. Cat. no. HSE 136. Canberra: AIHW.

AIHW, Australian Institute of Health and Welfare. 2013b. *Alcohol and other drug treatment services in Australia 2011–12*. Drug treatment series 21. Cat. no. HSE139. Canberra: AIHW.

Brennan, Alan., Chick, SE and Davies, R. 2006. A taxonomy of model structures for economic evaluation of health technology. *Health Economics*, 15(12), 1295-1310.

Briggs, A and Sculpher, M. 1998. An introduction to Markov modelling for economic evaluation. *Phamacoeconomics*, 13(4), 397-409.

Darke S, Ross J, Mills KL, Williamson A, Havard A, Teesson M. 2007. Patterns of sustained heroin abstinence among long-term, dependent heroin users: 36 months findings from the Australian Treatment Outcome Study (ATOS). *Addictive Behaviours*, 32(9), 1897-906.

Harding, A., Keegan, M and Kelly, S. 2010. Validating a dynamic population microsimulation model: Recent experience in Australia. *International Journal of Microsimulation,* 3(2) 46-64.

Horyniak, D., Peter Higgs, Rebecca Jenkinson, Louisa Degenhardt, Mark Stoové, Thomas Kerr, Matthew Hickman, Campbell Aitken and Paul Dietze. 2013. Establishing the Melbourne injecting drug user cohort study (MIX): rationale, methods, and baseline and twelve-month follow-up results. Harm Reduction Journal, 10(11), 1-14.

Karnon, J. 2003. Alternative decision modelling techniques for the evaluation of health care technologies: Markov process versus discrete event simulation. *Health Economics*, 12(10), 837-848.

Li, J. and O'Donoghue, C., 2013. A survey of dynamic microsimulation models: uses, model structure and methodology, International Journal of Microsimulation, 6(2), 3-55.

Lymer, S and Brown, Laurie. 2012. Developing a dynamic microsimulation model of the Australian health system: a means to explore impacts of

obesity over the next 50 years. *Epidemiology Research International*, vol. 2012, Article ID 132392, 13 pages.

Orcutt, GH. 1957. A new type of socioeconomic system. *Review of Economics and Statistics,* 39(2), 116-123.

Paddock, SM., Kilmer, Beau., Caulkins, J P., Booth, MJ and Pacula, RL. 2012. An epidemiology Model for Examining Marijuana Use over the life course. *Epidemiology Research International,* Vol. 2012, Article ID 520894, 12 pages.

Ringel, JS., Eibner, C., Girosi, F., Cordova, A and McGlynn, EA. 2010. Modelling health care policy alternatives. *Health Services Research,* 45(5), 1541–1558.

Ritter, A., McLeod, Ross and Shanahan, M. 2013. Government Drug Policy Expenditure in Australia-2009/10. *Drug Policy Modelling Program Monograph* 24.

Rutter, CM., Zaslavsky, AM and Feuer, EJ. 2011. Dynamic micro simulation models for health outcomes: a review. *Medical Decision Making*, 31(1), 10-18.

Statistics Canada. 2010. *POHEM-Population Health Model*. Available from: www.statcan.gc.ca/microsimulation/health-sante/health-sante-eng.htm [accessed 8 Apr 2014]

Teesson M, Mills K, Ross J, Darke S, Williamson A, Havard A. 2007. The impact of treatment on 3 years's outcome for heroin dependence: findings from the Australian Treatment Outcome Study (ATOS). *Addiction*, 103(1), 80-88.

World Bank. 2012. World Development Indicators 2012. Washington, DC. © World Bank. http://issuu.com/world.bank.publications/docs/9780821389850?e=0

Zarkin, GA., Dunlap, LJ., Hicks, KA and Mamo, Daniel. 2005. Benefits and costs of methadone treatment: results from lifetime simulation model. *Health Economics*, 14(11), 1133-1150.

Zucchelli, E., Jones, AM and Rice, N. 2012. The evaluation of health policies through dynamic microsimulation methods. *International Journal of Microsimulation,* 5(1), 2-20.

AUTHORS BIOGRAPHY

Nagesh Shukla (PhD): Dr. Nagesh Shukla is a researcher in the field of Industrial & Systems Engineering, particularly in the areas of data analytics, simulation modelling and computational intelligence. He has a PhD degree from University of Warwick, UK. His contributions have appeared in major international conferences, journals, book chapters, and technical reports. In 2013, he has been named as one of the Chief Investigators in NHMRC funded project. He also acts a reviewer to several high impact journals.

Phuong Hoang (PhD): He is an Economist/Research Fellow at the Drug Policy Modelling Program (DPMP) at the National Drug and Alcohol Research Centre (NDARC), the University of NSW, Australia. Prior to this, he was working in an ARC project on economic evaluation of policies regarding Assisted Reproductive Technologies (ART) in Australia.

Marian Shahanan (PhD): Dr Shanahan was awarded her PhD at UNSW in 2011 for her research assessing the costs and benefits of cannabis policies in the NSW context where the policy options included a hypothetical legalisation approach. She is currently a Senior Research Fellow at the National Drug and Alcohol Research Centre. Dr. Shanahan's background is in Health Economics. Current research includes assessing the cost-effectiveness of methadone post-release from prison, the cost effectiveness of various police diversion programs for cannabis, assessing the costs and benefits of treatment for heroin use.

Alison Ritter (PhD): Professor Alison Ritter is an internationally recognised drug policy scholar and the Director of the Drug Policy Modelling Program (DPMP) at the National Drug and Alcohol Research Centre (NDARC) at the University of New South Wales. She is an NHMRC Senior Research Fellow (2012 to 2016) leading a collaborative, multi-disciplinary program of research on drug policy. She is the President of the International Society for the Study of Drug Policy, Vice-President of the Alcohol and Drug Council of Australia and an Editor for a number of journals, including *Drug and Alcohol Review*, and the *International Journal of Drug Policy*. Professor Ritter has an extensive research grant track record. She has published widely in the field including three edited books; multiple book chapters and more than 200 other publications.

Vu Lam Cao: He is an Associate Research Fellow at SMART Infrastructure Facility, University of Wollongong. He has received his Masters in IT and ICT from the Uni-Wollongong. His research interest focus on agent based modelling and traffic micro-simulation modelling. Currently, Vu Lam's research focuses on modelling related to big data and health care.

Pascal Perez (MSc PhD): Professor Perez is currently the Research Director of the SMART Infrastructure Facility, University of Wollongong. He is a specialist of Integrative Social Simulation, using Multi-Agent Systems technologies to explore complex infrastructure systems. He is a member of the Technical Committee of the Australian Urban Research Infrastructure Network (AURIN). He is also a member of the Modelling and Decision Support Division of Simulation Australia and of the Modelling and Simulation Society of Australia and New Zealand (MSSANZ). In 2002, he received an ARC-International Linkage Fellowship to develop social modelling research at the Australian National University. He has published 100 refereed papers and book chapters. In 2006, he co-edited with his colleague David Batten the book *'Complex Science for a Complex World'* (ANU E Press).

VALIDATION OF A 4D LOW COST LAPAROSCOPIC TRAINING PLATFORM

M. Sguanci[a], F. Mandolfino[b] , M. Minuto[c] G. Vercelli[d] M. Gaudina[e] , V. Rumolo [f] M. Frascio[g]

[a]DISC - Department of general surgery
[b]DISC - Department of general surgery
[c]DISC - Department of general surgery
[d]DIBRIS – Department of Informatics, Bioengineering, Robotics and Systems Engineering
[e]DIBRIS – Department of Informatics, Bioengineering, Robotics and Systems Engineering
[f]DISC - Department of general surgery
[g]DISC - Department of general surgery

[a]marcosguanci@yahoo.it, [b]fcmandolfino@gmail.com [c] micheleminuto@hotmail.com
[d] gianni.vercelli@unige.it [e]marco.gaudina@gmail.com [f] valerio.rumolo@gmail.com [g]mfrascio@unige.it,

ABSTRACT

The use of simulation in laparoscopic surgery training appears to be qualitatively effective if supported by a suitable evaluation system.

The increasing demand of more complex laparoscopic simulators has inspired the creation of a 4d simulator which is a physical low-cost laparoscopic training platform that reproduces the tactile feedback: eLaparo4d) integrated with a software for virtual anatomical realistic scenarios (Unity3D V 4.1).

The aim of the present project is to show the platform validation results using two instruments: the face validity and the construct validity.

The results have been obtained by a 12 items standardized questionnaire focused on the "user's satisfaction" submitted to two 15 users groups .

4 basic skill have been chosen to be analyzed: laparoscopic focusing and navigation (2 different exercises), Hand – eye – coordination (HEC) (2 different exercises).

Keywords: low cost simulation, face validity, construct validity, training.

1. BACKGROUND

The use of simulation in laparoscopic surgery training appears to be qualitatively effective if supported by a suitable evaluation system.

The continually increasing demand of more complex laparoscopic simulators has inspired the creation of a 4d simulator which is a physical low-cost laparoscopic training platform that reproduces the tactile feedback: eLaparo4d) integrated with a software for virtual anatomical realistic scenarios (Unity3D V 4.1).

The School of Medicine of Genoa and the Biomedical Engineering and robotic department (DIBRIS) have cooperated to create a low-cost model based on existing and brand new software.

Aim of this work is to describe the the platform validation results using two instruments: the face validity and the construct validity.

2. MATERIALS AND METHODS

This study validates eLaparo4D simulator: face and construct validity.

2.1 The simulator system

The system is based on a nodejs (htpp://www.nodjes.org) application server that manages the visualisation system, the communication with hardware interfaces and the database where users' data are stored.

The server technology is indeed a sort of data gateway between the several different elements, regardless they are hardware or software. The following figure (figure 1) shows how communication data are exchanged from the very low part of the system (Hardware Interfaces, bottom) to the user interface (HTML Client,top).

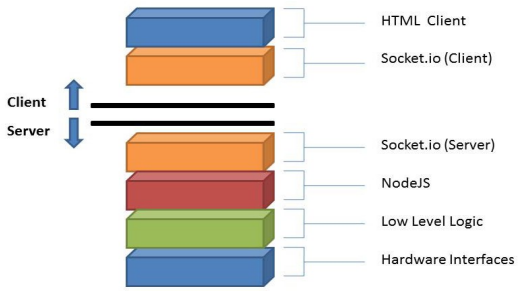

Figure 1: part of the system simulation

The user interface is a simple HTML5 web page

running a Unity3D engine (htpp://unity3d.com) plugin. We run several performance tests to compare Unity3D and native WebGL, getting same results. We finally decided to adopt
Unity3D engine due to its rapid development time. WebGL is a great technology but still too young to allow us working on a powerful and robust framework. The use of web pages as the main user interface allows us to be more versatile and in the future will give us the possibility, thanks to HTML5 powerful characteristics, to easily share contents in a live way with other systems. An interesting feature is, for example, having the possibility to be guided by an external supervisor, who is monitoring the training phase, while data are quickly exchanged via internet.

2.1.1 Visual and fisical modelling

As previously introduced, visual modelling is a very important aspect of the entire project.

A videolaparoscopic surgery simulator needs a detailed representation of the organs and the tissues inside of the human abdomen. The meshes included in eLaparo4D are developed in Blender 3D Modelling software (htpp://blender.org), and then imported in Unity3D, including textures and UV maps. Eventually, in Unity3D render shader materials are added to the raw meshes, to simulate the specific surface of each of the modelled tissues. In Figure 2, a screenshot of the current virtual environment is shown.

Figure 2: a screenshot from the current aspect of the virtual environment compared to a screenshot of the camera view of a real surgical operation.

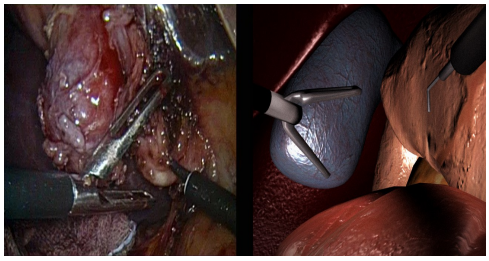

As remarked by our colleagues of the Videolaparoscopy Unit of the Department of Clinical Surgery, highly specific training sessions are required to help the operator achieving a proper skill set. In an ideal scenario, medical students should have access to a complete simulator composed of several training scenes, as part of a modular and step-based training process. While the main components and controls of the simulator should be in common, each scene should focus on a very specific surgery operation, differentiating in: the zone and the organs physically manipulated (the target), the particular surgical maneuvers performed (the task), and the type of manipuli used (the means).Considering these remarks, we developed a dynamic parametric physical simulation approach, arbitrary applicable to the rendered meshes in every scene and able to avoid system overloads. Such an approach permits the creation of different scenes starting from the same set of models and interaction algorithms, easily supporting a step-based training. In detail, each 3D object in the scene carries a selectable 3 layer collider component, driving a vertex deformation script. The first layer is a simple box collider; the

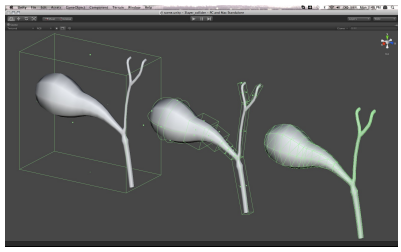

Figure 3: I.e of a collider layer for a gallbladder model

second one is a combination of simple shape colliders which cover, with good approximation, nearly all the volume of the object; the third is a precise mesh collider which exactly coincides with the vertex disposition of the object's mesh. In the foollowing figure (figure 3) is possible to see the 3 different collider layer for a gallbladder model.

2.1.2 Feedback system

Haptic feedback is implemented thanks to the use of three Phantom Omni devices from Sensable (htpp://sensable.com).

The first two are used as manipuli (grasper, hook or scissors) and the third one is used to move the camera within the virtual abdomen, as it happens in a real scenario. The system generates a resultant force when the user puts a manipulus in contact with a mesh, according to the executed task. Phantom devices have been chosen because reasonably low cost although precise enough for the needed level of realism. Furthermore, their stylus-like shape will permit a complete merging of the devices with the physical environment reconstruction; in particular, each stylus will be easily connected to real manipuli. Thanks to an Arduino board connected to a vibrating motor we have also included a vibration feedback. Vibration is used to enhance the realism of operations like tissue shearing (hook) and cutting (scissors).

2.2 The validation system

A valid simulator measures what it is intended to meas-ure.

There are a variety of aspects to validite; subjective approaches are the simplest.
In this sense, we have chosen 2 different kind of validation:

- The Face Validity
- The Construct Validity

Face validity usually is assessed informally by no experts and relates to the realism of the simulator; that is, does the simulator represent what it is supposed to represent?
This kind of validity relates to the realism of the simulator.
A questionnaire validation was created.
In this document 12 closed-ended questions were selected about the following topics:

ergonomics
structure
realism
tactile feedback
quality

For each question must be given a score according to the rating scale "Likert" (Highly inadequate, Insufficient, Sufficient, Good, very good).

Concurrent validity: is the extent to which the simulator, as an assessment tool, correlates with the "gold standard."
This testing can be achieved by evaluating two groups of subjects, with a different professional experience, with the simulator, comparing the performance scores. This necessitates establishing an objective structured assessment of technical skills (OSATS) evaluation by which the model or "gold standard" performance can be assessed reliably for comparison.(Max V. Wohlauer et al. , 2013)
About this, the simulator must be able to distinguish the experienced from inexperienced surgeons. This is best determined by testing a large number of surgeons with various degrees of training, experience, and frequency of performance of a specific surgical skill or procedure.
For competency assessment, the performance of an individual on a simulator should ideally predict, or at least correlate with, that individual's performance in the real environment of the operating room. As such, a valid and reliable measure of operating-room performance must be established. This allows differentiation between surgeons assumed to be clinically competent (experienced or expert clinicians) and noncompetent (junior or inexperienced residents). These evaluations are much simpler to perform when a specific task like Hand-eye coordination and laparoscopic navigation and focusing.

2.2.1 Subject

The total number of recruited participants in the study was 24. All participants were included in the face validity study.

A division into two subject groups was made to accomplish the study of construct validity.
The division criterion was the subject experience in laparoscopic surgery.

- Group 1: was composed by 12 novices (5 female, 7 male).
- Group 2: was composed by 12 experts (3 female, 9 male).

The mean age of the groups was years (range years) for novices and years (range years) for experts.
None of the novices had previous experience in virtual reality simulators.

2.2.3 Methodology

For the platform validation, 4 tasks have been selected. These tasks are focused to enhance the most basic skills.

Acquisition of basic skills: exercises related to the acquisition of tasks which allow students to reach basic gestures competences. They could practice using probes that simulate the haptic feedback according to the kind of action.

The 4 selected tasks are:

1. *laparoscopic - focusing - navigation*: This task aims to evaluate the ability to navigate a laparoscopic camera with a 30º optic. This is done by measuring the ability to identify 14 different targets placed at different sites
   Two different exercises were chosen:

   Exercise 1: the student, working with a 30° ptic, have to focus different solid targets in a static scenario. This task evaluates the macro – focusing.

   Exercise 2: the student working with a 30° ptic, have to focus a lot of hidden micro- targets, placed in different areas of the scenario.

2. *hand – eye – coordination (HEC):* This task aims to evaluate the ability to work with the non-dominant and dominat hand.
   The camera is static.
   Two different exercise were chosen:

Exercise 3: the student have to touch a defined point in an "organic scene" with the left and right instrument simultaneously

Exercise 4: the student have to touch a lot of spheres that appear sequentially and in random positions.
There is a time limit to center and touch each sphere with the right and left hand. In this task, the camera is static.

For each of these tasks, a certain number of metrics have been automatically recorded.
Metrics are defined as follows:

– *Total time.* Time that the user needs to accomplish the
Task.
– *Partial time.* Mean time that the user needs to accomplish a partial task.
– *Fulfillment.* Percentage of partial tasks done within the established time.
– *Penality:* number of penality about each task.

Which metrics are recorded for each task is shown in Table 1.

Task	Description	Metrics
Navigation	ability to navigate a laparoscopic camera with a 30º optic	Fulfillment (%) Total time (s) Score penality
Navigation and focusing	the student have to focus different solid targets in a static scenario	Fulfillment (%) Total time (s) Score penality
Coordination (HEC) 1st exercise	the student have to touch a defined point in an "organic scene"	Fulfillment (%) Total time (s) Score penality
Coordination (HEC) 2nd exercise	the student have to touch a lot of spheres that appear sequentially and in random positions.	Fulfillment (%) Total time (s) Score penality

Table 1 "Metrics and Tasks" in the Construct Validity

2.2.4 Questionnaire

All Expert subject were requested to fill a Face validity Questionnaire, referred to characteristics of the eLaparo4D simulator (11 questions).
The questions had to be answered in a 5-point Likert Scale.
The format of Likert item is:

- Strongly disagree
- Disagree
- Neither agree nor disagree
- Agree
- Strongly agree

2.2.5 Statistical analysis

Statistical analysis was performed using Excel software and SPSS.
Data are expressed in terms of mean ± standard deviation. The data from the Novice group and expert group are compared with the Mann-Whitney U test; about this, differences were considered significant at $P \leq 0.05$.
In this validation program, we decided to use also the Cronbach's Alpha Test to measure the "Reliability" of the internal consistency of the simulator.

3. RESULTS AND DISCUSSION

3.1 Results

Face Validity

The questionnaire analysis has showen the following data:

- Excellent degree of usefulness of simulation in reference to 'acquisition of skills, "basic" hand-eye coordination (4,4 ± 0,69)
- A real confidence in the ability of this device to allow an accurate performance measurement (4 ± 0,81)
- A great degree of realism in the management of the optic in the virtual scenario (3,9 ± 0,87)
- An excellent realism of targets (4,1 ± 0,56)
- An excellent degree of realism of the positioning of the instruments (3,9 ± 0,56)
- An high quality of the images (4 ± 0,81)
- A great Haptic feedback (sensation) (3,3 ± 0,67)

The Table 2 show the results of the Face Validity.

Characteristics	Experts (n=12)
Realism	3,6 ± 0,84
Degree of realism of the positioning of the instruments	3,9 ± 0,56
quality of the images	4 ± 0,81
Realism of targets	4,1 ± 0,56
Degree of "realism" movement	3,4 ± 0,96
Haptic feedback (sensation)	3,3 ± 0,67
Degree of realism in the management of the optic	3,9 ± 0,87
Degree of utility of the haptic feedback	3,5 ± 0,70
Degree of usefulness of the simulator about acquisition of "basic" skill (hand-eye coordination)	4,4 ± 0,69
Degree of usefulness of the simulation about acquisition of skills with non-dominant hand	3,9 ± 0,63
Degree of overall usefulness of the simulator about acquisition of basic laparoscopic	3,8 ± 1,03

techniques	
Confidence in the ability of this device to allow an accurate performance measurement	4 ± 0,81

Table 2 Face Validity Questionnaire results
Construct validity

The following table summarize the results of the comparison between the novices group and expert surgeons group.

Task	Metrics	Novice (n=12)	Expert (n=12)	P Value
Navigation Task 1 (First time)	Fulfillment (%)	91.66 ± 28.86	100.00 ± 0.00	0.374
	Total time (s)	53.00 ± 0.00	50.16 ± 10.46	0.171
	Score	11.48 ± 1.12	11.56 ± 1.23	0.488
	penality	1.09 ± 0.69	0.41 ± 0.79	0.472
Navigation Task 1 (Second time)	Fulfillment (%)	100.00 ± 0.00	100.00 ± 0.00	0.086
	Total time (s)	30.08 ± 4.64	31.00 ± 7.21	0.440
	Score	11.00 ± 0.00	10.62 ± 1.06	0.337
	penality	0.00 ± 0.00	0.25 ± 0.70	0.337
Navigation Task 2 (First time)	Fulfillment (%)	50 ± 52.22	66.66 ± 49.23	0.254
	Total time (s)	80.91 ± 14.93	69.41 ± 20.37	0.066
	Score	6.83 ± 3.32	7.00 ± 2.86	0.254
	penality	0.00 ± 0.00	1.12 ± 0.64	**0.004***
Navigation Task 2 (Second time)	Fulfillment (%)	91.66 ± 28.86	100.00 ± 0.00	0.156
	Total time (s)	50.41 ± 24.15	61.62 ± 14.37	0.149
	Score	9.25 ± 1.71	9.50 ± 0.53	0.337
	penality	0.3 ± 0.48	0.50 ± 0.53	0.251
Coordination Task 3 (First time)	Fulfillment (%)	100.00 ± 0.00	91.66 ± 28.86	0.374
	Total time (s)	29 ± 14.36	18.72 ± 15.12	**0.014***
	Score	8.83 ± 2.24	9.90 ± 1.37	0.077
	penality	0.00 ± 0.00	0.00 ± 0.00	NC
Coordination Task 3 (Second Time)	Fulfillment (%)	100.00 ± 0.00	100.00 ± 0.00	0.086
	Total time (s)	16.25 ± 6.99	10.25 ± 4.36	**0.026***
	Score	8.66 ± 2.42	10.62 ± 1.06	**0.006***
	penality	0.00 ± 0.00	0.00 ± 0.00	NC
Coordination Task 4 (First time)	Fulfillment (%)	0.00 ± 0.00	0.00 ± 0.00	0.488
	Total time (s)	67.66 ± 12.29	51.75 ± 11.24	**0.003***
	Score	6 ± 1.32	7.16 ± 1.64	0.051
	penality	4 ± 1.32	2.83 ± 1.64	0.051
Coordination Task 4 (Second time)	Fulfillment (%)	0.00 ± 0.00	90.90 ± 30.15	0.254
	Total time (s)	59.66 ± 13.04	40.50 ± 10.63	**0.003***
	Score	6.3 ± 1.88	8.12 ± 1.55	**0.030***
	penality	3.7 ± 1.88	1.87 ± 1.55	**0.030***

Table 3 Results of Construct validity

There were significant differences between the experienced group (Expert) and non-experienced group (Novice) in several tasks.
At least one of the metrics of each task presents significant differences.
It is only task 4 (coordination) the one that differentiates between experts and novices in all the evaluated parameters.
There were significant differences between the experienced group and non-experienced group in the task 3, in terms of "total time" and "score"; this task shows a better executions accomplished by experts than the ones accomplished by novices.
The task 2, about navigation, show a better percentage of fulfilment in favour of expert group (100% fulfillment).
Total time, shows significant diffrences in task 4,3,2.
There weren't significant differences between the experienced group and non-experienced group in the task 1.
As previously described in the methodology, metrics that are evaluated in all tasks are total time, fulfillment, score and penality

3.2 Discussion

Laparoscopic surgery simulators are important in the training process of surgeons in laparoscopic surgery.
A validation of simulators is always necessary in order to determine their capacity for surgeons training although as far as we know, there is not any mandatory validation strategy (6).
The Face validity and the Construct validity are two important steps of this process.
The Construct validity determines the capacity of the simulator to punctuate the execution according to the level of experience of the subject who is accomplishing the task.
So, a construct validated simulator will be able to distinguish between surgeons with different levels of experience in laparoscopic surgery.
The Face Validity is just based on the opinion and experience of surgeons and cannot be used in every case to define the validity of a new simulator.
As the face validity is very subjective, it is usually used at the first stages of validation. (Gallagher AG et al., 2003)
The aim of this work is to validate "eLaparo4D" simulator
accomplishing a face and construct validity in order to determine whether it is adequate for basic skills training.
Expert group agree with usefulness of the simulator in reference to 'acquisition of skills, "basic" hand-eye coordination and confidence in the ability of this device to allow an accurate performance measurement.
The realism of the targets and the scenario is a great characteristic, like the position of the instruments.
The haptic feedback is considered by expert as acceptable, most important elements in this kind of virtual simulators.
The results of the study show that there are significant differences between the execution of tasks by novices and by experts for the evaluated metrics.
Among all, navigation and coordination tasks show the clearer results.
The task1 about navigation not present any difference between the different levels of experience: this result can be due to the fact that novices have experience virtual games and in video camera use.
In task 3 and 4, the difference between novices and experts is evident; total time, score and penalty are in favour of experts.
Nevertheless, task 4 results analysis shows a percentage of fulfilment equal to 0% in both the groups.

The "total time" are evaluated in all tasks because is an important variable; novices need more time than experts to finish the tasks in all cases and experts fulfil the majority of the tasks and more efficiently than novices.
To evaluate the reliability, we decided to performe the correlation index to the metrics: total time and score.
The results of this test show an high value of correlation for the total time (0.664 – 66%) and a lower value for the score (0.296 – 30%).
From these values, the Split half Methodology was applied, to calculate the coefficient of Reliability; we applied the Spearman-Brown correction and the final result was: 0.79.
The table 4 show the coefficient.

Metric	Coefficient of Reliability
Total time	0.664
Score	0.296

Table 4 Correlation index result

This conclusion leads us to the point that eLaparod4D
could be used in training programs as an assessment tool.
Nevertheless, the limited size of the sample for this study implies that this conclusion should be checked again with a wider number of subjects.
In this sense we suppose to use the results of this work to choose objectives for a second study (Molina CR et al. , 2008)

ACKNOWLEDGMENTS

We would like to thank G. Vercelli, L. Lagomarsino, V. Zappi of Dept. of Informatics, Bioengineering, Robotics and Systems Engineering, E. Bellanti, L.Lagomarsino and S. Marcutti for their precious collaboration.

REFERENCES

1. htpp://www.nodjes.org
2. htpp://unity3d.com
3. htpp://sensable.com
4. htpp://blender.org
5. Max V. Wohlauer, Brian George, Peter F. Lawrence, Carla M. Pugh, Erik G. Van Eaton, Debra DaRosa. 2013. Review of Influential Articles in Surgical Education: 2002–2012. Journal of Graduate Medical Education 5:2, 219-226.
6. Gallagher AG, Ritter Em, Satava RM (2003) Fundamental principles of validation, and realiability: rigorous science for the assessment of surgical education and training. Surg Endosc 17:1525– 1529
7. Molina CR, de Win G, Ritter O, Keckstein J, Miserez M, Campo R (2008) Feasibility and construct validity of a novel laparoscopic skills testing and training model. Gynecol Surg 5(4): 281–290

VERIFICATION CONCEPT FOR AN ELECTRONEUROGRAM-BASED PROSTHESIS CONTROL

Volkhard Klinger

Department of Embedded Systems
FHDW Hannover
30173 Hanover, Germany

volkhard.klinger@fhdw.de

ABSTRACT
The use of nerve signals for a prosthesis control or limb stimulation is one great challenge in medical technology. It requires a recording of the electroneurogram (ENG) data and an identification of the motion-based action potentials of motoric, feedback and sensoric nerves within the corresponding neural bundle. We have realized a prototyping system for the data acquisition of ENG data, including an identification framework, described in (Klinger and Klauke 2013).
In this paper we introduce the verification concept of the identification process using synthetic datasets generated based on robot manipulator and electroneurogram simulator. The objective is to define a method to compare motion based trajectories and their corresponding ENG signals to prepare the future analysation and identification of human ENG data.

Keywords: ENG-based prosthesis control, system identification and verification, simulation framework, agent-based evolutionary computation, robot-manipulators

1. INTRODUCTION

The use of nerve signals to realize an intelligent control of prostheses or handicapped limbs is a key challenge in medical technology. Compared to the information acquisition via electroencephalogram (EEG) or electromyogram (EMG) signals, the use of ENG signals has several advantages (Klinger and Klauke 2013). So, our approach is the direct use of action potentials of peripheral neural bundles via an ENG (Gold, Darrell, Henze, and Koch 2007; Neymotin, Lytton, Olypher, and Fenton 2011). Based on these signals, a prosthesis, for example, an artificial hand or an artificial forearm, can be controlled specifically.
For the measurement of the very small electric signals up to sub-microvolt a technically optimized measuring circuit which permits the admission of electric axon signals in sub-µ area has been realized (Bohlmann, Klauke, and Klinger 2013}. The identification of the action potential movement patterns is based on methods of the machine learning (Bohlmann and Klinger 2010; Bohlmann, Klauke, Klinger, and Szczerbicka 2011). The proof of the identification concept is based on a verification framework described in this paper.

At first we present a short system overview and point out some aspects of the whole framework. Subsequently we give a brief description of the identification method. In subsection 1.3 we introduce the multipolar cuff electrode which provides some key characteristics for the used identification technique.
The main part of this paper is described in section 2. Here we present the verification concept based on a Matlab-based robot manipulator and explain the generation of stimulation patterns for the simulator, which is part of the verification concept. In section 3 we present results for the following aspects:

- Robot manipulator data based on specific sequence of motions
- Transformation into trigger pulses (action potentials) for the NEURON simulator
- NEURON simulation and generation of ENG data in accordance to the used multipolar cuff electrode
- Identification results

1.1. Overall System Architecture

In Figure 1 the overall concept, denoted as Smart Modular Biosignal Acquisition, Identification and Control System (SMoBAICS) in the following text, is shown in a block diagram. Two central components are to be recognized in this top-level: The data acquisition and signal conditioning in the analog front-end as well as the data evaluation and identification (Pattern Recognition, Learning).

In the data acquisition block the action potentials of the nerves are captured by a so called cuff electrode; the type of this electrode type is introduced in the following subsection. Following this the analog signals are being amplified and digitalized. Subsequently a two-stage evaluation and identification step follows. During these steps the ENG data stream has to be correlated to movement trajectories. We are using a multi-agent-based evolutionary algorithm optimized for a three step process (Klinger and Klauke 2013). The subdivision in two phases is necessary to allow a learning phase and an

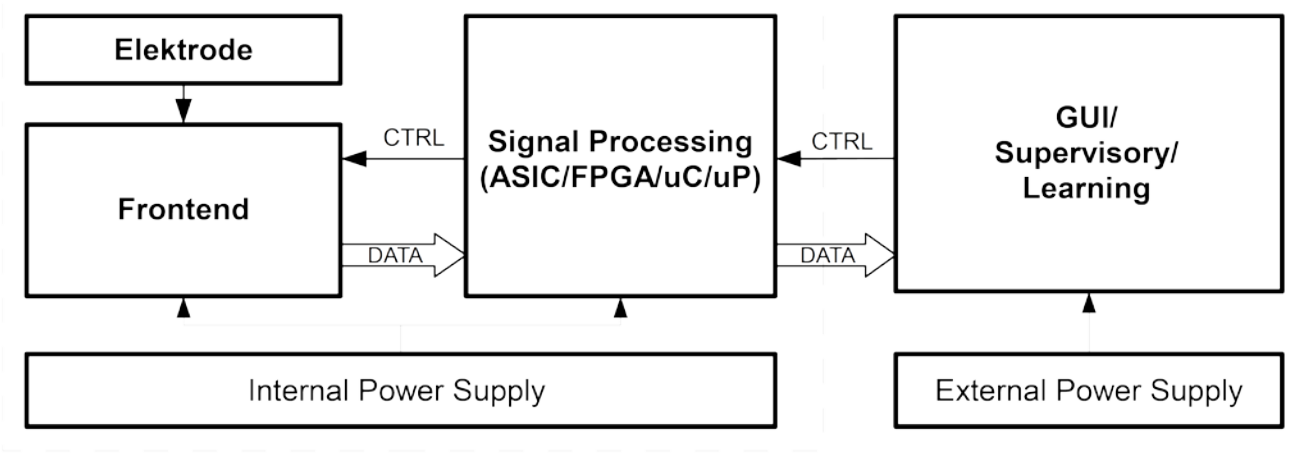

Figure 1. System architecture of SMoBAICS

operation phase. In the learning phase the base identification which allows a correlation between nerve signal and movement is carried out. The operation phase is using the identification results of the learning phase to realize a customization and adjustment due to parameter drift or electrode movement and to control the exoprosthesis. Therefore the base identification from the learning phase is used by a mobile processing device, which supports continuous learning. The objective is to integrate the necessary components for this phase within the organism using a system in package (SIP). New technologies, like energy harvesting, have to be used to operate this body mounted part.

1.2. Identification

The huge number of signal lines within a nerve - the axons - and the combination from actuatory, reactuatory and sensory information lines makes it practically impossible to perform a detailed analysis with the objective of a manual or automatic prosthesis control without using algorithmic tools. Therefore the machine learning and identification part is the most complex and the most important system module (Wodlinger and Durand 2011; Verdult2002). We are using a multi-agent-based evolutionary algorithm optimized for a three step process described in (Klinger and Klauke 2013). This work continues the former work about system identification presented in (Bohlmann, Klauke, Klinger, and Szczbericka 2011; Bohlmann, Klinger, and Szczerbicka 2009; Bohlmann, Klinger, and Szczerbicka 2010). At first a data pre-processing is executed to filter the data and to improve the data condition regarding the signal-noise ratio (SNR). The identification is subdivided into three-levels. In the first-level, the algorithm recognizes patterns of axon related action-potentials. This set of solutions is checked to well-known parameters, like impulse frequency, the relative magnitude of the nerve impulse amplitude and the refractory period. In addition, clusters are build up to model the different groups of activation and their related sensory information (feedback by proprioceptors). So, certain clusters in the neural bundle can be arranged to map muscle groups and their corresponding receptors. In the second level the agent-based set of solutions is combined to global solutions taking the causality between actor and sensory information into account. The third level correlates the first- and second-level solutions with trajectory information from a camera-system or a micro-electro-mechanical system (MEMS) for trajectory information, using inverse kinematics algorithms.

Once the identification procedure based on the recorded action potentials is successful, the recognized pattern can be used to drive a robotic prosthesis. Such devices are typically similar to serial manipulators, which can be modeled and controlled by applying well established methods from the field of robotics (Craig 2004; Sciavicco and Siciliano 2000; Khalil and Dombre 2002). Given the known direct and inverse kinematics of the serial mechanism, the task planning can either be performed in the joint space or in the task space. For the considered case, each motion pattern recognized by the action potential classifier corresponds to a predefined trajectory given in joint coordinates. Using the internal control unit of the prosthesis, the joint angle commands translate to the desired motion of the robotic device.

1.3. The Cuff Electrode

This type of electrode is put around the neural bundle to be examined. The single electrodes, part of the multipolar cuff-electrode, are inserted within biomedical silicone. This silicone protects the single electrodes and fixes them within the specific measurement arrangement. The main advantage of such an electrode is the non-invasive character. Properly designed this electrode can be used without cutting or traumatizing any nerves within a neural bundle. In contrast, using a sieve electrode the probability of an irreparably damage of the nerves is very high.

The cuff-electrode used in this application is a special cuff-electrode depicted in Figure 2. It consists of several electrodes organized in rings and segments. As elementary simulation set-up with minimal configura-

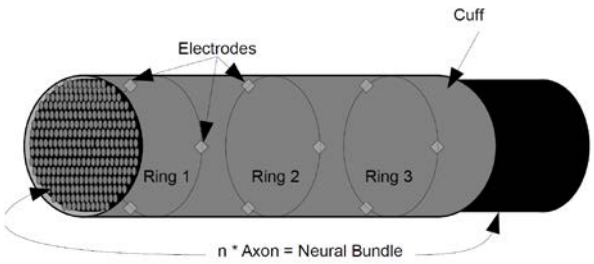

Figure 2. The Cuff Electrode

tion there are three segments (120°) and three rings necessary.

The three electrodes depicted there are evenly distributed on the circumference of the cuff (0°, 120°, 240°) to guarantee an uniform coverage of the action potentials triggered by the neural bundle for example via triangulation. Higher order of rings and segments depends on the space for the implanted cuff-electrode and the best available precision for electrode manufacturing. The number of axons of a neural bundles ranges up to several tens of thousands depending on the type of neural bundle and the selected application localization, like nervus ischiadicus, nervus radialis or nervus medianus.

2. VERIFICATION CONCEPT

To verify the identification process, it is necessary to generate well defined verification vectors. So, these vectors, called SimVectors, are used instead of recorded action potential data to allow specific verification scenarios. In addition, it is possible to reduce the number of animal trials using the verification and simulation framework.

To generate data according to the real existing biology mechanism we are using the well established NEURON framework for empirically-based simulations of neurons and networks of neurons (Carnevale and Hines 2006; Coates, Larson-Prior, Wolpert, and Prior 2003; Law and Kelton 2000) .

The different constraints, like myelin structures, all-or-none, two directions of information flow, frequency borders of the action potentials, etc. has been taken into account. We have configured the simulator and realized a complex neural bundle including our cuff electrode setup to generate verification data for several information transfer scenarios. The action potentials used for the NEURON-simulator are derived by human arm modeling via Matlab Robotics Toolbox (Corke 2011). With this model for verification we are able to concentrate on specific muscle groups and their reactuatory answer and therefore we are able to generate verification patterns.

Our first simple model which will provide proof of verification concept consists of 121 individual axons which run in parallel being arranged in a square grid. The dimensions of this array are depicted in Figure 3. Each axon has a diameter of 10 µm and a total length of 20 mm which is subdivided by 20 equally spaced nodes of Ranvier. Each Ranvier node has a length of 50 µm. These parameter are used with regard to the anatomical data from the selected laboratory animals (here: rats). It is obviously possible to redefine these parameters according other laboratory animals or later on human beings.

The simulation environment uses the Hodgkin-Huxley model to simulate the axon internal membrane, the ion channels and the extra cellular space (Hodgkin and Huxley 1952). So, the propagation of action potentials along the axons is modeled used these equations. Furthermore, the mechanisms concerning the passive membrane channels are included. In this context, each axon is considered myelinated while the Ranvier nodes are characterized by the absence of this surrounding sheath. In order to enable extra cellular recording, a mechanism is implemented that reports the contributions of local membrane currents to the total signal acquired by a recording electrode placed at a defined location with respect to the axon grid. Here, we consider the cuff electrode, introduced in subsection 1.3, which has three electrical contacts equally distributed along the interior wall of the cylindrical cross section. For simulation purposes, we define the radius of the circular contact arrangement according the dimensions of the defined nerve bundle. Furthermore, during simulations, this cuff electrode can be translated along the axon array in order to acquire the extra cellular potential at multiple locations as well as multiple time steps in accordance the multiple rings of the electrode.

Using the NEURON simulator, predefined or randomized excitation patterns can be applied to the modeled axons. An excitation is achieved by injecting a defined current in one end of an axon. The functionality of the simulation framework is further increased by the given ability to specify the number, duration and period length of the injection. By running the simulation, each

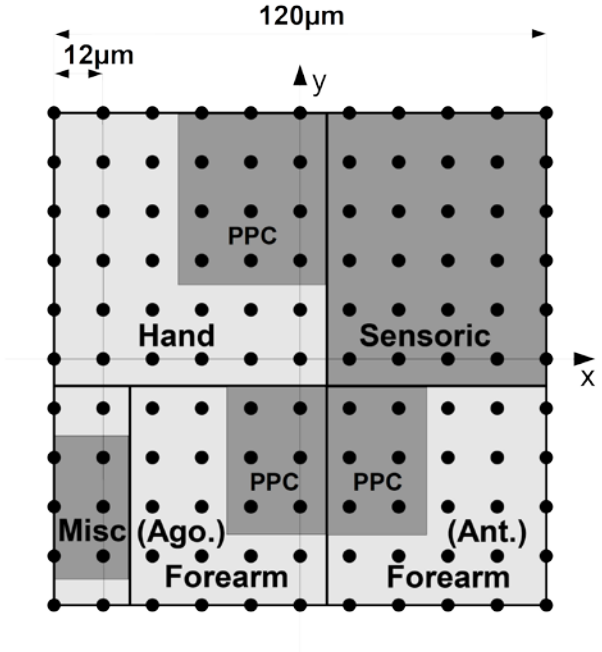

Figure 3. Used model for axon bundle

excitation pattern is translated into potentials acquired by the recording cuff electrode. Hence, identification algorithms processing time series of such potentials can easily be validated due to the fact that the excitation pattern, i.e., the ideal identification result, is known.

As an enhancement of the previously described simulation framework, the simplified model of a human arm was implemented in Matlab using the Robotics Toolbox. Based on this human arm model specific scenarios can be defined to generate sets of SimVectors for the verification process which provide complex interactions of muscle activities (actuatory) and feedback via proprioceptors (reactuatory).

The kinematics of the human arm can be approximated by a serial mechanism consisting of 7 active joints (Grecu, Dumitru, and Grecu 2009). The base coordinate frame is assumed to be located at the shoulder while the coordinate frame associated with the endeffector of the mechanism coincides with human wrist, see Figure 4. Both hand and fingers are omitted here. Following this approach, the simplified kinematics of the human arm can be expressed in terms of the Denavit Hartenberg parameters.

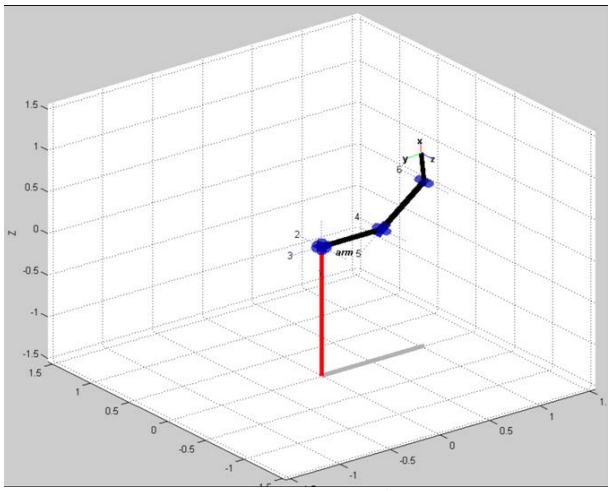

Figure 4. Matlab-based robot manipulator for human arm modeling

3. RESULTS

In order to validate the identification procedure proposed in this paper, we present here one scenario based on the movement of the forearm and the hand where the generation of the StimParameters is focused on the movement of the forearm. The resulting time series of simulated extra cellular recordings are fed to the identification algorithm.

In Figure 5 the joint acceleration, the joint moments, the joint angles and the joint velocity for the selected sequence of motion are shown. The process of movements demanded by the selected scenario and generated by the Matlab Robotics Toolbox is transformed into a sequence of action potentials according to the following criteria:

- Position of the axon according the axon membership to the specific muscle and proprioceptor sensors depicted in Figure 3.
- The frequency of actions potentials is set in accordance to the force vectors and the physiological data like maximum frequency and refractory period.
- The sequence of actuatory and reactuatory (proprioceptors) signals is set with regard to the causal relationship and the signal propagation times.

The sequence of signals is transformed into actions potentials and simulated by the NEURON simulator using the axon bundle configuration and the cuff electrode setup. The data acquired by this simulated cuff electrode is shown in Figure 6. In this Figure the frequency of the action potentials and their signal amplitudes, caused by the superposition of several actions potentials, is shown.

The Figures 7 and 8 show two different details from the overall signal sequence in Figure 6. Figure 7 shows the simulated data for three adjacent rings of the cuff electrode. The three time series are different because of the superposition of actuatory and reactuatory signals during the zoomed time period.

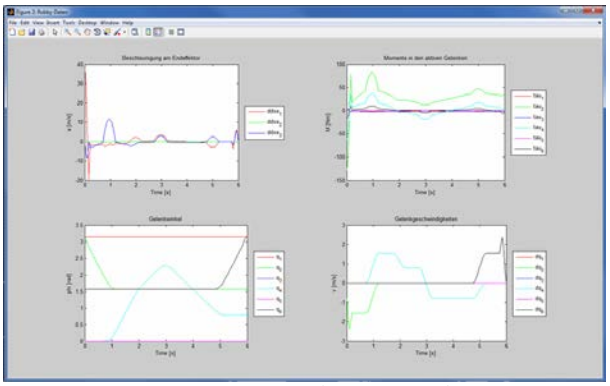

Figure 5. Joint data for sequence of motion

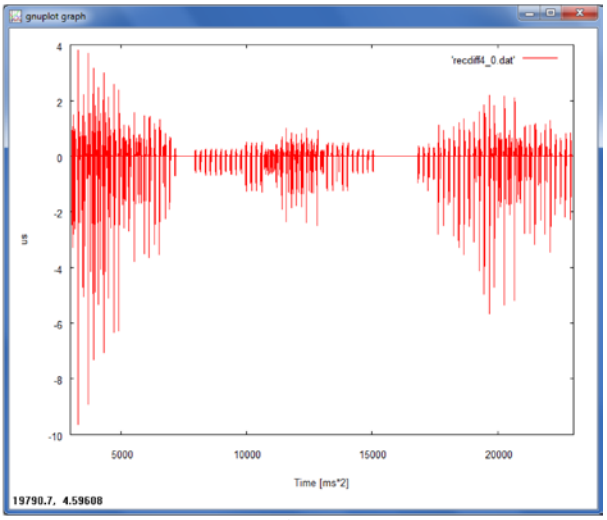

Figure 6. NEURON simulation of the actuatory and reactuatory action potentials of the selected sequence of motion (simulated ENG)

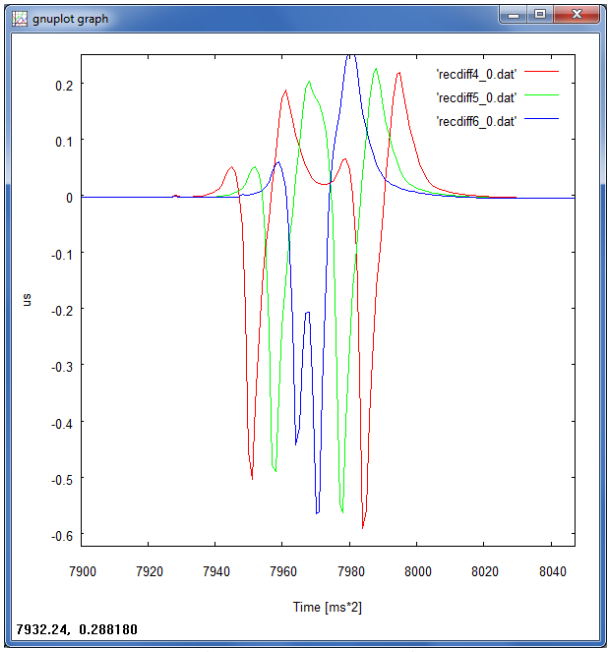

Figure 7. Zoom of Figure 6: Movement of action potentials

In Figure 8 the data acquired by three different segment electrodes of one electrode ring are shown. With regard to the position of the axon within the axon bundle the amplitudes are differing.

The identification method is using only the data acquired by the cuff electrode, no additional information. Here two different aspects of the identification process are shown:

- The detection of the direction to identify actuatory and reactuatory signals, and
- the clustering of action potentials to enable an assignment of the action potentials to specific areas.

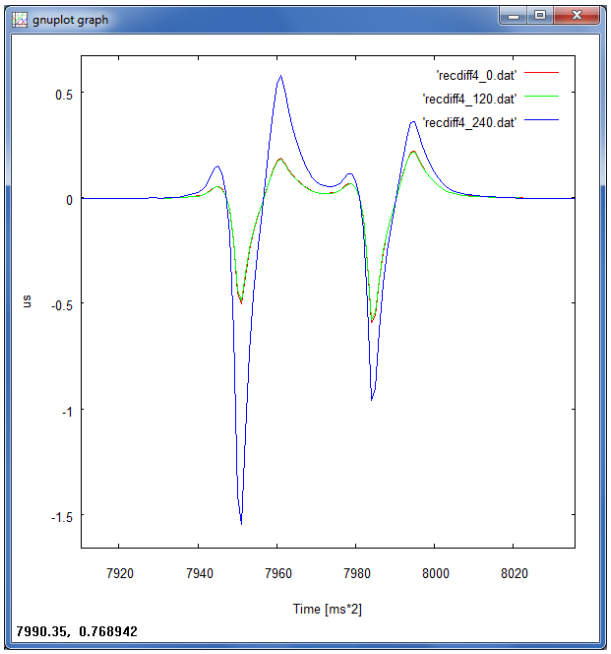

Figure 8. Zoom of Figure 6: Superposition and triangulation

Both aspects are necessary to realize a nerve signal based identification of the type of movement. In Figures 9 and 10 both aspects of the identification are shown, based on the SimVectors generated from the Robotics Toolbox. Figure 9 shows the direction detection, Figure 10 the cluster assignment.

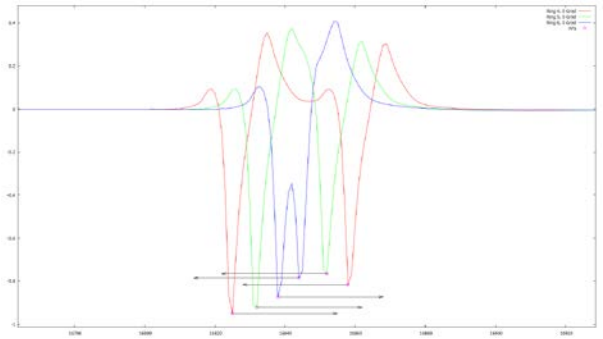

Figure 9. Restructured action potentials using the identification method and detection of actuatory and reactuatory action potentials

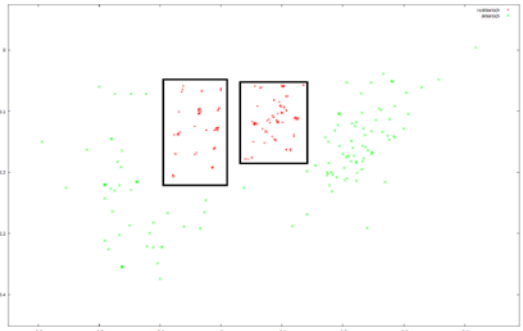

Figure 10. Clustering of the actuatory and reactuatory axons within the axon bundle according to the axon bundle model in Figure 3

4. SUMMARY AND FURTHER WORK

The SMoBAICS approach to identify of motion-based action potentials in neural bundles for exoprosthesis control or for handicapped limb simulation provides an integrated solution from ENG based action potential recording up to the identification procedure.

This paper focuses on the verification method based on generated action potentials used to enable the proof of the identification concept. On the basis of a movement trajectory, actuatory and reactuatory trajectory-based action potentials are simulated with the NEURON simulator according the axon bundle model. This simulation provides an ENG with regard to the special type of cuff electrode to enable a triangulation and direction detection. The identification method based on evolutionary algorithms (Bohlmann, Klinger, and Szczerbicka 2010; Klinger and Klauke 2013) reads these simulated ENG-data and reconstructs the action potentials, their motoric, feedback or sensoric characteristic and the location inside the axon bundle. Based on this identification a correlation between the action potentials and the corresponding movement actions is possible. Due to this solid foundation, the ENG-based motion detection for prosthesis control or

limb stimulation offers considerable potential. The used method based on a on robot manipulator and electroneurogram simulator allows a complex verification process and can be used for a large number of movement scenarios. The most important tasks in the next month will be:

- Adding noise to the SimVectors to analyze the identification process regarding the loss of signal to noise ratio.
- Including sensory feedback from hand's sensory areas in the simulation to take these additional nerve signals into account.
- Starting the clinical tests to achieve measurement results according the real existing biology mechanism.

Based on clinical tests the robustness of the identification method has to be optimized. To start these test the new measurement platform has to be finished. In addition inverse kinematics algorithms have to be integrated into the identification procedure.

ACKNOWLEDGEMENT

All in-vivo experiments are performed in collaboration with the Clinic for Neurosurgery at the Hannover Medical School (MHH).

REFERENCES

Sebastian Bohlmann, Arne Klauke, and Volkhard Klinger. In vivo-Experiment zur System-Validation des modularen Mess-Systems NGEPM-2. Forschungsberichte der FHDW Hannover (ISSN 1863-7043),, 02, 2013.

Sebastian Bohlmann, Arne Klauke, Volkhard Klinger, and Helena Szczerbicka. Model synthesis using a multi-agent learning strategy. In The 23rd European Modeling & Simulation Symposium (Simulation in Industry), Rome, Italy, September 2011.

Sebastian Bohlmann, Volkhard Klinger, and Helena Szczerbicka. HPNS - a Hybrid Process Net Simulation Environment Executing Online Dynamic Models of Industrial Manufacturing Systems. In Proceedings of the 2009 Winter Simulation Conference M. D. Rossetti, R. R. Hill, B. Johansson, A. Dunkin, and R. G. Ingalls, eds., 2009.

Sebastian Bohlmann, Volkhard Klinger, and Helena Szczerbicka. System Identification with Multi-Agent-based Evolutionary Computation Using a Local Optimization Kernel. In The Ninth International Conference on Machine Learning and Applications, pages 840–845, 2010.

Nicholas T. Carnevale and Michael L. Hines. The NEURON Book. Cambridge University Press, New York, NY, USA, 2006.

Jr. Coates, T.D., L.J. Larson-Prior, S. Wolpert, and F. Prior. Classification of simple stimuli based on detected nerve activity. 22(1):64–76, 2003.

Peter Corke. Robotics, Vision and Control – Fundamental Algorithms in MATLAB, volume 73 of Springer Tracts in Advanced Robotics. Springer, 2011.

J.J. Craig. Introduction to Robotics: Mechanics and Control. Prentice Hall, New Jersey, USA, 2004.

Carl Gold, Darrell A. Henze, and Christof Koch. Using extracellular action potential recordings to constrain compartmental models. Journal of Computational Neuroscience, 23(1):39–58, 2007.

V. Grecu, N. Dumitru, and L. Grecu. Analysis of huma arm joints and extension of the study to robot manipulator. In Proceedings of the nternational MultiConference of Engineers and Computer Scientists, Vol 2, March 18 - 20, pages 1348–1351, 2009.

A.L. Hodgkin and A.F. Huxley. A quantitative description of membrane current and its application to conduction and excitation in nerve. Journal of Physiology, 117:500–544, 1952.

W. Khalil and E. Dombre. Modeling, Identification & Control of Robots. Routledge, New York, USA, 2002.

Volkhard Klinger and Arne Klauke. Identification of motionbased action potentials in neural bundles using an algorithm with multiagent technology. In Werner Backfrieder, Marco Frascio, Vera Novak, Agostino Bruzzone, and Francesco Longo, editors, 2nd International Workshop on Innovative Simulation for Health Care (IWISH 2013), 2013.

Averill M. Law and W. David Kelton. Simulation Modeling and Analysis. McGraw-Hill, 2000.

S.A. Neymotin, W.W. Lytton, A.V. Olypher, and A.A. Fenton. Measuring the quality of neuronal identification in ensemble recordings. J Neurosci, 31(45):16398–409, 2011.

L. Sciavicco and B. Siciliano. Modelling and Control of Robot Manipulators. Springer, Berlin, Deutschland, 2000.

Vincent Verdult. Nonlinear System Identification: A State Space Appoche. PhD thesis, University of Twente, Faculty of Applied Physics, Enschede, The Netherlands, 2002.

B. Wodlinger and D. M. Durand. Recovery of neural activity from nerve cuff electrodes. In Annual International Conference of the IEEE Engineering in Medicine and Biology Society, pages 4653–4656, 2011.

AUTHORS BIOGRAPHY

VOLKHARD KLINGER has been a full time professor for embedded systems and computer science at the university of applied sciences FHDW in Hannover and Celle since 2002. After his academic studies at the RWTH Aachen he received his Ph.D. in Electrical Engineering from Technische Universit¨at Hamburg-Harburg. He teaches courses in computer science, embedded systems, electrical engineering and ASIC/system design. His email address is <Volkhard.Klinger@fhdw.de>.

AUTOMATED DOMAIN-SPECIFIC FEATURE SELECTION FOR CLASSIFICATION-BASED SEGMENTATION OF TOMOGRAPHIC MEDICAL IMAGE DATA

Gerald Zwettler[a,b,c], Werner Backfrieder[b]

[a]Bio- and Medical Informatics, Research and Development Department, University of Applied Sciences Upper Austria, Softwarepark 11, 4232 Hagenberg, AUSTRIA
[b]School of Informatics, Communication and Media, University of Applied Sciences Upper Austria, Softwarepark 11, 4232 Hagenberg, AUSTRIA
[c]Research Group Scientific Computing, Faculty of Computer Science, University of Vienna, Währingerstrasse 29/6.21, 1090 Vienna, AUSTRIA

[a]gerald.zwettler@fh-hagenberg.at, [b]werner.backfrieder@fh-hagenberg.at

ABSTRACT
Classification-based segmentation is an approach to establish generic analysis of medical image data. Significant feature sets covering different characteristics of regions to segment allow for robust discrimination of topologically defined classes. In this work a method for automated domain-specific feature selection to achieve a higher level of predictability is presented, incorporating multivariate feature analysis. For calculation of the probability density function, different approaches, like histogram analysis, enumeration of the entire feature space or umbrella Monte Carlo Integration are investigated. Furthermore, meta features calculated on entire classification results rather than on particular regions are introduced. Predictability of both, single local and meta features, is evaluated for different medical datasets as well for simulated intensity volumes, allowing testing and evaluating specific classification problems. The automated feature selection proofs to be accurate for classification-based segmentation utilizing well-known machine learning approaches.

Keywords: classification-based segmentation, multivariate feature analysis, Monte Carlo Integration, automated feature selection

1. INTRODUCTION

Precise segmentation of target anatomical structures from tomographic image datasets is an essential prerequisite for quantitative analysis and computer-assisted diagnostics. If all voxels of an anatomical structure are labelled, measurements on the extent and volume become feasible, for instance facilitating the monitoring of the disease progression. Furthermore, from available segmentations 3D surface models can be derived that can be utilized for surgery planning (Zwettler, Backfrieder, Swoboda, and Pfeifer 2009) or surgical training (Fürst and Schrempf 2012). Thereby the user interaction and subsequent analysis can be performed on the computer model or utilizing a virtual reality environment, enriched by haptic patient models that are derived from the anatomical segmentations and produced via emerging 3D printing devices. Precise segmentations are not only required for computer-based analysis, but also for registering multi-model image data of the same patient to combine high resolution morphological imaging (*CT*, *MRI*) and image data from the functional imaging domain (*PET*, *SPECT*). Only with available segmentation masks, the measured metabolic activity can be limited to organ borders to be quantitatively evaluated with respect to anatomical classifications (Beyer, Schwenzer, Bisdas, Claussen, and Pichler 2010).

In the last decades there has been intensive research work in the field of medical image processing to achieve preferably fully-automated segmentation approaches in specific diagnostic domains. Utilizing deformable models (McInerney and Terzopoulos 1996) and incorporating a priori knowledge on the target anatomical structure, morphologies with low variability in shape can be robustly segmented. Nevertheless, generic application of deformable models for arbitrary segmentation domains is not feasible as proper adjustment of the parameters and the a priori model is required. In contrast, Statistical Shape Models (Cootes, Taylor, Cooper, and Graham 1992) can be trained rather autonomously, if a large set of reference segmentations covering all relevant possible anatomical variations is available. Active appearance models (Cootes, Edwards, and Taylor 1998) introduce additional statistical properties of the targets structure expected intensity profile besides geometric features and Level sets (Osher and Sethian 1988) can handle changes in topology and anatomical variability but complex parameterization needs adjustment to the particular segmentation task. Furthermore, all of these sophisticated models are limited to segmentation of particular anatomical shapes, as border areas and overlapping segments cannot be handled, when segmenting multiple classes from input volume, covering all of the voxels at most.

Segmentation of the entire dataset from arbitrary imaging domains, i.e. assigning a class label to all available voxels, is up to now not feasible by utilizing

fully-automated model-based approaches. However, such entire segmentations can be achieved in a semi-automated way by utilizing conventional segmentation approaches like region growing (Gonzalez and Wintz 1987) or live wire contour detection (Schenk and Prause 2001) with appropriate filtering and morphological post-processing in a rapid prototyping image processing pipeline. A standardized process model for segmentation of arbitrary anatomical structures from variable tomographic image data has been presented in (Zwettler and Backfrieder 2013). While this approach is by far too user-intensive for practical application, the reference segmentations achievable in a semi-automated way are perfectly suited for training a priori models of specific segmentation domains.

A fully automated segmentation of all anatomical structures present from the particular input image modalities is achieved utilizing classification-based approaches, where at first fragmenting the input volume into regions of similar intensities, demarcated by gradients along the borders. For this pre-processing, e.g. watershed transform (Vincent and Soille 1991) applied to gradient magnitude can be utilized. To introduce additional robustness for this pre-segmentation, confidence-connected intensities, neighbourhood characteristics for iterative region merging and morphological post-processing are additionally incorporated (Zwettler and Backfrieder 2012). Given that pre-segmentation of the input image leads to fragmentation into mosaic-like regions with voxels predominantly belonging to one particular class, the actual segmentation can be achieved via multivariate feature classification. Therefore different characteristics of the particular anatomical structures, like intensity statistics, shape, location or co-occurrence metrics (Felipe, Traina and Traina 2003), are applicable. Most of these features are normally distributed, thus allowing classification with Gaussian mixture models, probability density function, Bayes networks or k-Means clustering. Furthermore, powerful classifiers from machine learning domain like neural networks (Vapnik 2000) or support vectors (Boser, Guyon and Vapnik 1992) are applicable. Besides, also heuristic approaches like genetic programming (Koza 1992) or genetic algorithms (Goldberg 1989) can be utilized for feature-based image classification.

In this work, *n=30* local features are evaluated with respect to their predictability, i.e. achievable classification precision for specific objectives, in different medical imaging domains. Thereby, *statistical*, *geometric*, *texture* and *transformation* features are utilized. For many of the proposed classifiers, the number of feature dimensions has to be limited due to numeric computability, over-training and noise sensitivity. Thus, in this work an approach is developed to automatically select the most appropriate feature set for a specific medical segmentation domain, according to single feature predictability considering feature correlation. Thereby, also the classification targets like high voxel match, high region classification confidence or individual class weights can be incorporated. To introduce additional robustness and to allow classification in a broader range of application, additional *m=13* meta features are introduced that are calculated on the class region statistics. These meta features are perfectly suited to be utilized for heuristic classification. For automated features selection, different cumulated predictability metrics, like multivariate PDF or histogram analysis are evaluated.

For testing and validation of the proposed features and proposed domain-specific feature selection, different medical datasets and simulated intensity volumes (Zwettler and Backfrieder 2014) are utilized.

2. MATERIAL

For testing and validation, MRI data from *BrainWeb* database (Cocosco, Kollokian, Kwan and Evans, 1997), anonymized patient studies from various imaging modalities and simulated intensity datasets are utilized as detailed in the following section.

2.1. Data from *BrainWeb*

In total *n=20* MRI datasets, reflecting spoiled FLASH sequences at flip angle *α=30* and an echo time (TE) of *9.2ms* and a repetition time (TR) of *22ms* with associated reference segmentations are utilized. The test sequence datasets denoted as *BRAINWEB_REF* in the following, have *0.5mm* voxel spacing at volume dimensions of *256×256×181* and *unsigned 8bit* scalar range. Reference segmentations fragment the dataset according to a topology of *k=12* classes reflecting anatomical structures to discriminate, namely *background* (0), *cerebrospinal fluid* (1), *grey matter* (2), *white matter* (3), *fat* (4), *muscles* (5), *skin* (6), *skull* (7), *vessels* (8), *around fat* (9), *dura mater* (10) and *bone marrow* (11).

Inter dataset class ratio variability of *BRAINWEB_REF* sequence is charted in Fig. 1, while axial slices #50 and #100 of *BrainWeb* dataset *ds1* are presented in Fig. 2.

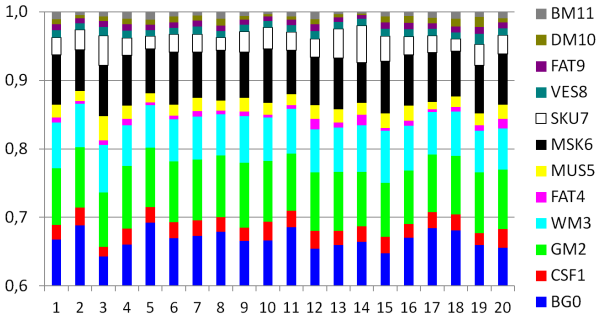

Figure 1: Inter dataset variability of the *n=20* datasets from *BREANWEB_REF*. Voxel ratio of the particular classes C_i significantly varies.

For *BrainWeb* datasets moreover manual reference segmentations are prepared as sequence *BRAINWEB_MAN*, discriminating between *k=6* classes, namely *white matter* (0), *grey matter* (1), *ventricle* (2), *background* (3), *tissue* (4) and *remaining* voxels (5).

Surface renderings for reference segmentations of *ds1* are presented in Fig. 3.

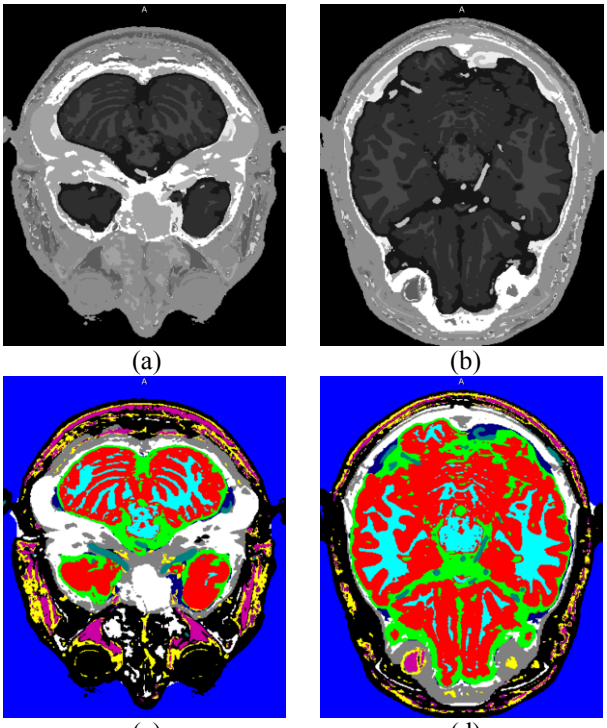

(a) (b) (c) (d)

Figure 2: First *BREANWEB_REF* dataset with input intensities and reference class labels.

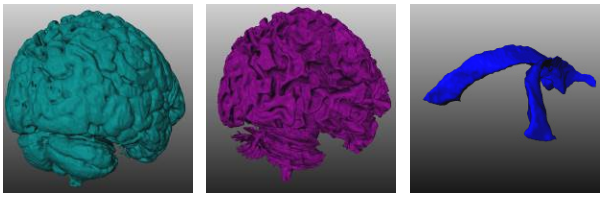

(a) (b) (c)

Figure 3: Surface Renderings on *BRAINWEB_MAN ds1* for grey matter (a), white matter (b) and ventricle (c).

2.2. Anonymized Patient Studies

Preparation of reference segmentation for true patient datasets necessitates the use of standardized image processing chains (Zwettler and Backfrieder 2013).

The sequence *HEART* thereby covers *n=15* datasets acquired with Siemens Somatom Sensation Cardiac 64-row MSCT, showing *512×512* slice dimensionality and *μ=288.5(92-461)* slices with an average spacing of *.359* in x/y direction and *.56* in z-direction. The defined topology discriminates between *k=9* classes, namely *lung* (0), *aorta* (1), *left ventricle* (2), *stents* (3), *right ventricle* (4), *liver* (5), *bones* (6), *tissue* (7) and *remaining* voxels (8).

Furthermore, abdominal CT datasets are utilized to build up sequence *ABDOMEN*, fragmenting input voxels into *k=13* classes, namely *background* (0), *intestinal tract* (1), *lungs* (2), *muscles* (3), *aorta* (4), *kidneys* (5), *stomach* (6), *vessels* (7), *liver* (8), *heart* (9), *bones* (10), *tissue* (11), and *remaining* voxels (12).

An overview of sequence *HEART* is given in Fig. 4 for *ds1* with axial slice #20 in (a) and labelled reference segmentations in (b) with surface renderings of the heart ventricles and aorta in (c). For *ds1* of *ABDOMEN* sequence, axial slice #50 is shown in (d) and reference segmentations in (e) with surface renderings of lungs, aorta and liver in (f).

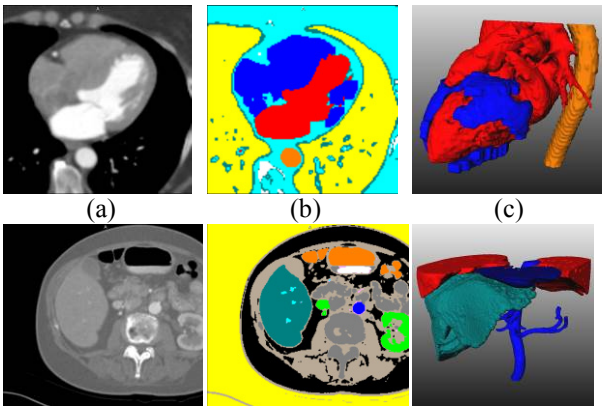

(a) (b) (c) (d) (e) (f)

Figure 4: Overview of *HEART* and *ABDOMEN* data.

2.3. Simulated Intensity Volumes

A newly developed intensity volume simulator (Zwettler and Backfrieder 2014) allows for generation of testing sequences with different shape morphology of the particular classes C_i. Besides, intra region intensity characteristics, inter dataset variability, surface characteristics, region size, voxel ratio and several more attributes can be parameterized for simulation.

Simulated test sequences with *n=15* datasets are generated at mask dimensionality of *128×128×128* and allow for simulation of *tubular*, *BLOB*-like, *plane*-like and *scatter* morphologies. Sequence *SIM_1* thereby features discrimination of *k=5* classes, see Fig. 5.

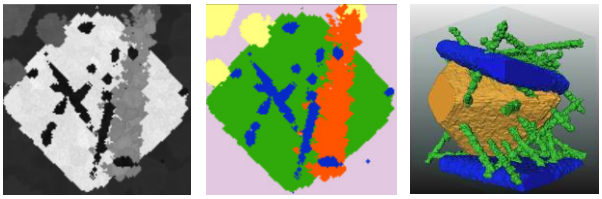

Figure 5: axial slice #50 of *SIM_1 ds1* (a) and associated reference segmentations (b) with surface rendering, showing tubular, plane and BLOB shape.

The testing sequences *SIM_2-SIM_8* only comprise two classes C_2 and C_3 with BLOB morphology showing identical characteristics that are differentiated from background class C_1. For the particular testing sequences, only specific characteristics are varied to allow for classification of classes C_2 and C_3 with respect to specific local and meta features, see Table 1.

3. METHODOLOGY

Whenever analysing statistically varied values of feature F_j calculated from a set of regions $D_i = \{R_1, R_2, \ldots, R_n\}$ assigned to a class C_i, the random feature values

generally can be modelled as normal distribution with $F_{ji} \sim N(\mu_{ji}, \sigma^2_{ji})$. Based on the single feature distributions, predictability at different positions in the multi-dimensional feature space and similarity evaluation with particular classes becomes feasible.

Table 1: Simulation Characteristics for *SIM_2-SIM_8*

ID	*difference of C_2 and C_3*
2	no difference ➔ utilized as ground truth
3	varied position within dataset
4	small differences in intensity profile
5	difference in connectedness, 1 vs. 60 islands
6	difference in mean region size
7	difference in class voxel ratio
8	intra region scalar correlation varied

3.1. Local and Meta Features

The *n=30* local features $\mathbf{F}_j$ considered in this work are calculated on particular regions R_i leading to static results, while the *m=13* introduced meta features $\hat{\mathbf{F}}$ are calculated on the classified region set D_i of a particular class C_i, allowing to incorporate single region classification results.

The total *43* considered features are grouped into four categories, namely *texture* features (Table 3), *statistical* features (Table 2), *geometric* features (Table 4) and *transformation* features (Table 5), covering different aspects on how to robustly discriminate the particular classes C_i.

With the *texture* features, as presented in Table 3, key intensity profile characteristics like mean region intensity, energy or entropy are incorporated.

The *statistical* features in Table 2 are mainly meta features, which evaluate statistics on region size calculated over all regions assigned to a particular class. Besides, class size and voxel ratio are calculated.

The *18 geometric* features enlisted in Table 4 refer to positional aspects of the particular regions, like mean position in x-, y-, and z-direction as well as mean city block distance from the image centre. Besides, surface-to-volume ratio and sphericity are calculated to address compactness.

Finally, for calculation of the *5 transformation* features from Table 5, co-occurrence matrix is derived from input image to calculate variance, entropy, energy and homogeneity. With these features, intensity profile characteristics can be well described.

Table 2: *statistical* features (9)

ID	definition	description
F_{12}	$F_{12}(\mathcal{R}) = \lvert\mathcal{R}\rvert$	region size
$\hat{F}_{13}$	$\hat{F}_{13}(\mathfrak{R}_{X_o}) = \min\ F_{12}(\mathfrak{R}_{X_o})$	min region size for class $\mathcal{X}_o$
$\hat{F}_{14}$	$\hat{F}_{14}(\mathfrak{R}_{X_o}) = \max\ F_{12}(\mathfrak{R}_{X_o})$	max region size for class $\mathcal{X}_o$
$\hat{F}_{15}$	$\hat{F}_{15}(\mathfrak{R}_{X_o}) = mean\ F_{12}(\mathfrak{R}_{X_o})$	mean region size for class $\mathcal{X}_o$
$\hat{F}_{16}$	$\hat{F}_{16}(\mathfrak{R}_{X_o}) = quantile(0.5, F_{12}(\mathfrak{R}_{X_o}))$	median region size for $\mathcal{X}_o$
$\hat{F}_{17}$	$\hat{F}_{17}(\mathfrak{R}_{X_o}) = quantile(0.25, F_{12}(\mathfrak{R}_{X_o}))$	quantile 25 region size for $\mathcal{X}_o$
$\hat{F}_{18}$	$\hat{F}_{18}(\mathfrak{R}_{X_o}) = quantile(0.75, F_{12}(\mathfrak{R}_{X_o}))$	quantile 75 region size for $\mathcal{X}_o$
$\hat{F}_{19}$	$\hat{F}_{19}(\mathfrak{R}_{X_o}) = std\ F_{12}(\mathfrak{R}_{X_o})$	σ in region size for $\mathcal{X}_o$
$\hat{F}_{20}$	$\hat{F}_{20}(\mathfrak{R}_{X_o}) = \frac{1}{\lvert I\rvert} \cdot \sum_{i=1}^{\lvert\mathfrak{R}_{X_o}\rvert} \lvert\mathcal{R}_i\rvert$	component size ratio of $\mathcal{X}_o$

Table 3: *texture* features (11)

ID	definition	description
F_1	$F_1(\mathcal{R}) = mean\ I(\mathcal{R})$	mean region intensity value
F_2	$F_2(\mathcal{R}) = \min I(\mathcal{R})$	minimum intensity in $\mathcal{R}$
F_3	$F_3(\mathcal{R}) = \max I(\mathcal{R})$	maximum intensity in $\mathcal{R}$
F_4	$F_4(\mathcal{R}) = std\ I(\mathcal{R})$	standard deviation of intensity values in region $\mathcal{R}$
F_5	$F_5(\mathcal{R}) = quantile(0.5, I(\mathcal{R}))$	median intensity value in region $\mathcal{R}$
F_6	$F_6(\mathcal{R}) = quantile(0.25, I(\mathcal{R}))$	quantile 25 intensity value in region $\mathcal{R}$
F_7	$F_7(\mathcal{R}) = quantile(0.75, I(\mathcal{R}))$	quantile 75 intensity value in region $\mathcal{R}$
F_8	$F_8(\mathcal{R}) = \sum_{i=s_{min}}^{s_{max}} p_i \cdot \log p_i$	entropy of intensities
F_9	$F_9(\mathcal{R}) = \sum_{i=s_{min}}^{s_{max}} p_i^2$	energy of intensities
F_{10}	$F_{10}(\mathcal{R}) = \max_{i=s_{min}}^{s_{max}} p_i$	maximum probability of intensities
F_{11}	$F_{11}(\mathcal{R}) = \frac{1}{s_{max}-s_{min}} \cdot \sum_{i=s_{min}}^{s_{max}} p_i$	mean probability of intensities

Table 4: *geometric* features (18)

ID	definition	description
F_{21}	$F_{21}(\mathcal{R}) = \frac{surf(\mathcal{R})}{\lvert\mathcal{R}\rvert}$	surface to volume ratio
F_{22}	$F_{22}(\mathcal{R}) = \psi(\mathcal{R})$	sphericity
F_{23}-F_{25}	$F_{23}(\mathcal{R}) = C_{oM}(\mathcal{R})_x$	region center of mass for x-coordinate (F_{23}), y-coordinate (F_{24}) and z-coordinate (F_{25})
F_{26}	$F_{26}(\mathcal{R}) = distCB(C_{oM}(\mathcal{R}), C_{oM}(\mathfrak{R}_{X_o}))$	city block distance of region center-of-mass to expected position
F_{27}-F_{29}	$F_{27}(\mathcal{R}) = \frac{1}{\lvert\mathcal{R}\rvert} \sum_{i=1}^{\lvert\mathcal{R}\rvert} \lvert c_{i_x} - C_{oM}(\mathcal{R})_x\rvert$	mean city-block distance from center-of-mass in x direction (F_{27}), y direction (F_{28}) and z direction (F_{29})
F_{30}	$F_{30}(\mathcal{R}) = \frac{1}{\lvert\mathcal{R}\rvert} \sum_{i=1}^{\lvert\mathcal{R}\rvert} distCB(c_i, C_{oM}(\mathcal{R}))$	mean city block distance to center-of-mass
F_{31}-F_{33}	$F_{31}(\mathcal{R}) = \frac{1}{\lvert\mathcal{R}\rvert} \sum_{i=1}^{\lvert\mathcal{R}\rvert} \lvert c_{i_x} - C_{oM}(I)_x\rvert$	mean city-block distance from image I center-of-mass in x direction (F_{31}), y direction (F_{32}) and z direction (F_{33}).
F_{34}	$F_{34}(\mathcal{R}) = \frac{1}{\lvert\mathcal{R}\rvert} \sum_{i=1}^{\lvert\mathcal{R}\rvert} distCB(c_i, C_{oM}(I))$	mean city block distance to image I center-of-mass
$\hat{F}_{35}$	$\hat{F}_{35}(\mathfrak{R}_{X_o}) = numOfIslands(\mathfrak{R}_{X_o}, \mathcal{N}_{18})$	expected number of autonomous islands
$\hat{F}_{36}$-$\hat{F}_{39}$	$\hat{F}_{36}(\mathfrak{R}_{X_o}) = C_{oM}(\mathfrak{R}_{X_o})_x$	center-of-mass calculated for all regions of class $\mathcal{X}_o$ in x direction ($\hat{F}_{36}$), y direction ($\hat{F}_{37}$) and z direction ($\hat{F}_{38}$)

Table 5: *transformation* features (5)

ID	definition	description
F_{39}	$F_{39}(\mathcal{C}_\mathcal{R}) = \sum_{i=s_{min}}^{s_{max}} \sum_{j=s_{min}}^{s_{max}} (i-j)^2 \cdot p(i,j)$	variance of region
F_{40}	$F_{40}(\mathcal{C}_\mathcal{R}) = \sum_{i=s_{min}}^{s_{max}} \sum_{j=s_{min}}^{s_{max}} p(i,j) \cdot \log p(i,j)$	entropy of region
F_{41}	$F_{41}(\mathcal{C}_\mathcal{R}) = \sum_{i=s_{min}}^{s_{max}} \sum_{j=s_{min}}^{s_{max}} p(i,j)^2$	energy of region
F_{42}	$F_{42}(\mathcal{C}_\mathcal{R}) = \sum_{i=s_{min}}^{s_{max}} \sum_{j=s_{min}}^{s_{max}} \frac{p(i,j)}{1+\lvert i-j\rvert}$	homogeneity of region
F_{43}	$F_{43}(\mathcal{C}_\mathcal{R}) = \max\ p(i,j)$	maximum value as max co-occurrance

3.2. Single Feature Predictability

Features $\mathbf{F}_j$ showing a high level of predictability are considered to be best suited to discriminate the considered classes C_i. As the normal distributions of the particular classes are expected to at least partially overlap, classification generally cannot be performed

without bearing some level of uncertainty, see Fig. 6 for illustration of one-dimensional feature set with distributions for classes $C_1 - C_3$ partially overlapping.

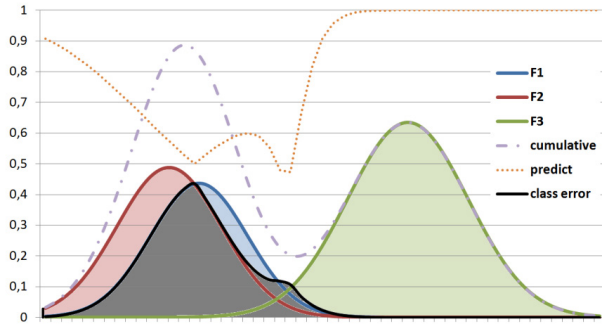

Figure 6: Bayes error in feature classification. The overlapping area marked in black of the class feature distributions F_1, F_2 and F_3 derived from classes C_1, C_2 and C_3 for feature $\mathbf{F}_j$ is classified at low confidence with $pred_j$=.771 as F_1 and F_2 are largely overlapping.

The local probability density function (*pdf*) of the particular class feature value distributions is thereby defined for a particular class X_o as

$$pdf(x, \mathcal{X}_o, \mathcal{F}_{l_o}) = \frac{1}{\sqrt{2\pi\sigma_{l_o}^2}} \exp\left(-\frac{(x-\mu_{l_o})^2}{2\sigma_{l_o}^2}\right) \quad (1)$$

where the pdf is weighted according to region occurrence ratio, voxel class ratio or utilizing specific weight for the particular classes in the sense of Bayesian inference as delineated in Equ. 2. This way, the particular key classification objective is defined and differences in region or voxel occurrence probability of the particular classes can be modelled.

$$P(\mathcal{X}_o|x) = pdf(f, \mathcal{X}_o, \mathcal{F}_{l_o}) \cdot P(\mathcal{X}_o) \quad (2)$$

Predictability (*pred*) is evaluated at each discrete position of the feature space with

$$pred(y, \mathcal{F}_{l_o}) = \frac{\max\limits_{\mathcal{X}_i \in \mathfrak{X}} pdf(y, \mathcal{X}_i, \mathcal{F}_{l_o}) \cdot P(\mathcal{X}_i)}{\sum\limits_{\mathcal{X}_i \in \mathfrak{X}} pdf(y, \mathcal{X}_i, \mathcal{F}_{l_o}) \cdot P(\mathcal{X}_i)} \quad (3)$$

so that overall predictability of a particular feature with respect to all considered classes X_i can be formulated as

$$pred(\mathcal{F}_l) = \frac{\int_{y=-\infty}^{\infty} \max\limits_{\mathcal{X}_i \in \mathfrak{X}} pdf(y, \mathcal{X}_i) \cdot P(\mathcal{X}_i)}{\int_{y=-\infty}^{\infty} \sum\limits_{\mathcal{X}_i \in \mathfrak{X}} pdf(y, \mathcal{X}_i) \cdot P(\mathcal{X}_i)}. \quad (4)$$

3.3. Multivariate Class Similarity

For common classification tasks the sole utilization of single features generally is considered to be insufficient. Instead, several features are utilized to derive the best matching class label of a region R_i from the particular feature vector. With every additionally incorporated feature, the dimensionality of the feature space is increased by one, thereby increasing the overall achievable predictability, see Fig. 7 for two-dimensional feature space with distributions for classes $C_1 - C_3$ less overlapping compared to each single feature dimension.

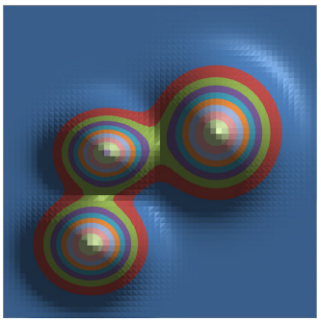

Figure 7: With additional feature dimension $\mathbf{F}_k$ showing $pred_k$=.743 to be combined with $\mathbf{F}_j$ from Fig. 6, overall predictability is increased to $pred_{jk}$=.9707.

For calculation of cumulated predictability from single feature dimensions, correlation has to be considered. With higher feature correlation τ_{ij}, of the involved features $\mathbf{F}_j$ and $\mathbf{F}_k$, the increase in overall predictability due to the extended feature space drops.

Calculation of multi-dimensional probability density function pdf_{gmm} is achieved with

$$pdf_{gmm}(X, \mathcal{X}_o, \mathfrak{F}_o) = \frac{1}{(2\pi)^{d/2} \cdot \sqrt{|\Sigma|}} \cdot exp\left(-\frac{1}{2}(X - \mu_{\mathfrak{F}_o})' \mathbf{\Sigma^{-1}} (X - \mu_{\mathfrak{F}_o})\right) \quad (5)$$

for input vector $X = \{x_1, \ldots, x_d\} \in \mathbb{R}^d$ with covariance matrix $\Sigma \in \mathbb{R}^{d \times d}$ calculated for pairwise covariances as

$$COV(X_k, X_l) = \frac{1}{n-1} \cdot \sum_{i=1}^{n} (x_{k_i} - \bar{X}_k) \cdot (x_{l_i} - \bar{X}_l) \quad (6)$$

3.4. Automated Domain-Specific Feature Selection

With the formulations defined in section 3.3, predictability of a certain feature set can be calculated for particular segmentation domains by statistically evaluating a set of reference regions $D_i = \{R_1, R_2, \ldots, R_n\}$ preserved for each class C_i to be discriminate. Nevertheless, with increasing dimensionality of the feature space, the proper calculation strategy for integration over the feature space from local evaluation of the pdf_{gmm} has to be analysed in depth. Therefore, the following calculation strategies are applicable, namely:

- Partial integration by evaluating pdf_{gmm} at discrete and equally distributed positions per feature dimension is only applicable for a very small feature vector size, as the total number of required evaluation positions exponentially grows with respect to increased feature space dimensionality. A reduction of sampling positions per dimension would allow for handling higher-dimensional feature spaces but entail a drop in result quality as the sampling frequency becomes deficient.
- *Monte Carlo integration* (*MCI*) (Metropolis 1987) allows for sampling of the feature space at a predefined number of random positions. This way,

also higher dimensions can be handled. Nevertheless, insufficient sampling frequency as mentioned for the partial integration approach, remains unaddressed. With decreasing sampling density, the risk for leaving significant parts of the feature space unconsidered during MCI increases. Imprecision introduced by MCI is especially high when single class distribution show small variability and thus might not be hit by any of the sampling positions at all or if the feature space is generally sparsely populated.

- The *umbrella* variation of *Monte Carlo* integration addresses the problem of feature space sparseness by sampling only at positions derived from the particular class feature value deviations, incorporating Bayes inference with respect to region or voxel class probabilities.
- Similar results can be achieved, when evaluating the pdf_{gmm} exclusively at positions of the multi-dimensional feature space that are derived from the incorporated set of reference regions. Nevertheless, applicability of this approach highly depends on a sufficient number of reference segmentation datasets. Furthermore, inaccuracies are introduced from feature distributions that do not perfectly approach Gaussian shape, as the pdf_{gmm} sampling is performed according to true region feature data.
- Finally, a *histogram* approach can be utilized, evaluating a multi-dimensional histogram for all classes C_i. This way, the true feature value distribution of the particular classes is approximated best. Thus, higher accuracy for the evaluated predictability values is to be expected for those features, e.g. for geometric properties, that do not perfectly approach Gaussian shape. To overcome the problem of features space sparseness, filtering is applied with respect to the particular bin count per dimension, which is downscaled with higher dimensionality, see Table 6.

Table 6: Histogram calculation parameters with respect to dimensionality $\mathcal{D}$

	smoothing filter	histogram bins	
$\mathcal{D}$	kernel size k	bin size s	total $s^{\mathcal{D}}$
1	10	200	200
2	8	100	10,000
3	5	50	125,000
4	3	20	160,000
5	2	10	100,000
6	1	8	262,144
7	0	6	279,936
8	0	5	390,625
9	0	4	262,144
10	0	3	59,049

Despite the different enlisted calculation strategies applicative to multi-feature predictability estimation, the algorithm for automated domain-specific feature selection remains the same. For automated selection of a feature set $\mathcal{F}_{local}$ and a feature set $\mathcal{F}_{meta}$ for a particular classification domain, defined by class-labelled regions R_i derived from the preserved set of reference segmentations, at first the feature with highest *pdf* is selected. In the following, the feature vector is iteratively extended until the target number of dimensions is approached, by selecting the feature $\mathbf{F}_j$ that maximizes the pdf_{gmm} achievable by the particular feature vector length, at each iteration.

Although in theory the overall achievable predictability pdf_{gmm} is expected to monotonically increase with every additional feature dimension $\mathbf{F}_j$, depending on the calculation strategy also decreasing overall predictability values might be noticed. This effect results from the smaller histogram bin size at higher dimensionality, which subsequently leads to a collapse of neighbouring bins and thus a pretended reduction in predictability. The same holds for *MCI* approaches, where the sampling frequency drops at increased dimensionality. Thus, any possible drop in overall predictability pdf_{gmm} thereby only results from the numerical calculation strategy, not due to effectively reduced classification capability. Nevertheless, for the actual classification problem, the chosen iterative feature selection approach allows for best feature selection with an ever increased predictability from each single feature added to the feature space.

4. IMPLEMENTATION

The algorithms developed for this work in the field of feature analysis and feature selection are implemented in *C++*. For *I/O* operations and random number generation, *boost* library (Boost 2014) is utilized as external library. Although, the core boost concepts are meanwhile added to *C++11* standard, the utilization of boost programming paradigms started with the development of the *MIPP* framework (Swoboda et al. 2008) back in 2007 was perpetuated for reasons of consistency. Besides, no further external code was utilized.

4.1. Image Volume Data Layout

The data layout for image volumes is a crucial aspect with respect to genericity and performance. For this work, 2D images and 3D volumes are represented as real 2D and 3D matrices of scalar values respectively.

Commonly, image processing frameworks like ITK (Kitware 2014) feature a one-dimensional data layout for images of arbitrary dimensionality, ensuring a maximum level of genericity. Nevertheless, with required index conversions from 1D to n-D at each pixel access, this design would not feature the excessive use of mask operations as required for gradient calculation, common filtering and morphological opening/closing operations.

Thus, 2D and 3D matrices of scalar values are preferably utilized, allowing direct access to the particular pixel/voxel positions via index tuples. The chosen approach does not show significant disadvantages with respect to memory management

(paging, memory allocation,...), and thus perfectly meets the procedural algorithmic requirements.

4.2. Histogram Data Layout

For histogram analysis in the context of multivariate feature analysis, also volume data of higher (at least 4D and 5D) has to be considered. Consequently, for this particular domain a higher level of genericity is required. Thus, only for histograms and the required associated operations, like filtering, a 1D layout for the voxel data with index conversions for access is applied.

5. RESULTS

In the following, first single feature predictability is analysed prior to addressing multidimensional feature spaces and automated domain-specific feature selection.

5.1. Results on Single Feature Predictability

At first, single feature predictability is evaluated for the $n=30$ local and $m=13$ meta features evaluated on $k=12$ classes of *BRAINWEB_REF* dataset series, with predictability results for the considered local features $\mathbf{F}_j$ charted in Fig. 8 and the meta features $\hat{\mathbf{F}}$ presented in Fig. 9. The predictability is thereby calculated with partial integration (P_{stat}), from reference region feature vectors (P_{reg}), utilizing MCI (P_{mc}), based on reference region histogram (P_{hist}) and based on umbrella MCI (P_{mcu}), with *pdf* weighting chosen to maximize the number of correct classified regions in contrast to a maximized number of correctly classified voxel. Despite the chosen predictability calculation strategy, the particular local features show a similar trend.

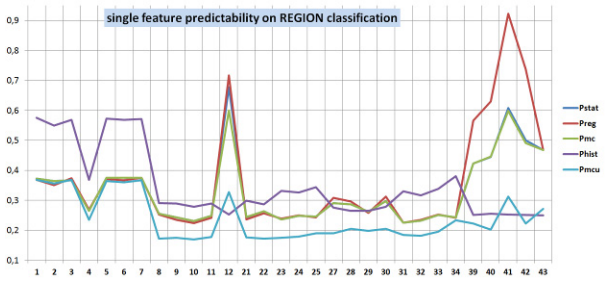

Figure 8: Predictability of local features $\mathbf{F}_k$ calculated for $n=20$ *BRAINWEB_REF* datasets.

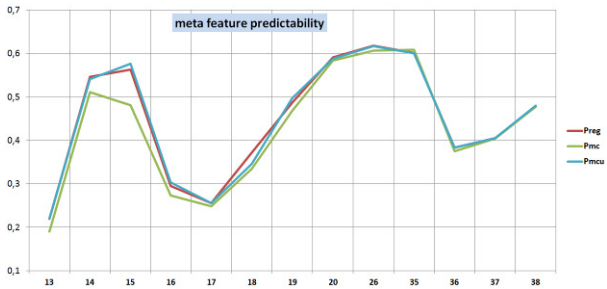

Figure 9: Predictability of meta features $\hat{\mathbf{F}}$ calculated for $n=20$ *BRAINWEB_REF* datasets.

Besides single feature predictability, also feature correlation is relevant for later to follow multivariate feature analysis. Correlation matrix calculated for the first $k=15$ local features is presented in Fig. 10. As expected, the region intensity features ($\mathbf{F}_1$-$\mathbf{F}_7$) show a high level of correlation. The same holds for texture metrics directly calculated on image intensity profile ($\mathbf{F}_8$-$\mathbf{F}_{11}$). Nevertheless, with the different feature groups considered, enough feature independence is available for multi-dimensional feature analysis at high level of achievable predictability.

	1	2	3	4	5	6	7	8	9	10	11	12	21	22	23	24	25	27	28	29
1		0,98	0,98	0,33	1,00	1,00	1,00	0,14	0,16	0,06	0,20	0,03	0,16	0,18	0,02	0,08	0,03	0,03	0,06	0,12
2	0,98		0,95	0,20	0,98	0,99	0,97	0,24	0,25	0,15	0,28	0,03	0,23	0,26	0,02	0,08	0,01	0,07	0,09	0,17
3	0,98	0,95		0,46	0,98	0,97	0,99	0,05	0,08	0,01	0,12	0,01	0,10	0,11	0,02	0,08	0,06	0,02	0,01	0,07
4	0,33	0,20	0,46		0,31	0,25	0,38	0,22	0,21	0,28	0,16	0,03	0,02	0,08	0,01	0,02	0,15	0,01	0,02	0,01
5	1,00	0,98	0,98	0,31		0,99	0,99	0,13	0,15	0,06	0,19	0,03	0,15	0,17	0,02	0,08	0,03	0,03	0,05	0,12
6	1,00	0,99	0,97	0,25	0,99		0,99	0,15	0,17	0,08	0,20	0,03	0,16	0,18	0,02	0,08	0,02	0,03	0,05	0,12
7	1,00	0,97	0,99	0,38	0,99	0,99		0,11	0,13	0,03	0,17	0,03	0,15	0,16	0,02	0,08	0,04	0,03	0,05	0,11
8	0,14	0,24	0,05	0,22	0,13	0,15	0,11		0,94	0,81	0,95	0,01	0,72	0,85	0,01	0,01	0,01	0,23	0,23	0,35
9	0,16	0,25	0,08	0,21	0,15	0,17	0,13	0,94		0,90	0,98	0,02	0,64	0,75	0,00	0,01	0,01	0,16	0,17	0,27
10	0,06	0,15	0,01	0,28	0,06	0,08	0,03	0,81	0,90		0,81	0,02	0,50	0,59	0,00	0,01	0,01	0,13	0,14	0,22
11	0,20	0,28	0,12	0,16	0,19	0,20	0,17	0,95	0,98	0,81		0,03	0,70	0,79	0,00	0,01	0,03	0,21	0,23	0,32
12	0,03	0,03	0,01	0,03	0,03	0,03	0,03	0,01	0,02	0,02	0,03		0,15	0,00	0,00	0,00	0,01	0,67	0,67	0,48
21	0,16	0,23	0,10	0,02	0,15	0,16	0,15	0,72	0,64	0,50	0,70	0,15		0,49	0,00	0,04	0,03	0,34	0,38	0,39
22	0,18	0,26	0,11	0,08	0,17	0,18	0,16	0,85	0,75	0,59	0,79	0,00	0,49		0,01	0,03	0,08	0,32	0,34	0,49
23	0,02	0,02	0,02	0,01	0,02	0,02	0,02	0,01	0,00	0,00	0,00	0,00	0,00	0,01		0,03	0,01	0,00	0,00	0,01
24	0,08	0,08	0,08	0,02	0,08	0,08	0,08	0,01	0,01	0,01	0,01	0,00	0,04	0,03	0,03		0,12	0,04	0,04	0,03
25	0,03	0,01	0,06	0,15	0,03	0,02	0,04	0,01	0,01	0,01	0,03	0,01	0,03	0,08	0,01	0,12		0,04	0,04	0,00
27	0,03	0,07	0,02	0,01	0,03	0,03	0,03	0,23	0,16	0,13	0,21	0,67	0,34	0,32	0,00	0,04	0,04		0,78	0,69
28	0,06	0,09	0,01	0,02	0,05	0,05	0,05	0,23	0,17	0,14	0,23	0,67	0,38	0,34	0,00	0,04	0,04	0,78		0,75
29	0,12	0,17	0,07	0,01	0,12	0,12	0,11	0,35	0,27	0,22	0,32	0,48	0,39	0,49	0,01	0,03	0,00	0,69	0,75	

Figure 10: Correlation matrix calculated for the first $k=15$ local features $\mathbf{F}_k$ evaluated on *BRAINWEB_REF*.

The simulated dataset series *SIM_2-SIM_8* are perfectly suited to evaluate the local and meta features showing highest predictability for the specific classification scenarios. Results on the $k=30$ local features are presented in Fig. 11 and for the meta features in Fig. 12., with single feature predictability reported relative to results on *SIM_2* as ground truth. Thus, a peak indicates, that for the particular scenario, the particular feature $\mathbf{F}_j$ is at least superior utilizable for classification.

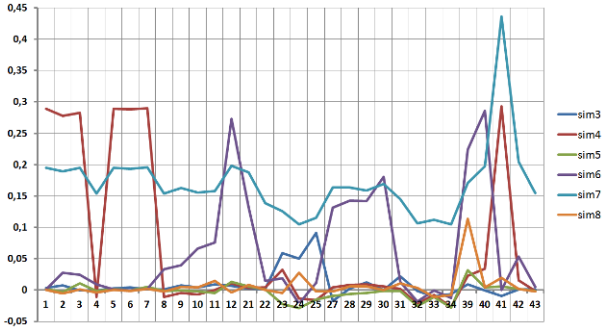

Figure 11: Single local feature predictability calculated for *SIM_3-SIM_8* relative to *SIM_2* as neutral classification scenario.

Analysis on the simulated datasets SIM_3-SIM_8 leads to the following findings:

- For *SIM_3* with only class position being varied, geometric features ($\mathbf{F}_{23}$-$\mathbf{F}_{25}$) are best.
- For *SIM_4* with varied mean intensity level, intensity features ($\mathbf{F}_1$-$\mathbf{F}_7$) contribute most for overall predictability.

- Meta feature $\hat{\mathbf{F}}_{35}$ best addresses the difference in connectedness according to number of islands for *SIM_5*.
- For *SIM_6* the mean region size ($\mathbf{F}_{12}$) and for *SIM_7* voxel-ratio meta feature $\hat{\mathbf{F}}_{20}$ are best suited, whereas the intra region intensity characteristics simulated with *SIM_8* necessitate utilization of co-occurrence features ($\mathbf{F}_{39}$-$\mathbf{F}_{43}$).

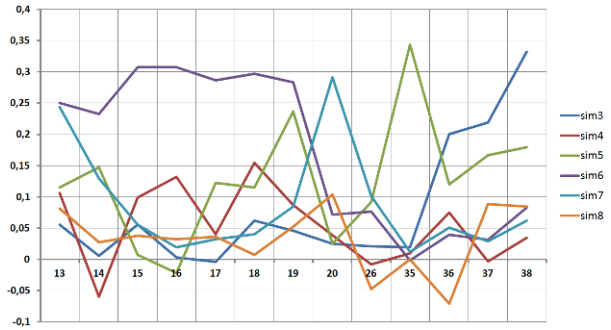

Figure 12: Single meta feature predictability calculated for *SIM_3*-*SIM_8* relative to *SIM_2* as neutral classification scenario.

Generally, predictability of the particular features shows a general tendency despite the particular segmentation domain and an overall high level, which correlates indirectly with the number of defined classes *k* in the particular classification domains, see Fig. 13.

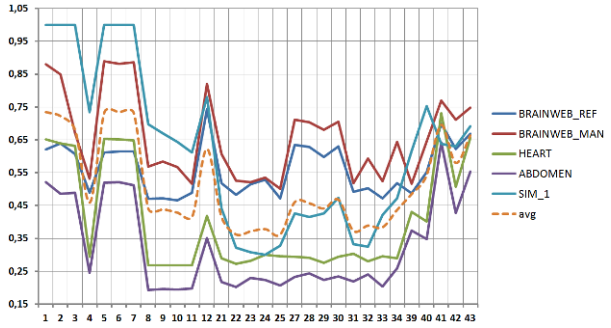

Figure 13: Single meta feature predictability calculated for *BRAINWEB_REF*, *BRAINWEB_MAN*, *HEART*, *ABDOMEN* and *SIM_1*.

5.2. Results on Multivariate Class Similarity and Domain-Specific Feature Selection

Although the particular local features show a common trend for the different segmentation and classification domains as previously discussed in Fig. 13, automated feature selection leads to different results for the utilized testing sequences as shown in Table 7. While for all of the considered datasets, feature $\mathbf{F}_6$ is chosen at first rank, the features selected at rank $\mathbf{F}_{II}$ to $\mathbf{F}_V$ highly depend on the particular classification domain. Feature $\mathbf{F}_6$ thereby best handles outliers compared to the other similar intensity features. Automated feature selection based on P_{hist} as shown in Table 7 generally leads to an increased overall predictability with every additional feature, while due to calculation reasons, the results at higher dimensionality also quantitatively drop due to collapsing bins, see Fig. 14. In contrast, utilizing P_{mcu}, the cumulated results show monotonic increase also at higher dimensions, see Fig. 15.

Table 7: Domain-specific feature selection based on histogram predictability P_{hist}.

dataset		$\mathcal{F}_I$	$\mathcal{F}_{II}$	$\mathcal{F}_{III}$	$\mathcal{F}_{IV}$	$\mathcal{F}_V$
B_REF	$\mathcal{F}_i$	6	33	34	21	29
	P_{hist}	.99171	.90909	.98315	.89093	.93510
	$P_{total_{hist}}$	.99171	.99378	.99287	.98570	.97232
B_MAN	$\mathcal{F}_i$	6	8	34	40	29
	P_{hist}	.97430	.92915	.92717	.92342	.92069
	$P_{total_{hist}}$	.97430	.98281	.98335	.97645	.95609
HEART	$\mathcal{F}_i$	6	25	24	23	21
	P_{hist}	.79306	.48754	.52078	.50716	.44183
	$P_{total_{hist}}$	.79306	.81167	.82332	.80702	.76524
ABDOM	$\mathcal{F}_i$	6	29	23	24	25
	P_{hist}	.71942	.48264	.48561	.46589	.45236
	$P_{total_{hist}}$	.71942	.73392	.75085	.73710	.70514
SIM_1	$\mathcal{F}_i$	6	40	1	8	2
	P_{hist}	.99956	.82879	.99938	.80552	.99945
	$P_{total_{hist}}$	.99956	.99897	.99763	.98726	.97692

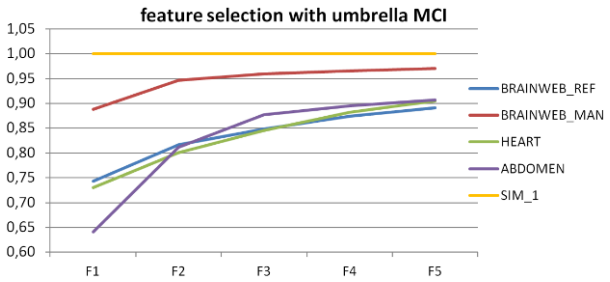

Figure 14: Overall P_{mcu} for increased number of selected *local* features.

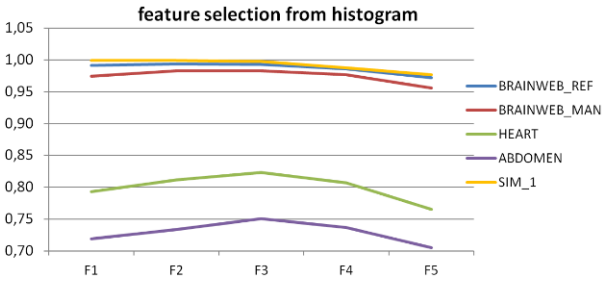

Figure 15: Overall P_{hist} for increased number of selected *local* features.

For the simulated datasets *SIM_2*-*SIM_8*, the results on automated local feature selection, as shown in Table 8, as well as automated feature selection of the best meta features, as presented in Table 9, accord with the previous findings on domain-specific single feature predictability as argued before.

Regarding the histogram-based overall predictability calculation strategy P_{hist}, density of the feature space with respect to the chosen dimension-dependent bin count as well as the applied filter parameterization has to be evaluated. Results are presented for *BRAINWEB_MAN* dataset in Fig. 16 by visualizing the 3D histogram for different feature sets. With features ($\mathbf{F}_5$, $\mathbf{F}_{12}$, $\mathbf{F}_{39}$), due to outliers in the region size dimension, density of the feature space is low and

would necessitate for histogram equalization (a). Geometric positional features (F_{23}, F_{24}, F_{25}) allow refection of the class morphology itself (b). The feature set (F_1, F_8, F_{25}) that is considered best according to automated feature selection, shows a dense feature space and well-defined decision boundaries between the neighbouring class distributions (c).

Table 8: Selected *local* features for simulated datasets.

	selected $\mathcal{F}_i$			predictability $P_{\mathcal{C}_{mcu}}$			
dataset	$\mathcal{F}_I$	$\mathcal{F}_{II}$	$\mathcal{F}_{III}$	$\mathcal{C}_1$	$\mathcal{C}_2$	$\mathcal{C}_3$	$P_{total_{mcu}}$
SIM_2	41	24	23	1.00	.539	.536	.7232
SIM_3	41	25	24	1.00	.804	.809	.8840
SIM_4	5	21	33	1.00	.996	.996	.9974
SIM_5	41	42	43	1.00	.497	.772	.7805
SIM_6	40	41	43	1.00	1.00	1.00	1.000
SIM_7	3	23	24	1.00	.200	.842	.8412
SIM_8	42	39	8	1.00	.755	.883	.8916

Table 9: Selected *meta* features for simulated datasets.

	selected $\hat{\mathcal{F}}_i$			predictability $P_{\mathcal{C}_{mcu}}$			
dataset	$\hat{\mathcal{F}}_I$	$\hat{\mathcal{F}}_{II}$	$\hat{\mathcal{F}}_{III}$	$\mathcal{C}_1$	$\mathcal{C}_2$	$\mathcal{C}_3$	$P_{total_{mcu}}$
SIM_2	14	17	19	1.00	.892	.619	.8371
SIM_3	14	38	36	1.00	.983	.974	.9858
SIM_4	18	14	26	1.00	.947	.951	.9661
SIM_5	35	17	13	1.00	1.00	1.00	1.000
SIM_6	15	13	14	1.00	1.00	1.00	1.000
SIM_7	20	13	14	1.00	1.00	1.00	1.000
SIM_8	20	14	13	1.00	.875	.876	.9173

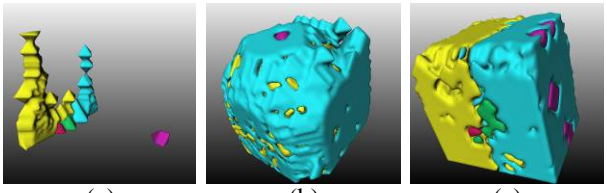

(a) (b) (c)

Figure 16: Visualization of 3D histogram with different utilized feature sets, showing decision boundaries for *white matter* (red), *grey matter* (green), *background* (magenta), *tissue* (yellow) and *remaining* voxel (cyan) from *BRAINWEB_MAN* datasets.

While feature selection can be parameterized to maximize region or voxel classification respectively, also predictability of the particular classes can be evaluated in detail, as shown in Fig. 17 for *k=13* classes of *ABDOMEN* sequence. With features additionally incorporated for classification lead to higher overall predictability, also the predictability of the particular classes C_i increases by trend. Generally, for tomographic patient datasets, particular structures can only be classified at low confidence due to overlapping in the feature distributions. Thus, the incorporation of meta features is highly required to further improve distinctness for classification. Feature selection can also be adjusted to balance single class results or apply specific weights, besides tying to maximize region or voxel classification confidence.

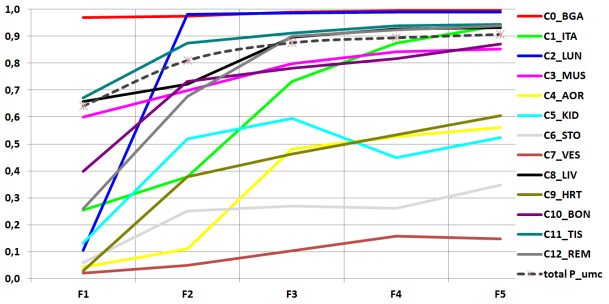

Figure 17: Single class predictability for *ABDOMEN* sequence according to increased number of features.

5.3. Results on Final Classification

Finally, classification of the pre-segmented datasets according to the automatically selected features has to be evaluated utilizing conventional classifiers from the machine learning domain. Segmentation results from neural network classification utilizing *HeuristicLab* (Wagner 2014) on *BRAINWEB_MAN* sequence are presented in Fig. 18. Besides some artefacts wrongly connected with grey and white matter volume and some marginal missing parts of the ventricle, the achievable classification results are of high quality.

For the three classes *grey matter*, *white matter* and *ventricle* a region classification precision of *.952* is achieved, incorporating *k=10* local features. With respect to the voxel error introduced by hybrid watershed pre-segmentation of *.969*, overall voxel classification precision is to be quantified with *.914*.

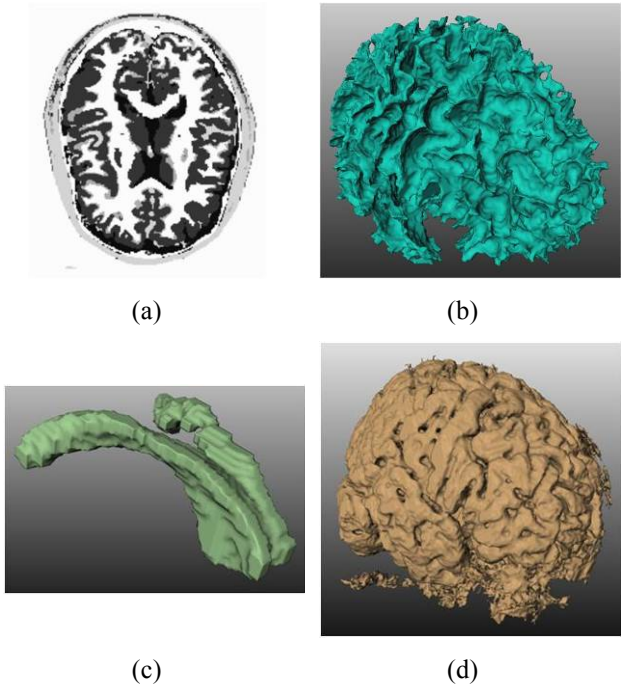

(a) (b)

(c) (d)

Figure 18: Classification results on *BRAINWEB_MAN* achieved with neural networks. Axial slice of labelled classes in (a) and surface renderings of *white matter* (b), *corpus callosum* (ventricle) (c) and the *grey matter* (d).

6. DISCUSSION AND CONCLUSIONS

A strategy for domain-specific selection of local features with respect to maximized region of voxel classification precision has been presented, also adjustable to different objectives by user-defined weights.

Introduced meta features provide potential for additional predictability in the medical segmentation and classification domain and are perfectly suited to be incorporated for genetic algorithms. Future developments will focus on application of these meta features to better steer the partially stochastic classification results of single individuals towards the optimal solution in evolutionary algorithms.

Besides, additional classifiers like genetic programming, support vectors or random forests will be evaluated with respect to achievable classification precision.

With respect to histogram-based approaches, sparseness of the feature space at higher dimensions will necessitate the future utilization of histogram equalization.

REFERENCES

Beyer, T., Schwenzer, N., Bisdas, S., Claussen C.D., and Pichler, B.J., 2010. MR/PET – Hybrid Imaging for the Next Decade. In *MAGNETOM Flash 3/2010*.

Boost, 2014. Boost C++ libraries, http://www.boost.org/, last visited 14/5/2014.

Boser, B.E., Guyon, I.M., Vapnik, V., 1992. A training algorithm for optimal margin classifiers. In *Proc. of Computational Learning Theory*, 144-152.

Cocosco, C.A., Kollokian, V., Kwan, K.-S., Evans, A.C., 1997. BrainWeb: Online Interface to a 3D MRI Simulated Database. In *NeuroImage* 5(4), 425.

Cootes, T.F., Taylor, C.J., Cooper, D.H., Graham, J., 1992. Training Models of Shape from Sets of Examples. In *Proceedings of the British Machine Vision Conference*, 9-18., Leeds, U.K.

Cootes, T.F., Edwards, G.J., Taylor, C.J., 1998. Active Appearance Models. In *Proceedings of the 5th European Conference on Computer Vision*, 484-498. June 2-6, Freiburg (Germany).

Felipe, J., Traina, A.J.M., Traina, C., 2003. Retrieval by Content of Medical Images Using Texture for Tissue Identification. In *Proc. of the 16th IEEE Symposium on Computer-Based Medical Systems CBMS'03*, 175-181.

Fürst, D., Schrempf, A., 2012. PATIENTSIM – Development of an Augmented Reality Simulator for Surgical Training of Vertebroplasty and Kyphoplasty. In *Proceedings of the 9th IASTED*.

Gonzalez, R.C., Wintz, P., 1987. *Digital Image Processing*. London: Addison Wesley.

Goldberg, D.E., 1989. *Genetic Algorithms in Search, Optimization and Machine Learning*. Boston, USA: Addison-Wesley Longman.

Kitware, Inc., 2014. ITK- The Insight Segmentation and Registration Toolkit, http://www.itk.org/ITK/, last visited 14/5/2014.

Koza, J.R., 1992. *Genetic Programming*. Massachusetts, USA: MIT Technology.

McInerney, T., Terzopoulos, D., 1996. Deformable Models in Medical Image Analysis : A Survey. In *Medical Image Analysis* 1 (2):91-108.

Metropolis, N., 1987. The Beginning of the Monte Carlo Method. In *Los Alamos Science*, 125-130.

Osher, S., Sethian, J.A., 1988. Fronts Propagating with Curvature-Dependent Speed: Algorithms Based on Hamilton-Jacobi Formulations. In *Journal of Computational Physics* 79:12-49.

Schenk, A., Prause, G.P.M., 2001. Optimierte semi-automatische Segmentierung von 3D Objekten mit Live-Wire und Shape-Based-Interpolation. In *Bildverarbeitung für die Medizin* 2001, 202-206.

Swoboda, R., Backfrieder, W., Zwettler, G., Pfeifer, F., 2008. MIPP: A Medical Image Processing Platform based on ITK, VTK and Eclipse RCP. In *The Insight Journal* 3(2), 1-36.

Vapnik, V., 2000. *The Nature of Statistical Learning Theory*. New York, USA: Springer.

Vincent, L., Soille, P., 1991. Watersheds in Digital Space – An Efficient Algorithm Based on Immersion Simulations. In *IEEE Transactions on Pattern Analysis and Machine Intelligence 13(6)*, 583-598.

Wagner, S., 2014. Architecture and Design of the Heuristiclab Optimization Environment. In *Advanced methods and Applications in Computational Intelligence, Topics in Intelligent Engineering and Informatics Series*, Springer, 197-261.

Zwettler, G., Backfrieder, W., Swoboda, R., Pfeifer, F., 2009. Fast Fully-automated Model-driven Liver Segmentation Utilizing Slicewise Applied Levelsets on Large CT Data. In *Proceedings of the 21st European Modeling and Simulation Symposium*, 161-166.

Zwettler, G., Backfrieder, W., 2012. A New Hybrid Algorithm Based on Watershed Method, Confidence Connected Thresholding and Region Merging as Preprocessing for Statistical Classification of General Medical Images. In *Proceedings of the 24th European Modeling and Simulation Symposium EMSS2012*, 73-81.

Zwettler, G., Backfrieder, W., 2013. Generic Model-Based Application of Modular Image Processing Chains for Medical 3D Data Analysis in Clinical Research and Radiographer Training. In *Proc. of the International Workshop on Innovative Simulation for Healthcare IWISH2013*, 58-64.

Zwettler, G. and Backfrieder, W., 2014. Simulation of Tomographic Medical Image Data for Training of Generic Segmentation Models Utilizing Multivariate Feature Classification. In *Proc. of the SummerSim2014*, Monterey, USA, pp.10 (article in press).

ROBUST SURFACE BASED REGISTRATION IN AN OPEN FRAMEWORK FOR IMAGE GUIDED SURGERY

Werner Backfrieder[(a)], Gerald Zwettler[(b)]

[(a)]Department of Biomedical Informatics, University of Applied Sciences Upper Austria, Hagenberg, Austria
[(b)] Biomedical Research and Development Centre, University of Applied Sciences Upper Austria, Hagenberg, Austria

[(a)]Werner.Backfrieder@fh-hagenberg.atl, [(b)] Gerald.Zwettler@fh-hagenberg.at

ABSTRACT
Image guided surgery has established as a valuable routine methodology in modern operation theatres, especially when targeting obscured morphology or for exact positioning of tools. In cerebral surgery image guidance has a long tradition, even in orthopedics; recently it also extends to abdominal surgery. The software packages are highly task specific and complex, thus the systems are hardly extendible. But in a research environment, an open software architecture is highly desirable. In this work a surgical navigation framework is presented based on a hardware abstraction layer, with a DeviceServer as a central service. It allows seamless communication with any type of tracking, video, and haptic devices via network and makes the actual application platform and language independent. The top software layer is a generic surgical navigation framework based on the Matlab® scripting language. The great functionality and easy handling of Matlab® facilitates rapid prototyping of new components in image guided surgery. The development needs no highly specialized software experts and is suitable for the interdisciplinary staff of a research lab. As a showcase for the newly developed system, a registration algorithm to match the coordinate systems of an optical tracking system and patient image data is implemented. It is a surface-to-points algorithm, characterized by robustness, stability and usability. Iterative registration is implemented as a steepest gradient procedure and distances are measured with a three dimensional chamfer map. The registration yields accurate overlay of the coordinates, allowing exact positioning of surgical tools. Because of the easy handling and extensibility, the developed rapid prototyping environment has high potential in clinical research facilities.

Keywords: image guided surgery, medical image processing, virtual reality, augmented reality

1. INTRODUCTION

Modern image based surgical navigation developed within the last three decades. The historical roots of intraoperative navigation go back to frame-based stereotaxis, a technique utilizing preoperative images to facilitate inter-operative guidance, thus enabling the exact targeting of intracranial structures to place needles, catheters or electrodes. The surgical trajectory is guided to avoid damage in functional centers of the brain and to minimize craniotomy, thus providing saver surgery and shorter anastasis.

In the 1990s the concept of frameless stereotaxis was introduced to neurosurgery. It was the first modern navigation system employing the capabilities of novel imaging modalities and real-time tracking of surgical instruments, both merged by powerful computer technology and graphics (Enchyev 2009). Image guided navigation is characterized by two phases, the planning phase outside the operating room (OR) comprising preoperative data acquisition, visualization and planning, and the intra-operative phase in the OR, with registration of image and patient coordinates, tool-tracking and intraoperative visualization. This needs special equipment to meet the standards of an aseptic environment. This modern methodology was highly beneficial for patient care and economical aspects of treatment (Paleologos et al. 2000).

The technique is refined with the development of functional MRI, enabling the exact localization of functional foci, e.g. the centers of motoric activities, speech, or visual perception in the brain cortex. The planning of the surgical trajectory accounts for avoiding functional handicaps after surgery (Nimsky et al. 2005).

Preoperative image acquisition is not sufficient for exact localization of tools in the image volumes, especially in soft tissue surgery, e.g. the brain-shift after opening the dura mater. It is compensated by intra-operative imaging or computational assessment of the deviations with respective virtual deformation of the image volume (Hatiboglu et al. 2009, Liu et al. 2014, Reinbacher et al. 2014, Scheufler et al. 2011).

Orthopedic surgery is a broad field for surgical navigation techniques, ranging from hip and knee to spine surgery. The applications comprise exact replacement of pathologic morphology, the positioning of artificial joints or screws and the use of surgical robots (Blackeny et al. 2011, Kelly and Swank 2009, Mason et al. 2007, Verdú-López et al. 2014).

Much research effort is done in this field on model based navigation. In contrast to the previously discussed

image guided methods, a model of the surgical target is adopted according to intra-operative measurements of control points. This needs no imaging modalities and prevents the patient from potential risk of radiation (Habor 2013).

The development leads to navigation of information, i.e. the aggregation of all kind of information from all available sources stored in Pictures Archiving and Communication System (PACS) and the Hospital Information System (HIS). Data are filtered and processed for intuitive representation in the OR. This "digital OR" is the high end development of the top system providers (Malarme et al. 2008).

The discussed systems differ in complexity and performance, but most of them are software monoliths with even closed source code and specifications, thus adaption to special user needs or extension of functionality is bound to vendor-specific customer support or it needs extensive knowledge of modern software technologies. In this work an open software framework for rapid prototyping of surgical navigation tools with the high level scripting language Matlab® on top is presented. Matlab® covers a wide range of mathematical, statistical and computational problems and allows easy development of complex solutions. As a showcase, a surface-to-points registration algorithm is developed and implemented for user friendly and robust registration with an optical tracking system.

2. METHODS

Accurate registration is an essential requirement for the transformation of world coordinates, acquired by the tracking system, into the patient (image) coordinate system. Most off-the-shelf applications for surgical navigation use point to point registration. This requires fiducial landmarks, since inherent anatomical landmarks are mostly not reliable or strongly manifested. These fiducial landmarks often need minor surgical intervention, e.g. a set of bone screws is fixed at the skull, or some bulky equipment, models as they are used for dental casts, is bonded to the patient's teeth (Bettschart et al. 2012, Morea et al. 2011, Aldana et al. 2010). In the next step, the markers are measured sequentially with the pointing device of the tracking system, where a strict order has to be kept to guarantee point-to-point relationship of the markers and the respective positions in the image volume. Summarized, since point-to-point registration is still the method of choice, it may be erroneous and needs some practice. A further pitfall is the stability of the markers, since they must not move during the time interval between image data acquisition and actual surgical intervention.

In this work a more robust und user friendly method for registration is presented. It takes advantage of inherent landmarks, thus the efforts for mounting and careful conservation are obsolete, and even the registration procedure is elementary. As an inherent landmark any external surface of the patient is proper. In the testing environment at the surgical lab of the Biomedical Research Facility at Hagenberg, Upper Austria, a plastic skull phantom with a 6 part rubber brain model is available. Image volumes are acquired with a Siemens Cardiac Sensation 64 scanner, 220 slices with a 512x512 matrix, 16 bit per pixel, voxel-size 1x0.4x0.4mm^3. A three panel display of the phantom is shown in Fig. 1. The skull bone is mimicked by plastics and the soft tissue parts, i.e. the brain, are modeled with rubber, the darker gray indicates the lower attenuation coefficients of the brains.

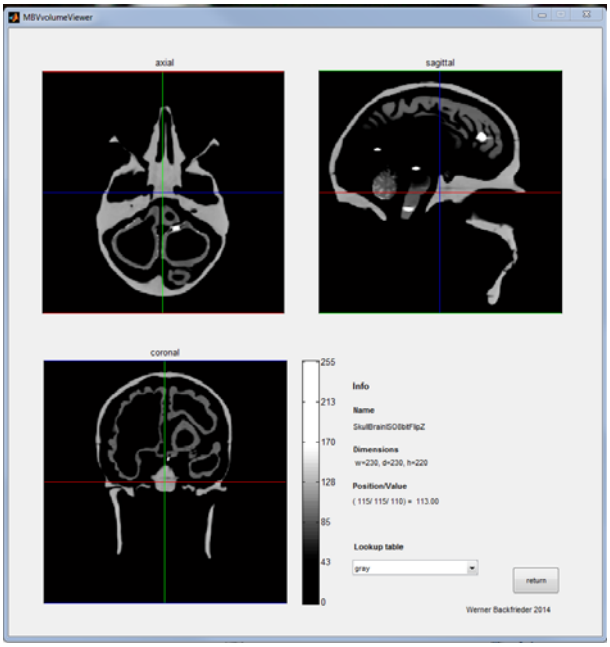

Figure 1: Transversal, sagittal and coronal slices through the x-ray CT scan of the phantom.

The registration procedure starts with the sampling of surface points on the upper skull. The tip of the surgical device is moved along the skullcap and these points are recorded. This set of points is registered against the surface, extracted from the image volume. This is a typical surface-to-points matching algorithm. It differs from the well-known point-to-point techniques in the aspect, that there are no correspondent points in the image volume. An alternative is the ICP algorithm, where always the closest subset of points out of the total surface set is registered against the sampled points.

2.1. Surface to points matching

Registration is a classical optimization problem, where the extremal values of a cost function are determined. In this case the cost function is the sum of the shortest distances of the points to the surface. The assessment of this shortest distance is generally costly. In the worst case the distances to all available surface points must be calculated and then the minimum is chosen. As part of an iterative procedure, this approach needs a high amount of computing power. In contrast a pre-calculated surface-to-distance map allows the direct lookup of the closest distance. The chamfer algorithm is an extremely efficient method to calculate such a distance map by only two passes of a volume-mask

through the image volume. The algorithm takes advantage of already known distances in the direct neighborhood of the pixel, whose distance is just determined and comprises the steps described below.

2.1.1. Initialization

The surface map is initialized with known distances; these are the voxels building up the surface. The surface is determined by interactive thresholding the image volume, gaining the parts of interest in the intensity interval. Dilation, a basic operation from binary mathematical morphology, with a cross shaped structure element is applied to the thresholded object (Heijmans and Ronse 1990). The original binary image volume is subtracted from the dilated, yielding the outer surface of the object. The surface voxels are assigned zero distance and all other voxels are set to infinity, cf. Fig 2.

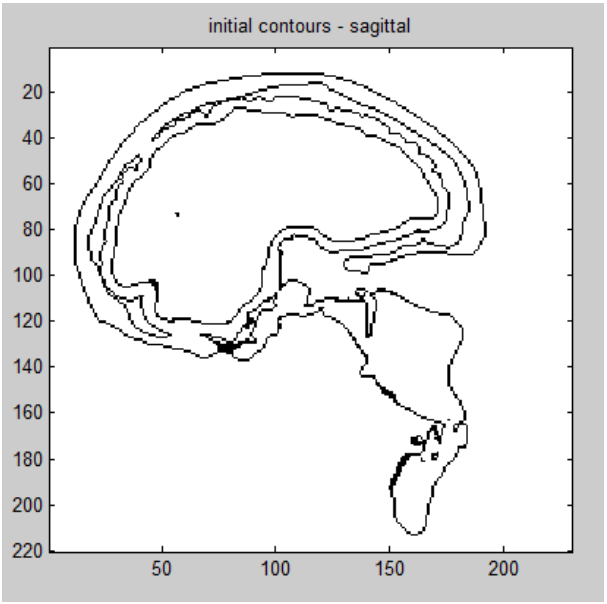

Figure 2: Contours of a sagittal slice, defining zero distance in the initial distance map.

2.1.2. Calculation of distances

The shortest distances are calculated accordingly to chamfer transform in two passes (Treves et al. 1998). In the first pass the image stack is decreased, slice by slice. Within each slice the calculation is proceeded from the top left corner down to the bottom right corner. The volume mask comprises the 26-neighbourhood of a pixel, but in the first pass only a subset of this neighborhood is considered; cf. Fig 3, where all three layers of the mask are shown. At an actual pixel position all known distances in the vicinity defined by the mask are considered. Then the distance-difference from the actual pixel to these selected vicinity pixels is added. Finally the minimum value is assigned as new distance to the central position. The second pass processes the voxels in the opposite direction and the volume mask is complementary. As a result a volume map with distances is obtained, with comparatively little computational effort, proper for even greater volume data. The three main sections of the volumetric distance map are shown in Fig 4.

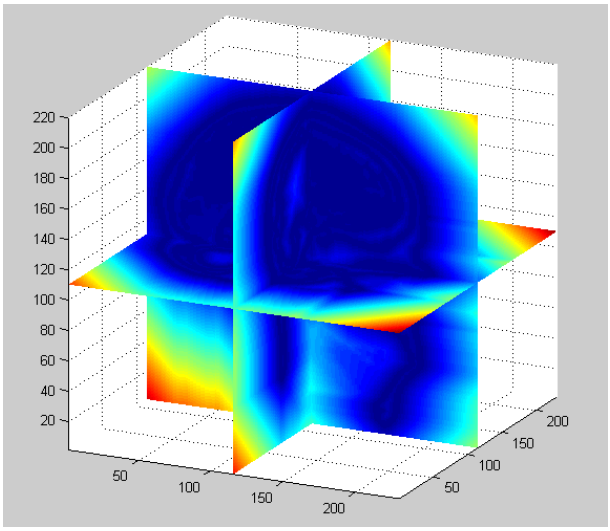

Figure 3: Chamfer distance map, displayed with intersecting slices.

2.1.3. Optimization

For surface-to-points registration rigid body transform is sufficient, since there are no systematic distortions, both in CT-image data and position data, provided by the tracking system. Rigid body motion is characterized by six degrees of freedom, both three for translation $\boldsymbol{t}=(t_x,t_y,t_z)^T$ into all directions and rotation. In this case we refer to the Euler angles in (z,y',z'') convention. The transform is described by the homogeneous 4 by 4 matrix (Goldstein 2006)

$$T=\begin{pmatrix} R & t \\ 0 & 1 \end{pmatrix}, \qquad (1)$$

and

$$R = R_z R_{y'} R_{z''} \ , \qquad (2)$$

built by the rotation matrices around the axes, fixed to the object

$$R_z=\begin{pmatrix} \cos\gamma & -\sin\gamma & 0 \\ -\sin\gamma & \cos\gamma & 0 \\ 0 & 0 & 1 \end{pmatrix},$$

$$R_{y'}=\begin{pmatrix} \cos\beta & 0 & -\sin\beta \\ 0 & 1 & 0 \\ -\sin\beta & 0 & \cos\beta \end{pmatrix}, \qquad (3)$$

$$R_{z''}=\begin{pmatrix} \cos\alpha & -\sin\alpha & 0 \\ -\sin\alpha & \cos\alpha & 0 \\ 0 & 0 & 1 \end{pmatrix},$$

with the rotation angles γ around the z-axis, β around y' and α around the z''. Optimization is implemented as steepest gradient method, with different relaxation parameters for rotation and translation.

3. IMPLEMENTATION

This registration procedure is a showcase for the rapid prototyping environment for surgical planning and navigation, based on Matlab®. The central module of this development environment is the seamless interface to the tracking tools and other surgical environments. The implementation is built on the Java library support of Matlab®, thus a stable and real-time integration of all surgical navigation devices is provided.

3.1. Architecture

The principal part of the rapid prototyping environment is the hardware abstraction layer (HAL) (Zwettler and Backfrieder 2013), it allows seamless communication with all types navigation hardware. In the center of the HAL is the DeviceServer (Zwettler and Backfrieder 2013b), it defines a communication standard enabling the integration of different hardware, like tracking environments, force sensors, haptic interaction devices or 3D surface scanners. These devices are directly attached to one or several host computers running the DeviceServer application. Thereby, communication between the attached devices and the DeviceServer is based on vendor-specific communication protocols and API's. When integrating a hardware device into the DeviceServer, abstraction from the complex API's, different messaging formats and transmission protocols is achieved. A compact set of harmonized scripting commands is defined for each device, utilizing extended Backus-Naur-Form (EBNF) grammar format for control command definition (ISO/IEC14977 1996).

Clients just communicate with the DeviceServer application over standard network protocols, thus achieving general connectivity and platform independence for all higher level applications demanding input and feedback from devices. The small set of HW-specific commands defined with the EBNF grammar is implemented with available vendor-specific API functionality. Commands can be transmitted to the DeviceServer via a console client, the application client port, a RAW network communication port and the telnet communication port, see Fig.5. The DeviceServer can handle an unrestricted number of clients concurrently. The EBNF command definition allows for wrapper generation in arbitrary programming languages. The command transfer is accomplished via network proxies to achieve programming language and platform independence. Currently C++ and Java wrapper generation is supported.

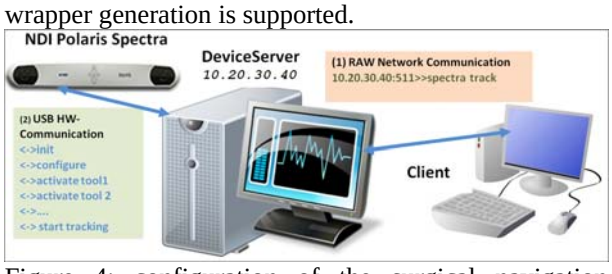

Figure 4: configuration of the surgical navigation environment. The devices are attached to the host computer running the DeviceServer. A client application communicates via network with the tools.

4. RESULTS

The integration of the device server into a Matlab® environment proofed to be a highly productive rapid prototyping tool. Ease of development, the diversity of software solutions, and quick proof of concepts are outstanding characteristics of that implementation. Communication with surgery tools is not disturbed by any significant latency and actually real time response is achieved.

Table 1: marker references

Name	x	y	z	Δr
R1	181.43	104.56	98.15	
M1	183.77	106.45	99.96	2.99
R2	179.63	59.58	56.47	
M2	177.42	62.71	57.00	3.21
R3	118.01	192.97	71.74	
M3	115.61	195.29	70.08	3.18
R4	56.49	84.93	28.53	
M4	57.15	85.10	26.00	2.62
R5	45.74	97.31	95.62	
M5	43.04	100.07	95.15	2.84
			ΣΔ	2.96+/-0.25

The proposed method for real-world to image registration proofed to be feasible. Point sampling on the upper skull bone is easy and reliable; the curvature of the bone is distinct to provide good and unique matching of the contours, thus minimizing positioning errors in further navigation operations.

As a benchmark of the novel registration procedure, the deviations of tracker measurement and image based positioning, at the fiducial markers (five plastic spheres, 5mm diameter), cf. Fig 6a, are summarized. In the planning step the markers are segmented and the center of mass of each marker is calculated. During the control step, the tip of the tool is pointed onto each marker and its position in image space, i.e. the registered position is measured. Table 1 summarizes the reference values (R), the measured values (M) and the resulting deviations. The mean deviation is 2.97+/-0.25mm, indicating good registration. With a radius of the marker spheres of 2.5mm, the efficient accuracy is in the range of the tracker tolerance of 0.5mm. A rendering of the segmented objet in comparison with a photo of the real scenery is shown in Fig. 6b.

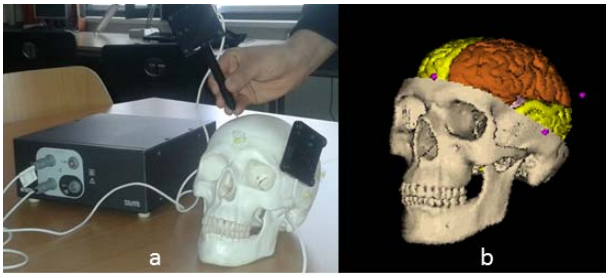

Figure 5: Phantom with attached position tool, surgical pointer and tracking unit (a), and segmented image space (b).

5. DISCUSSION

In this work a novel rapid prototyping environment for applications in surgical navigation and surgery planning is presented. As a showcase of the framework a robust, easy to handle method for registration of image and world coordinates was implemented and tested. Results manifest high accuracy of registration. There exists a great bunch of systems for surgical navigation, based either on virtual reality (VR) or augmented reality (AR), supporting variable hardware components and differing in complexity. But most of the systems are not open for further extensions and development by the user, or they need high level expertise in VR programming, mathematics or computational geometry. The proposed system, based on a hardware abstraction layer, is not limited to devices from specific vendors; it is open and allows unique access to all devices. On top is the scripting language Matlab®, with its enormous functionality, enabling rapid development of even complex extensions to an existing navigation environment. Access to hardware tools performs in real-time, display of complex sceneries may slightly lag behind. This can be solved by implementing critical code-pieces in Matlab-Mex, the native C interface.

The proposed registration method may not be applicable with soft tissue surfaces, since during surgery mostly turgor deforms the surface and registration becomes inconsistent. But for spine surgery, when bone screws must be positioned exactly into the vertebral body, not penetrating the vertebral channel, this method has high potential for intra-surgical registration.

This rapid prototyping environment allows the implementation of novel concepts and algorithms for surgical navigation with rather little effort.

REFERENCES

Aldana, P.R., MacGregor, T.L., James, H.E., Marcus, R.B. Jr, Indelicato, D.J., 2010. Titanium screws as fiducial markers for image-guided stereotactic proton irradiation in pediatric central nervous system tumors: a technical report. Pediatr Neurosurg. 2010;46(3):227-31

Bettschart, C., Kruse, A., Matthews, F., Zemann, W., Obwegeser, J.A., Grätz, K.W., Lübbers, H.T., 2014. Point-to-point registration with mandibulo-maxillary splint in open and closed jaw position. Evaluation of registration accuracy for computer-aided surgery of the mandible. J Craniomaxillofac Surg. 2012 Oct;40(7):592-8.

Blakeney, W.G., Khan, R.J., Wall, S.J., 2011. Computer-assisted techniques versus conventional guides for component alignment in total knee arthroplasty: a randomized controlled trial. J Bone Joint Surg Am 93:1377–1384.

Enchev,Y., 2009. Neuronavigation: geneology, reality, and prospects. Neurosurg Focus, 27(3): E11. Evans, W.A., 1994. Approaches to intelligent information retrieval. *Information Processing and Management*, 7 (2), 147–168.

Goldstein H., 2006. Klassische Mechanik, WILEY-VCH-Verlag, Weinheim 2006, S. 652.

Habor, D., Neuhaus. S., Vollborn, T., Wolfart, S., Radermacher, K., Heger, S., 2013. Model based assessment of vestibular jawbone thickness using high frequency 3D ultrasound micro-scanning - Proceedings of SPIE Medical Imaging, pp. 8675-33.

Hatiboglu, M.A., Weinberg , J.S., Suki, D., Rao, G., Prabhu, S.S., Shah, K., Jackson, E., Sawaya, R., 2009. Impact of intraoperative high-field magnetic resonance imaging guidance on glioma surgery: a prospective volumetric analysis. *Neurosurg* 64(6):1073–1081.

Heijmans, H.J.A.M, Ronse, C., 1990. The algebraic basis of mathematical morphology I. Dilations and erosions, Computer Vision, Graphics, and Image Processing, Volume 50, Issue 3, June 1990, Pages 245-295

ISO/IEC 14977: 1996(E). In: http://www.cl.cam.ac.uk/~mgk25/iso-14977.pdf

Liu, Y., Kot, A., Drakopoulos, F., Yao, C., Fedorov, A., Enquobahrie, A., Clatz, O., Chrisochoides, NP.,2014. An ITK implementation of a physics-based non-rigid registration method for brain deformation in image-guided neurosurgery. Front Neuroinform. 2014 Apr 7;8:33.

Kelley, T.C., Swank, M.L., 2009. Role of navigation in total hip arthroplasty. *J Bone Joint Surg Am* 91(Suppl 1):153–158.

Malarme, P., Wikler, D., Warze'e, N., 2008. Digital operating room., 3(1): 145-148.

Mason, J.B., Fehring, T.K., Estok, R., Banel, D., Fahrbach, K., 2007. Meta-analysis of alignment outcomes in computer-assisted total knee arthroplasty surgery. *J Arthroplasty* 8:1097–1106

Morea, C., Hayek, J.E., Oleskovicz, C., Dominguez, G.C., Chilvarquer, I., 2011. Precise insertion of orthodontic miniscrews with a stereolithographic surgical guide based on cone beam computed tomography data: a pilot study. Int J Oral Maxillofac Implants. 2011 Jul-Aug;26(4):860-5.

Nimsky, C., Ganslandt, O., Hastreiter, P.,Wang, R., Benner, T., Sorensen, A.G., Fahlbusch, R., 2005. Preoperative and intraoperative diffusion tensor imaging-based fiber tracking in glioma surgery. *Neurosurg* 56(1):130–138

Paleologos, TS., Wadley, JP., Kitchen, ND., Thomas, DG., 2000. Clinical utility and cost-effectiveness of interactive image-guided craniotomy: clinical comparison between conventional and imageguided meningioma surgery. *Neurosurg* 47(1): p 40–48

Reinbacher, KE., Pau, M., Wallner, J., Zemann, W., Klein, A., Gstettner, C., Aigner, R.M., Feichtinger, M., 2014. Minimal invasive biopsy of intraconal expansion by PET/CT/MRI image-guided

navigation: A new method. J Craniomaxillofac Surg. 2014 Mar 19.
Scheufler, K.M., Franke, J., Eckardt, A., Dohmen, H., 2011. Accuracy of image-guided pedicle screw placement using intraoperative computed tomography-based navigation with automated referencing, part I: cervicothoracic spine. *Neurosurg* 69(4):782–795.
Treves, ST, Mitchell, KD, Habboush, IH. 1998. Three dimensional image alignment, registration and fusion. Q J Nucl Med. 1998 Jun;42(2):83-92.
Verdú-López, F., Vanaclocha-Vanaclocha, V., Gozalbes -Esterelles, L., Sánchez-Pardo, M., 2014. Minimally invasive spine surgery in spinal infections. J Neurosurg Sci. 2014 Jun;58(2):45-56.
Zwettler, G., Backfrieder, W., 2013. Architecture and Design of a Generic Device Server for Virtual Reality Hardware Integration in Surgical Navigation - LECTURE NOTES IN COMPUTER SCIENCE, Vol. 8112, No.1, 2013, pp. 166-173
Zwettler, G., Backfrieder, W., 2013b. Generic Device Server Implementation for Virtual Reality Hardware Integration in Surgical Training - Computer Aided Systems Theory (Eurocast 2013), Las Palmas, Spain,2013, pp. 118-119

AUTHORS BIOGRAPHY

Werner Backfrieder received his degree in technical physics at the Vienna University of Technology in 1992. Then he was with the Department of Biomedical Engineering and Physics of the Medical University of Vienna, where he reached a tenure position in 2002. Since 2002 he is with the University of Applied Sciences Upper Austria at the division of Biomedical Informatics. His research focus is on Medical Physics and Medical Image Processing in Nuclear Medicine and Radiology with emphasis to high performance computing. Recently research efforts are laid on virtual reality techniques in the context of surgical planning and navigation.

Gerald A. Zwettler was born in Wels, Austria and attended the Upper Austrian University of Applied Sciences, Campus Hagenberg where he studied software engineering for medicine and graduated Dipl.-Ing.(FH) in 2005 and the follow up master studies in software engineering in 2009. In 2010 he has started his PhD studies at the University of Vienna at the Institute of Scientific Computing. Since 2005 he is working as research and teaching assistant at the Upper Austrian University of Applied Sciences at the school of informatics, communications and media at the Campus Hagenberg in the field of medical image analysis and software engineering with focus on computer-based diagnostics support and medical applications.

A COMPUTATIONAL COMPARISON BETWEEN LINEAR AND PULSED EXTRACORPOREAL MEMBRANE OXYGENATION (ECMO) BASED ON HEMODYNAMICS IN THE AORTA

Vera Gramigna[(a)], Maria Vittoria Caruso[(b)], Attilio Renzulli [(c)], Gionata Fragomeni [(d)]

[(a) (b) (d)] Department of Computer and Biomedical Engineering, *"Magna Graecia"* University, Catanzaro, 88100, Italy
[(c)] Cardiac Surgery Unit, *"Magna Graecia"* University, Catanzaro, 88100, Italy

[(a)]gramigna@unicz.it, [(b)]mv.caruso@unicz.it, [(c)]renzulli@unicz.it, [(d)]fragomeni@unicz.it

ABSTRACT

The experience of combining extra-corporeal membrane oxygenation (ECMO) with intra-aortic balloon pump (IABP) for the treatment of acute heart failure in critically ill adults can in principle have a synergistic and complementary effect. ECMO is a medical procedure used to supply oxygen to the blood circulation of patient with cardiac/ pulmonary failure. Since linear flow in ECMO is often responsible for some clinical problems, aim of this study was to evaluate the hemodynamic difference in the aorta due to linear and pulsed ECMO, the latter obtained with the IABP, currently the most commonly used mechanical circulatory support device. A multiscale model, realized coupling a 3D CFD analysis with a lumped parameters model (resistance's boundary conditions), was carried out. The numerical results showed that the aortic flow followed the balloon radius behavior's change. Therefore pulsatility similar to the arterial one, in respect of the linear standard behaviour (IABP not inserted), occurred.

Keywords: Extracorporeal Membrane Oxygenation (ECMO), Intra Aortic Balloon Pump (IABP), Computation Fluid Dynamic (CFD), Multiscale Model

1. INTRODUCTION

In the last years, the limitations of the most commonly methods (such as the extra-corporeal membrane oxygenation -ECMO- and the intra-aortic balloon pump -IABP-) which were unable, if used singularly, to achieve ideal outcomes in patients with severe disease, contributed to diffusion of technique that combine the two methodologies for the treatment of acute heart failure in adults. In fact, even if the IABP can improve blood flow to internal organs, allowing the weakened heart to recover its function, it cannot replace the physiological pumping of the heart. For patients whose cardiac muscle is already severely damaged, IABP support may not raise cardiac output sufficiently to meet the body's needs, creating the necessity for further circulatory support (Pengyu 2014). The principle of ECMO, long-term extracorporeal support used to treat patients with severe cardiac/ pulmonary failure, is based on prolonged partial cardiopulmonary bypass. When the ECMO is used to keep the heart at rest, the connection aorta - right atrium is adopted and the two cannulas are inserted via surgical cut down. Even if the survival rate is high, cerebrovascular injury may be an important complication. In fact, the significant changes in cerebral circulation that happen during induction of ECMO (decreased arterial pulsatility and rapid changes in arterial partial pressure of oxygen and carbon dioxide) compared with the previous state (patient is hypoxemic for hours), are often responsible for cerebral damage (Papademetriou 2011) .

Mathematical methods and Computational Fluid Dynamics (CFD) have recently emerged as a powerful design tool in hemodynamic context. Different studies were focused on the CFD-based design strategies applied to blood flow in pumps and other blood-handling devices (Behbahani 2009). Nevertheless little is known about fluid dynamics changes in aorta during IABP- induced pulsed ECMO.

The aim of this study was to investigate the flow pattern in the ascending aorta and in the epiaortic vessels between non-pulsatile standard ECMO (linear and constant flow) and pulsatile ECMO (induced by IABP) in a computational fluid dynamics (CFD) model and to look for hemodynamic differences. In the present study, flow pulsatility during CPB was realized through the use of the IABP, whose principal component is a polyethylene balloon which inflates and deflates according to the cardiac cycle (Biglino 2010).

2. MATERIALS AND METHODS

2.1. ECMO Circuit

The principal components of the ECMO circuit considered in this study were: a Stöckert Centrifugal Pump (SCP) combined with the Stöckert Centrifugal Pump Console (Stockert Instrumente GmbH, Munich,

Germany), a membrane oxygenator (Quadrox D, Maquet, Jostra) with integrated heart exchanger, an oxygen/air blender, and an oximetry monitor.

2.2. The geometrical model

A 3D real patient-specific model of the aorta was obtained from a series of in vivo contrast-enhanced axial CT-scan slices, done for clinical reasons. The medical images used in the present study were a collection of DICOM files and the reconstruction of three-dimensional model was performed through a process of semiautomatic segmentation using a commercial open source software (Itk snap software, http://www.itksnap.org). Finally, the derived faced surface was simplified for the CFD analysis using the reverse engineering process (Figure 1). Informed consent was granted for the patient, before enrolling him in the research.

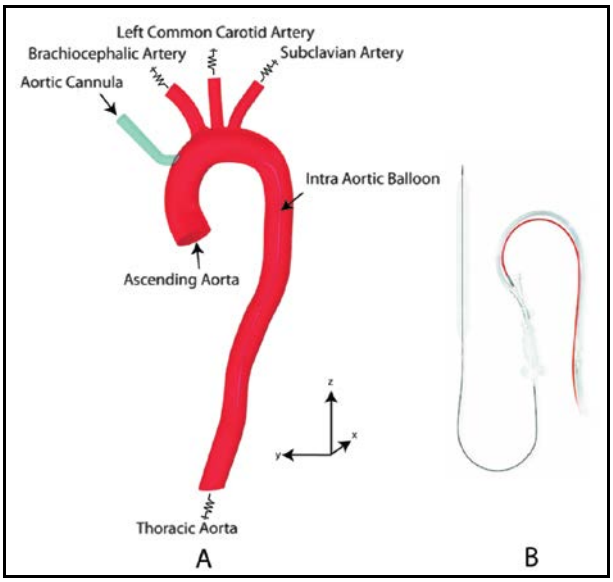

Figure 1: Multiscale model (A) and used IABP (B). The model includes the arterial cannula, the deflated IABP and the lumped parameters model (resistance's boundary conditions) used for the four vessels.

The model reproduced the ascending aorta, the three epiaortic vessels (innominate or brachiocephalic artery, left common carotid artery, left subclavian artery), and the thoracic aorta.

A standard ECMO arterial cannula (24 Fr Medtronic Inc., Minneapolis, MN, USA) was added to the ascending aorta on the site that is routinely adopted at our institution (Cardiothoracic Surgery Unit, Department of Medical and Surgical Sciences), 2 cm below the take off of the innominate artery on the anterior wall of the aorta and with a tilt angle of 45° (Figure 1).

To reproduce the physiological flow pulsatility, the Intra Aortic Balloon Pump (IABP) was used (Chang 2010, Lim 2013). Its principal component is a polyethylene balloon placed after the left subclavian artery and before the iliac bifurcation, which inflates and deflates according to the cardiac cycle: it is fully inflated in mid diastole and fully deflates in systolic peak. The intra-aortic balloon (Sensation 7 Fr. 40 cm3 with CS300 IABP System, Datascope, Maquet GmbH and Co. KG, Rastatt, Germany) was set in the descending aorta (Biglino 2010), 2 cm below the left subclavian artery, as in clinical practice (Onorati et al. 2009a, 2009b and 2009c) (Figure 1). The geometry was simplified ignoring the conical terminal parts and considering only the central cylinder, with a volume of 0.9 ml in deflation phase and of 38.7 ml at the full inflated instant, giving an 84% lumen obstruction in the descending aorta (Biglino 2010, Kem 1999, Lim 2013).

2.3 Mathematical model, boundary conditions and simulations details

Blood was considered as a Newtonian flow (Quarteroni 2000, Vignon-Clementel 2006, Formaggia 2009, Gao 2005) whose motion was described using the three-dimensional incompressible Navier-Stokes equations:

$$\nabla \cdot \mathbf{u} = 0 \quad (1)$$

$$\rho\,(\partial \mathbf{u}/\partial t) + \rho(\mathbf{u}\cdot\nabla)\mathbf{u} = \nabla\cdot[-p\mathbf{I} + \mu(\nabla\mathbf{u} + (\nabla\mathbf{u})^{T}] + \mathbf{F} \quad (2)$$

where **u** represented the fluid velocity vector, p the pressure, μ the dynamic viscosity, ρ the density of blood, **I** the identity matrix and **F** the volume force field, which was neglected in the computational study because the effect of gravity was ignored (the patient was supine during the surgical procedure). ρ and μ were equal to 1060 Kg/m^3 and 0.0035 Pa·s, respectively.

Moreover, in this study was hypothesized that the all flow delivered only through the ECMO arterial cannula (continuous flow of 5.5 L/min) and the aorta was considered as clamped (no flow came out from aortic valve). The laminar model was chosen to simulate the blood flow motion because, with a flow of about 5.5 L/min, the Reynolds number was about 3400 in arterial cannula and about 1200 in ascending aorta.

Considering an assistance level of 1:1, the balloon inflation behaviour was approximated with an 8 degree Fourier general model. The balloon inflation started 0.2 s after the beginning of the diastole and the maximum volume was reached in 0.25 s, considering a cardiac cycle of about 1 s, so a “false” systolic peak, due to IABP, occurred at 1.45 sec. Moreover, the balloon displacement in the x, y directions was controlled by a parametric solver.

A multiscale study, realized coupling a 3D CFD analysis and a lumped parameters model (0D boundary conditions), was carried out by using COMSOL 4.3a (COMSOL Inc, Stockholm, Sweden), a finite-element-based commercial software package.

As inlet boundary condition, a continuous flow value of 5.5 L/min, delivered through the arterial cannula, was used, while as outlet boundary conditions (Vignon-Clementel 2006a, 2006b), a 0D model made only of resistances (Lee 2002, Olufsen 2000, Benim 2011) was adopted to represent the arterial system of

the downstream branch regions (smaller arteries, arterioles, capillaries, venules and veins). Resistances at the four outflow exits (innominate artery, left common carotid artery, left subclavian artery and thoracic aorta) were imposed by the following pressure equation:

$$p=p_0+R\cdot Q \quad (3)$$

where p_0 was an aortic outlet pressure of 80 mmHg, Q indicated the instantaneous volumetric flow rate through each respective outflow exits, calculated at each time instant from the local velocity profile, and R the resistance. We used a constant outlet pressure offset of 80 mmHg to obtain a physiologically range of pressures in the system. R values were optimized for each vessel in order to create a referential model, characterized by the real flow rates, for every patient in the same circumstances: $2.9\cdot10^8$ Pa·s/m^3 for the brachiocephalic artery, $6.0\cdot10^8$ Pa·s/m^3 for left common carotid and left subclavian arteries and $0.6\cdot10^8$ Pa·s/m^3 for the thoracic aorta.

Moreover the vessel and the arterial cannula walls were assumed to be rigid and no-slip boundary conditions were applied.

Mesh was assessed in order to obtain a good quality for linear and pulsed cases and included two boundary layers and tetrahedral elements: 75980 elements for first case and 367742 elements for second case. The different number of elements occurred because in linear case (without IABP) tridimensional models consisted only of the aorta anatomy and the arterial cannula, while in assisted one there was also the balloon in the descending aorta.

For the fluid-dynamic analysis, to evaluate the blood flow perfusion in the aorta and epiaortic vessels, two time-depending parametric simulations were performed and the Pardiso solver was used to solve the Navier-Stokes equations. The P1-P1 finite element method was used for the space discretization in the equations of the blood motion. For all simulations three balloon inflation phase were considered to eliminate the transitory initial effects and only one was analyzed (from 2 to 3 sec).

Hemodynamic parameters for all vessels were evaluated and the comparison between linear and IABP-induced pulsatile ECMO flow rates was assumed as index of epiaortic perfusion improvement.

3. RESULTS AND DISCUSSIONS

Flow rates in inflation instant for each vessel in linear and pulsed ECMO were evaluated and percent flow (%) in respect to the aortic cannula flow of 5.5 L/min were calculated (Table1). Moreover hemodynamic changes between linear and pulsed ECMO were analyzed during the cardiac cycle by means of percent error (P-L) between linear (L) and pulsed (P) ECMO. In the inflation instant, considered as a “false” systolic peak, IABP produced an increase of flow rates in all epiaortic vessels, with a mean value of about 12.87%, 13.81%, 16.18% in brachiocephalic, left common carotid and left subclavian arteries, respectively. Moreover, the presence of IABP produced pulsatility in the flow behavior, as in physiological case, but with lowest peak value of each vessel (Figure 2).

Table 1: Flow Rate in the inflation instant for each vessel in linear and pulsed ECMO and percentage difference (P-L) between the two cases. I: Ascending Aorta; II: Brachiocephalic Artery; III: Left Common Carotid Artery; IV: Left Subclavian Artery; V: Thoracic Aorta.

Vessel	LINEAR (L)		PULSED (P)		P - L
	[L/min]	%	[L/min]	%	%
I	0,00	0,00	0,01	0,12	0,12
II	1,04	18,86	1,75	31,73	12,87
III	0,74	13,43	1,50	27,24	13,81
IV	0,87	15,84	1,76	32,01	16,18
V	2,48	45,03	0,46	8,34	-36,69

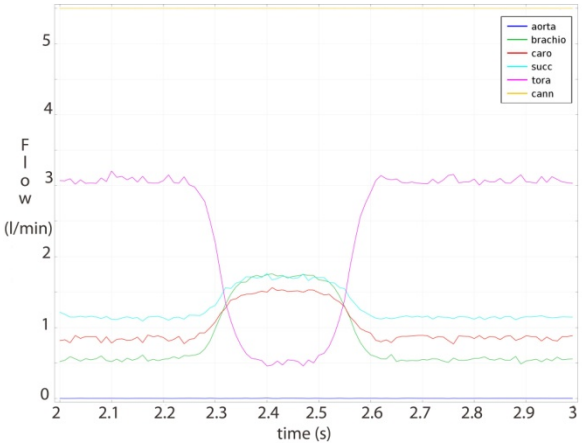

Figure 2: Flow distribution (l/min) during one IABP cycle

Analyzing streamlines behavior in aortic model, Figure 3 highlighted a dramatic difference in the blood flow dynamic through the epiaortic vessels between linear (A) and pulsed case (B and C). In fact in the first case the flow hit the inner wall of aortic arch and headed to thoracic aorta, while in the second case the flow was directed to the subclavian artery and thoracic aorta when the balloon was deflated, and to the left common carotid and left subclavian arteries in deflation phase. Moreover, the counterpulsation in inflation phase produced a steady flow pattern in each epiaortic vessel, which, on the contrary, appeared whirling in the linear case.

This model allowed the study of hemodynamic parameters in a model of aorta in linear situation and in presence of IABP during ECMO. Moreover, it could be allow quantitative prediction of hemolysis and supports the engineer in identifying recirculation areas and other regions with an increased probability for blood clotting (Behbahani 2009).

4. LIMITATIONS AND FUTURE PERSPECTIVES

Although the main contribution of this work was the implementation of a 3D-0D model to evaluate the modifications of aortic hemodynamics during IABP pulsed ECMO, it presents several limitations.

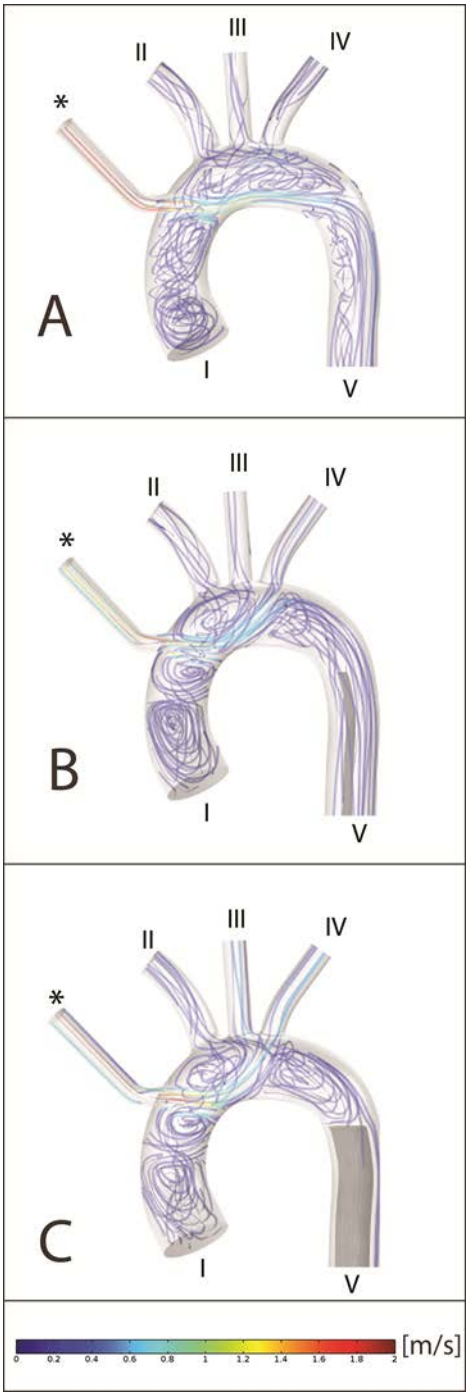

Figure 3: Velocity stream lines (m/s) during the aortic cross-clamp time in control case (A) ECMO-IABP off- and in the pulsed case: (B) ECMO-IABP on- at the deflation instant and (C) ECMO-IABP on- at the inflation instant. I: Ascending Aorta; II: Brachiocephalic Artery; III: Left Common Carotid Artery; IV: Left Subclavian Artery; V: Thoracic Aorta; *: Aortic cannula.

First the resistance values were supposed constant during assisted cases, but it was not true in real situations (Onorati et al. 2009a, 2009b and 2009c). For example, as reported in (Krishna et al. 2009), balloon inflation during diastole causes displacement of the stroke volume, and hence activation of the aortic baroreceptors. The peripheral resistance is reduced, thus improving blood flow. This resistance change was not taken into account in our study. Thus, the improvement of the present model would be the estimation of resistance values and their behavior during cardiac cycle, by means, for example, of a pressure-drop model (Itu L. et al. 2012). Moreover it would also be useful to study a multiscale fluid-structure simulation to analyze vascular wall modification in pathological cases. The idea will be to use results obtained from *ex-vivo* experimental tensile tests on aortic tissue as data of structural mechanical behavior and of wall deformation laws.

REFERENCES

Behbahani, M., 2009. A Review of Computational Fluid Dynamics Analysis of Blood Pumps. *European Journal of Applied Mathematics*, 20, 363–397.

Benim, A.C., Nahavandi, A., Assmann, A., Schubert, D., Feindt, P., Suh, S.H., 2011. Simulation of blood flow in human aorta with emphasis on outlet boundary conditions. *Applied Mathematical Modelling*, 35(7), 3175-3188.

Biglino G., 2010. *Experimental study of the mechanics of the intra-aortic balloon*. Thesis (Ph.D). Brunel University.

Chang Y., Bin G., 2010. Modeling and identification of an intra-aorta pump. *ASAIO J*, 56(6):504-9.

Datascope Corp. *Sensation 7Fr. IAB Catheter, Instructions for use*, Maquet. Available from: http://ca.maquet.com/clinicianinformation/instructions-for-use/iab-catheters/ [accessed 10 April 2013].

Formaggia, L., Quarteroni, A., Veneziani, A., 2009. *Cardiovascular Mathematics, Modeling and simulation of the circulatory system*, Volume 1, Springer. Milan.

Gao, F., Watanabe, M., Matsuzawa, T., 2005. Three-dimensional Computational Mechanical Analysis for 3-layered Aortic Arch Model under Steady and Unsteady Flow with Fluid-structure Interactions. *Proceedings of the Eighth International Conference on High-Performance Computing in Asia-Pacific Region, IEEE Computer Society*. pp. 161. November 30-December 03, Beijing, (China).

Itu L., Sharma P., Ralovich K., Mihalef V., Ionasec R., Everett A., Ringel R., Kamen A., Comaniciu D., 2012. Non-Invasive Hemodynamic Assessment of Aortic Coarctation: Validation with In Vivo Measurements. *Annals of Biomedical Engineering*, 41(4), 669–681.

Kern M. J., Aguirre F. V., Caracciolo E. A., Bach R. G., Donohue T. J., Lasorda D., Ohman E. M., Schnitzler R. N., King D. L., Ohley W. J., Grayzel

J., 1999. Hemodynamic effects of new intra-aortic balloon counterpulsation timing methods in patients: a multicenter evaluation. *American Heart Journal*, 137, 1129-1136.

Krishna M., Zacharowsk K., 2009. Principles of intra-aortic balloon pump counterpulsation. *Continuing Education in Anaesthesia, Critical Care & Pain*, 9(1), 24-28.

Lee, D., Chen, J.Y., 2002. Numerical simulation of steady flow fields in a model of abdominal aorta with its peripheral branches. *Journal of Biomechanics*, 35 (8), 1115–1122.

Lim K. M.., Lee J. S., Gyeong M.-S., Choi J.-S., Choi S. W., Shim E. B., 2013. Computational Quantification of the Cardiac Energy Consumption during Intra-Aortic Balloon Pumping Using a Cardiac Electromechanics Model. *Cardiovascular Disorders*, 28, 93-99.

Olufsen, M.S., Peskin, C.S., Kim, W.Y., Pedersen, E.M., Nadim, A., Larsen J., 2000. Numerical simulation and experimental validation of blood flow in arteries with structured-tree outflow conditions. *Annals of Biomedical Engineering*, 28(11), 1281-1299.

Onorati, F., Santarpino, G., Presta, P., Caroleo, S., Abdalla, K., Santangelo, E., Gulletta, E., Fuiano, G., Costanzo, F.S., Renzulli, A., 2009. Pulsatile perfusion with intra-aortic balloon pumping ameliorates whole body response to cardiopulmonary bypass in the elderly. *Critical Care Medicine*, 37(3), 902-911.

Onorati, F., Santarpino, G., Rubino, A., Cristodoro, L., Scalas, C., Renzulli, A. 2009. Intraoperative bypass graft flow in intra-aortic balloon pump-supported patients: differences in arterial and venous sequential conduits. *Journal of Thoracic Cardiovascular Surgery*, 138(1), 54-61.

Onorati, F., Santarpino, G., Rubino, A.S., Caroleo, S., Dardano, A., Scalas, C., Gulletta, E., Santangelo, E., Renzulli, A., 2009. Body perfusion during adult cardiopulmonary bypass is improved by pulsatile flow with intra-aortic balloon pump. *International Journal of Artificial Organs*, 32(1), 50-61.

Papademetriou M. D. 2011. *Multichannel Near Infrared Spectroscopy to monitor cerebral oxygenation in infants and children supported in extracorporeal membrane oxygenation (ECMO).* Thesis (Ph.D). University College London.

Ma P., Zhang Z., Song T., Yang Y., MSa, Meng G., Zhao J., Wang C, Gu K., Peng J., Jiang B., Qi Y., Yan R., Ma X., 2014. Combining ECMO with IABP for the Treatment of Critically Ill Adult Heart Failure Patients. *Heart, Lung and Circulation*, 23, 363–368.

Quarteroni A., Tuveri M., Veneziani A., 2000. Computational Vascular Fluid Dynamics: problems, models and methods. *Computing and Visualization in Science*, 2, 163-197.

Vignon-Clementel I. E., Figueroa C. A., Jansen K. E., Taylor C. A., 2006. Outflow boundary conditions for three dimensional finite element modeling of blood flow and pressure in arteries. *Computer Methods in Applied Mechanics and Engineering*, 195, 3776–3796.

Vignon-Clementel, I., 2006. *A couple multidomain method for computational modeling of blood flow*, Thesis (PhD). Stanford University.

DESIGN AND MODEL A NOVEL ANKLE FOOT ORTHOSIS

Trung Nguyen[(a)], Takashi Komeda[(b)], Hung Dao[(c)]

[(a)(b)]Shibaura Institute of Technology
Research Organization for Advanced Engineering
307 Fukasaku, Minuma-ku, Saitama City, Saitama 330-8570, Japan
[(a)]thanhtrung.hust@gmail.com, [(b)]komeda@se.shibaura-it.ac.jp, [(c)]hunget.bk@gmail.com

ABSTRACT
A lower limb orthosis is a type of external supporting devices that are used to support the patients who have problems due to trauma, incomplete spinal cord injury, stroke, etc. in the process of treatment and recovery. In the three articulations of lower extremity, ankle joint bears more weight than the other joints. Almost the current active, passive ankle orthosis systems focus on controlling dorsiflexion, plantar flexion around ankle joint or both of them. In reality, however, the locomotion of human is continuous movement of Center of Pressure (CoP) points underneath the foot. This paper suggests a novel ankle orthosis system based on CoP. This new model can control dorsiflexion, plantarflextion to prevent foot from foot slap and foot drop effect for patients who have trouble with their ankle. This paper will demonstrate the design and the model of the novel orthosis system.

Keywords: Ankle Foot Orthosis (AFO), Center of Pressure, Design, foot slap, foot drop.

1. INTRODUCTION

Locomotion is a fundamental movement of human and has reciprocal influences with the other organs in the human body. For those who have gait impairment have to face significant health consequences, including loss of bone mineral content, bedridden situation, increased incidence of urinary tract infection, muscle spasticity, impaired lymphatic and vascular circulation, impaired digestive operation, and reduced respiratory and cardiovascular capacities (Phillips and et al. 1987). The physical therapy for these gait impairments varies depending on the cause of gait disorders. Prevalent causes leading gait impairments are neurological disorder and injuries, such as trauma, spinal cord injuries, multiple sclerosis, and Parkinson's disease.

Robotic therapy is more and more used in gait rehabilitation after stroke because of having a number of advantages. These advantages include reducing the physical burden for the therapist, ability to provide a large volume of movement in a safe environment, enhancing capacities of monitor performance of the lower limb during rehabilitation.

Currently, the AFO can be divided into two main groups as either passive of active AFO. The first type, passive AFO (Becker Orhopedic 2009, Kitaoka and et al. 2006, Novachec and et al. 2007), is used when human subject transfer force to move the ankle joint. On the contrary, for the other type of AFO, the actuators generate torque to control the system. The passive AFO, which is further classified by material, has some virtues such as: light weight, economy, and ability to provide assistance stiffness from some few Newton meters up to 20 N.m of resistive torque. However, the main essential point needs to be improved for this type of system is control capacity. The control of the passive AFO depends on the activation of spring, valves, or switches in open-loop as the user walk (Shorter and et al. 2013). Besides, the passive AFO has another limitation that is impossible to generate propulsion force during terminal stance phase. In order to improve the robustness capacity of controller, overcome the drawback points of the passive AFO, the active AFO(s) was developed using different external force sources to control ankle articulation. These energy sources include Magneto Rheological (MR) damper (Naito and et al. 2009), Series Elastic Actuator (SEA) (Svensson and Holmberg, 2008), McKibben pneumatic actuator (Ferris, Czerniecki and Hannaford 2005) and etc. The active AFO(s), which improve the weak points of the passive AFO, however, still contain some limitations. For the AFO system that uses the MR damper, they are capable of controlling foot motion, but they are impossible to generate the propulsive force in the push-off phase. The AFO developed by a group of MIT using SEA (Hwang, Kim and Kim 2007) can assist patients with both plantarflexion and dosirflexion. However, this system did not fully support when push-off phase. It only reduced the impedance of the AFO to allow full plantarflexion movement.

In this paper, we present a novel 3D model of active AFO that can support patients with both plantarflexion and dosirflexion movements, prevent the weak ankle foot from both foot drop and foot slap. Moreover, the new system is also capable of supporting the foot to generate propulsive force at terminal stance phase.

The structure of the remaining paper is described as follows. The paper starts with the introduction of a normal walking cycle. After that, the mechanical design as well as 3D model of the new AFO is shown. The controller selection and controllable feasibility of the

AFO are presented in the followed section. Finally, the conclusion and future works are demonstrated.

2. A NORMAL GAIT CYCLE

A normal level-walking gait cycle is defined as starting with the heel strike of one foot and terminating at the next heel strike of the same foot (Inman, Ralston, and Tood 1981, Perry 1992). This cycle is subdivided into two sub cycles as the stance phase (about 60% of a gait cycle) and swing phase (about 40% of a gait cycle) as in Figure 1. Whereas the swing phase (SW) is a portion of the gait cycle when the foot is off the ground, the stance phase (ST) is from heel-strike when the heel contacts with the ground to toe-off when the same foot leave the ground. According to the ref(s) (Palmer 2002, Gate 2004) the ST phase can be divided into three sub-subphases: Controlled PlantarFlexion (CP), Controlled Dosirflexion (CD) and Powered Plantarflexion (PP) (Berniker and Herr 2008).

- The CP begins at heel-strike and ends at the foot-flat. In this process the heel and forefoot initially contact with the ground.
- The CD begins at the foot - flat and continues until the ankle reaches a state of maximum dorsiflexion.
- The PP begins after CD and finishes at the instant of toe-off.

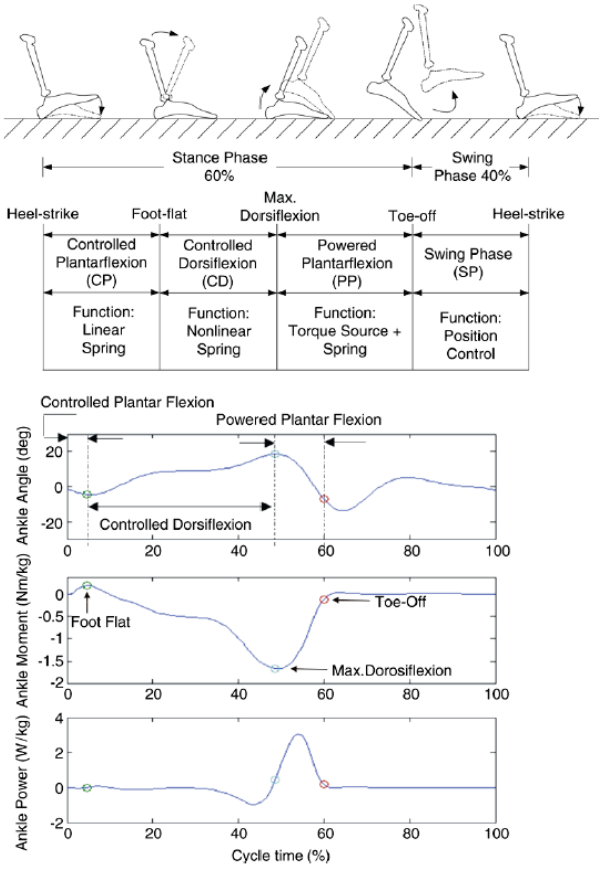

Figure 1: Normal Ankle biomechanics when level walking (Berniker and Herr 2008).

3. MECHANICAL STRUCTURE OF THE NOVEL AFO

The idea to develop the new active AFO is generated from the movement of the CoP during locomotion. The CoP (gait line) is the average vector of all force that acts on the bottom of the normal foot as it goes through the stance phase. This line goes from the lateral heel side of medial forefoot and leave at the toe of the foot. This movement goes very fast from the rearfoot to forefoot (Grundy, Tosh and McLeish RD 1975)

We developed a novel active AFO to control two important points of CoP line: the lateral rearfoot and medial forefoot point by using one DC Servomotor. The Table 1 expresses the control role of the each point when implementing to control the AFO. In the gait cycle mentioned in the Table1 the SW phase is more specifically divided into Initial SW (ISW), Medium SW (MSW) and Terminal SW (TSW).

		Stance phase			Swing phase		
		CP 5%	CD 40 %	PP 15 %	ISW 10 %	MSW 15 %	TSW 15 %
Controlled part	Rearfoot point	○	○	×	×	×	×
	Forefoot point	×	×	○	○	○	○

Table 1: Controlling role of rearfoot and forefoot point.

In order to separate one torque source from a DC Servomotor into two different sources to control two points, a three bevel gear mechanism that are perpendicularly assembled is used as in Figure 3.a. These three bevel gears include a main bevel gear connected to the motor, a rearfoot bevel gear that has a clearance fit on the rearfoot shaft to control rearfoot point, and a forefoot bevel gear which also clearance fit on the forefoot shaft to control forefoot point. Moreover, it is necessary to design some mechanism to change the torque flow from the rearfoot shaft to the forefoot shaft and vice versa. These mechanisms are summarized as in Figure 2:

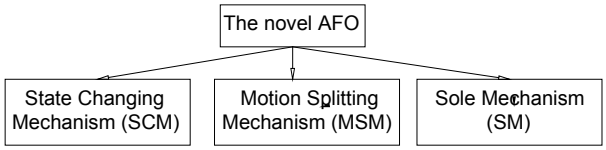

Figure 2: Mechanisms of the AFO.

3.1. Motion Splitting Mechanism

The mission of the MSM is to change the torque flow from the DC Servomotor into two different shafts: the rearfoot shaft and forefoot shaft.

After designing and choosing, the final structure of the MSM is shown in the Figure 3. The torque flow is transferred as follows: Motor -> Main bevel gear -> Rearfoot (forefoot) bevel gear -> Rearfoot (Forefoot) shaft -> Rearfoot (Forefoot) point on the sole.

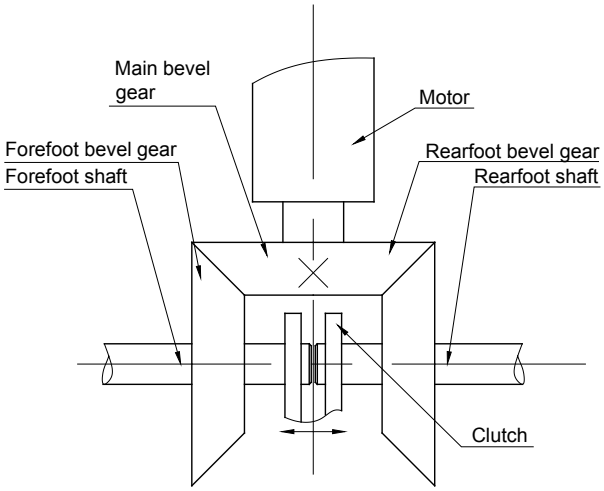

a) Bevel gears structures.

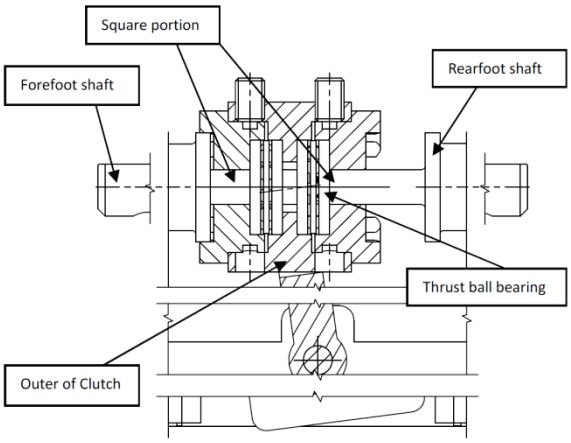

b) Motion Splitting Mechanism.

Figure 3: The bevel gears structure and Motion Splitting Mechanism.

The system uses clutches to transfer the energy from the rearfoot/forefoot bevel gear to the rearfoot/forefoot clutch shaft, respectively. Because the shaft's velocity is not high, then in order to transmit the energy from rearfoot/forefoot clutch to rearfoot/forefoot shaft the system uses a square section shaft portion as well as a square section hole on the clutches as in Figure 3.b.

3.2. Changing State Mechanism

In the operation of the MSM, in order to change from controlling the rearfoot shaft to controlling the forefoot shaft and vice versa, it is necessary to have an external mechanism to alter the clutches states. The states' clutches are ON/OFF forefoot/rearfoot clutch on the clutch portion of the bevel gear.

The current model used two different Electromagnets to control the ON/OFF states for the two clutches. From the 3D model expressed in Figure 4, in order to close the forefoot clutch (on the left side) the system's controller has to turn the rearfoot electromagnet off and turn the forefoot electromagnet on to generate the pull force. This force makes the level rod rotate around O point and pull the clutch move to the left side.

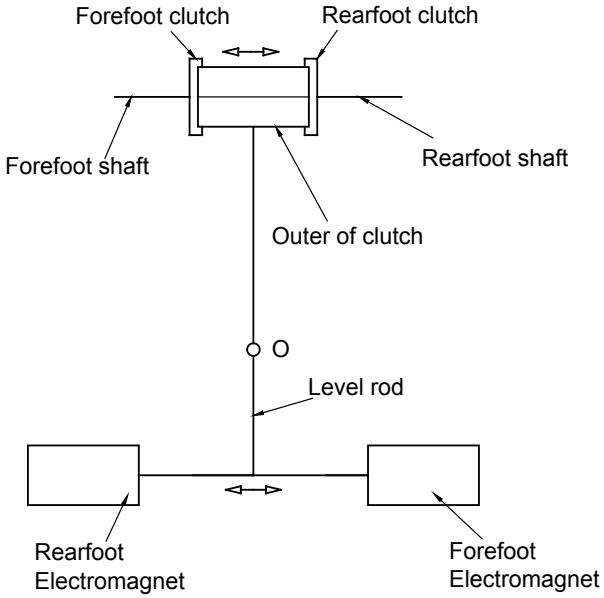

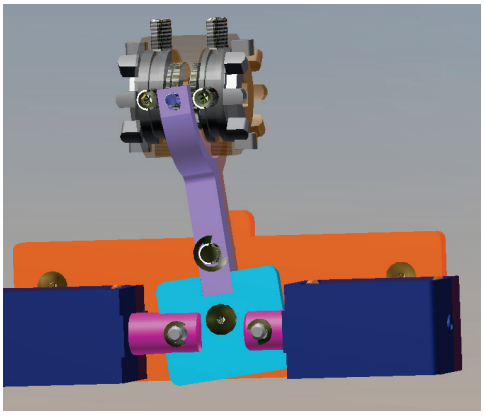

Figure 4: The changing State Mechanism.

3.3. The sole mechanism of the AFO

The sole of the AFO has roles of transferring the controlled forces from the motor to the ground to rotate the ankle joint at stance phase and to rotate ankle articulation only at swing phase. In the current design, the model used the hinge structure for the AFO's sole mechanism. Each of rearfoot and forefoot sole portions has two plates which are upper and lower plate as in Figure 5.

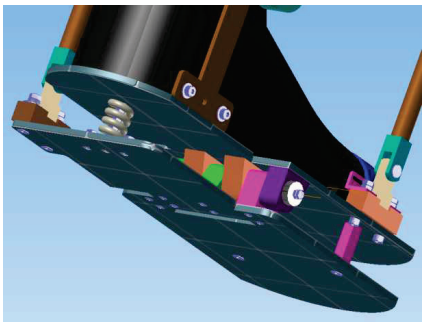

Figure 5: AFO's sole structure.

At the initial contact time, the impact force increases very fast and can be harmful for the

pathologic ankle foot as well as for the mechanical parts and motor system. To reduce this effect, a compression spring is assembled between the upper and the lower plate of the rearfoot.

In summary, after design the new active AFO which has some proposed mechanisms, the final 3D model is presented in the Figure 6. It is also noted that in this model we also attached a potentiometer to measure the ankle angle. Besides, the system has two hinge mechanisms to hang the system on the foot's shank. By using the hinge structure the system can increase the force transferring area between the AFO and human shank even though the dimension of the shank is changed with different patients.

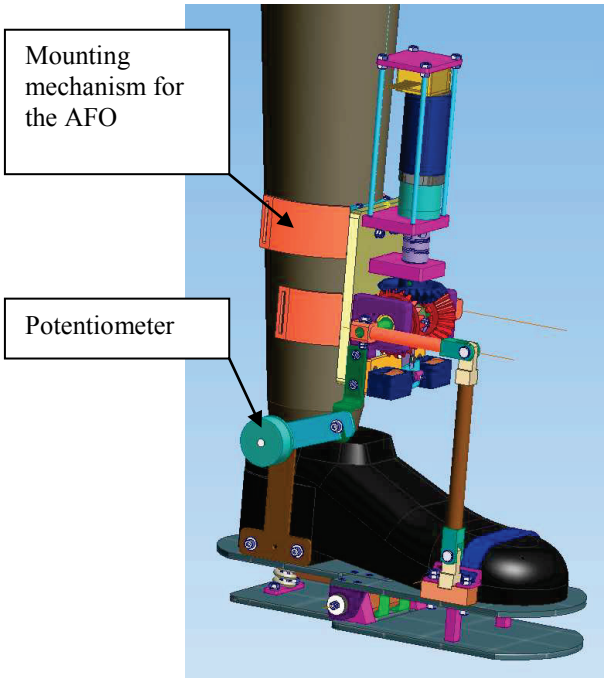

Figure 6: 3D model of the new AFO which is also attached the mounting mechanism and potentiometer.

4. FEASIBILITY ANALYSIS

In order to analysis the possibility of controlling of the system, the system was assumed to be controlled by using a position controller.

According to the above discussion, the system uses the state controller to detect the phase of gait and control them. These states include CP, CD, PP and Swing state as in Table 1. Following is the feasibility analysis of controlling for each of the state:

4.1. Controlled Plantarflexion and Controlled Dorsiflexion

According to Table 1 and Figure 1 these sub-subphases start from the initial contact and ends at the maximum dorsiflexion angle. The system used the rearfoot point to control this stage. As in Figure 7, during this stage the rearfoot part of the AFO always contacts with the ground. Moreover, in the sagittal plane, there are rotational joints of A, B, C, and D.

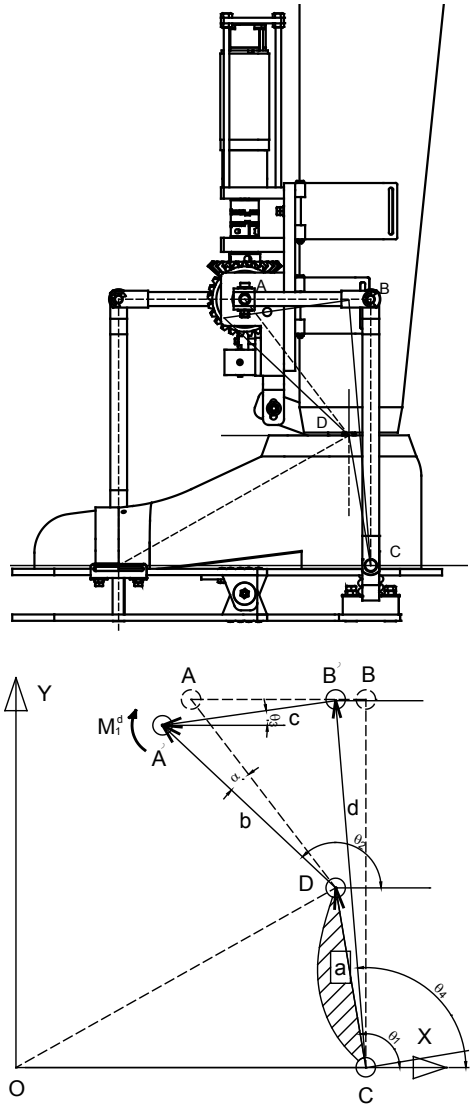

Figure 7: Positon controlling model at the 1st stage.

Because during the 1st stage, the rearfoot plate always contacts with the ground, the CD link is fixed to the floor. As a result, the ABCD linkage is equal to four-bar mechanism. It is necessary to find out the angle relation between the rearfoot shaft angle θ_3 and the angle at ankle θ_2.

Using complex number to solve this problem:

$$\overrightarrow{CD}+\overrightarrow{DA}-\overrightarrow{CB}-\overrightarrow{BA}=0 \qquad (1)$$

$$a.e^{j\theta_1}+b.e^{j\theta_2}-c.e^{j(180+\theta_3)}-d.e^{j\theta_4}=0$$

After deploying the above mathematic model, we have:

$$K_1.\cos\beta_2+K_2.\cos\beta_3+K_3=\cos(\beta_2-\beta_3)$$

where

$$K_1=-\frac{a}{c};K_2=-\frac{a}{b}\ and\ K_3=\frac{-a^2-b^2-c^2+d^2}{2.b.c}$$

$$\beta_2=\theta_1-\theta_2;\beta_3=\theta_1-\theta_3;$$

Then

$$K_1.\cos\beta_2 + K_2.\cos\beta_3 + K_3 = \cos\beta_2.\cos\beta_3 + \sin\beta_2.\sin\beta_3 \quad (2)$$

Besides,

$$\sin\beta_3 = \frac{2.\tan(\frac{1}{2}\beta_3)}{[1+\tan^2(\frac{1}{2}\beta_3)]} \; and \; \cos\beta_3 = \frac{1-\tan^2(\frac{1}{2}\beta_3)}{1+\tan^2(\frac{1}{2}\beta_3)}$$

Replacing to the above functions (2):

$$A.\tan^2(\frac{1}{2}\beta_3) + B.\tan(\frac{1}{2}\beta_3) + C = 0 \quad (3)$$

The function (3) has two roots as:

$$\theta_3 = \theta_1 - \beta_3 = \theta_1 - 2.\tan^{-1}[\frac{-B \pm \sqrt{B^2 - 4.A.C}}{2.A}] \quad (4)$$

The roots (4) of angle θ_3 can be calculated by the geometric dimensions of the system as: a, b, c, d and ankle angle. There is a notice that the absolute value of the angle θ_3 is less than 90 degree, then in the two roots (4) there is only one value that is sufficient the condition. As a result, it is possible to control the CP and CD of the first stage.

4.2. Powered Plantarflexion and Swing phase

The system uses the forefoot point to control PP and SW sub-phase. During the PP duration, the forefoot plate always contacts with the ground and the rearfoot plate does not. However, the angle between the rearfoot and the ground at instant time is able to be calculated based on the values of hip, knee and ankle value. According to Figure 8

$$\gamma = h + k + a \quad (5)$$

Where: h, k and a are the angle value of hip, knee and ankle joint, respectively.

As a result, at instant time, the CO linkage can be recognized as a fixed linkage. Then, the ABCO is equal to four-bar structure and it is similar as the calculation aforementioned. The relationship between the rearfoot shaft and ankle value as follow:

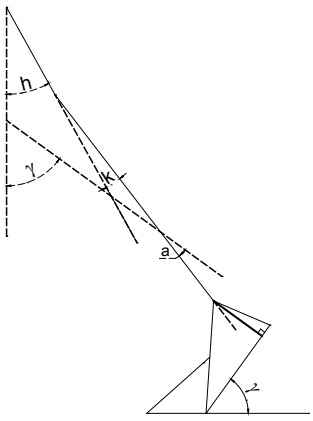

Figure 8: Value between the rearfoot plate and ground.

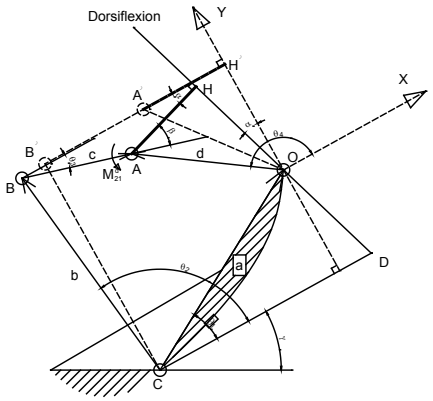

Figure 9: Position control model for PP

$$\beta = \alpha + \theta_3 = \alpha - \theta_1 + 2.\tan^{-1}[\frac{-B \pm \sqrt{B^2 - 4.A.C}}{2.A}] \quad (5)$$

Where:

$$A = (1+K_2).\cos\beta_4 - K_1 + K_3$$

$$B = -2.\sin\beta_4$$

$$C = (K_2 - 1)\cos\beta_4 + K_1 + K_3$$

$$K_1 = -\frac{a}{d}; K_2 = \frac{a}{c} and \; K_3 = \frac{a^2 + c^2 + d^2 - b^2}{2.c.d}$$

For the Swing phase, if the coordination is attached to the shank the AO of the ABCO mechanism is fixed. The relationship between controlled angle of the rearfoot shaft and the ankle angle values.The relationship between the rearfoot shaft ankle and the ankle angle is described

$$\beta = \alpha + \theta_3 = \alpha + \theta_1 - 2.\tan^{-1}[\frac{-B \pm \sqrt{B^2 - 4.A.C}}{2.A}] \quad (6)$$

Where

$$A = (1+K_2).\cos\beta_4 + K_3 - K_1$$

$$B = -2.\sin\beta_4$$

$$C = K_1 + K_3 - (1-K_2)\cos\beta_4$$

$$K_1 = -\frac{a}{d}; K_2 = \frac{a}{c} and \; K_3 = \frac{a^2 + c^2 + d^2 - b^2}{2.c.d}$$

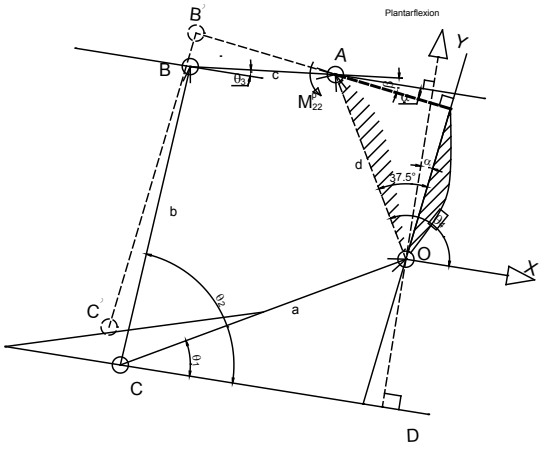

Figure 10: Position control model for the SW.

5. CONCLUSION

The paper presented the mechanical design, 3D model of a novel ankle foot orthosis. This model could help patient with ankle impairment prevent from foot drop, foot slap and improve capacity of dorsiflexion and plantarflexion. Moreover, the feasibility of the new model was also analyzed and discussed to ensure the controllable ability of the system.

In the future, the first prototype of the novel AFO will be produced and make some experiments to evaluate the system. Furthermore, in this prototype is also attached some force sensors to sense the impact force underneath of the sole to support the controller of the system.

REFERENCES

Phillips, L., Ozer, M., Axelson, P., and Fonseca., J., 1987. Spinal Cord Injury: A Guide for Patient and Family. Raven Pr.

Becker Orthopedic, Troy, M., 2009, 2003.

Kitaoka, H. B., Crevoisier, X. M., Harbst, K., D. Hansen, B. K., and Kaufman, K., 2006. "The effect of custom-made braces for the ankle and hindfoot on ankle and foot kinematics and ground reaction forces". *Archives Phys. Med. Rehabil.,* 87(1), pp. 130–135.

Novacheck, T. F., Beattie, C., Rozumalski, A., G.Gent, and G.Kroll, 2007. Quantifying the spring-like properties of ankle-foot orthoses (afos). *J. Prosthetics Orthotics, 19(4),* pp. 98–103.

Shorter, K.A., Xia, J., Elizabeth, Hsiao-Wecksler, T., and Kogler, G.F., 2013. Technologies for powered ankle-foot orthotic systems: Possibilities and challenges. *IEEE/ASME Transactions on Mechatronics,* 8(1), pp. 337–347,.

Naito, H., Akazawa, Y., Tagaya, K., Matsumoto, T., and Tanaka, M., 2009. An ankle-foot orthosis with a variableresistance ankle joint suing a magnetorheological-fluid rotary damper. *Jour. Of Biomechanical Sience and Engineering,* 4(2), pp. 182–191.

Svensson, W., and Holmberg, U., 2008. Ankle-foot-orthosis control in inclinations and stairs. *In in Proc. IEEE Int. Conf. Robot., Autom. Mechatronics,* pp. 1301– 306, 21-24 Sept. 2008, Chengdu.

Ferris, D.P., Czerniecki, M., and Hannaford, B., 2005. An ankle-foot orthosis powered by artificial pneumatic muscles. *J. Appl. Biomech.,* 21(2), pp. 189–197.

Hwang, S., Kim, J., and Kim, Y., 2007. Development of an active ankle-foot orthosis for hemiplegic patients. *In 1st Int.Convention Rehabil. Eng. Assistive Technol.: Conjunction 1st Tan Tock Seng Hospital Neurorehabil. Meet*., pp. 110–113.

Gate, D. H., Characterizing ankle function during stair ascent, descent, and level walking for ankle prosthesis and orthosis design, *Master's thesis, Boston University,* 2004.

Au, S., Berniker, M., Herr, H., Powered ankle-foot prosthesis to assist level-ground and stair-descent gaits., *Neural networks Journal*, vol. 4, No. 21, 2008.

Grundy, M., Tosh, P.A, and McLeish RD, S. L., 1975. An investigation of the centres of pressure under the foot while walkings. *Jour. of Bone and joint surgery.,* 57(1), pp. 98–103.

AUTHORS BIOGRAPHY

TRUNG NGUYEN received the B.E. (2008) degree in mechanical engineering from Hanoi University of Science and Technology, Vietnam and M.E. (2012) in Shibaura Institute of Technology, Japan.

He interests include lower limb orthosis for hemiplegia, control theory, motion planning, modeling and simulation.

Takashi KOMEDA received the Ph.D. degree from the University of Tokyo in 1987.

He became a Lecturer and an Associated Professor at Shibaura Institute of Technology in 1987 and 1990. He has been a full Professor since 1997. His interest is mechatronics for medical and rehabilitation applications.

FMECA MODELLING AND ANALYSIS IN BLOOD TRANSFUSION CHAIN

G. Borelli[(a)], F. V. Caredda[(b)], A. Fanti[(c)], G. Gatto[(d)], G. Mazzarella[(e)], P. F. Orrù[(f)], A. Volpi[(g)], F. Zedda[(h)]

[(a)] AOB - Azienda Ospedaliera G. Brotzu, Piazza Ricchi 1, 09121 Cagliari – Italy
[(b)] Centro Interdipartimentale di Ingegneria e Scienze Ambientali, University of Cagliari, Via S. Giorgio 12 - 09124, Cagliari – Italy
[(c) (d) (e)] Dipartimento di Ingegneria Elettrica ed elettronica, University of Cagliari, Piazza d'Armi, 09123, Cagliari – Italy
[(f) (h)] Dipartimento di Ingegneria Meccanica, Chimica e Materiali, University of Cagliari, Piazza d'Armi - 09123 Cagliari - Italy
[(g)] Dipartimento di Ingegneria Industriale, University of Parma, Via G.P. Usberti 181A- 43124, Parma – Italy

[(a)] gianlucaborelli@aob.it, [(b)] vale_caredda@tiscali.it, [(c)] alessandro.fanti@diee.unica.it, [(d)] gatto@diee.unica.it, [(e)] mazzarel@diee.unica.it, [(f)] pforru@unica.it, [(g)] andrea.volpi@unipr.it, [(h)] francescozedda@gmail.com,

ABSTRACT
This paper describes the modelling and analysis of the processes and activities used in the Blood Transfusion Centre of Hospital Brotzu (Cagliari – Italy), via FMECA (Failure Modes Effects and Criticalities Analysis) method, in order to enhance patient safety and improve clinical risk management. The first part of the study consists on an analysis of the present blood transfusion chain processes (AS-IS), obtained by reverse engineering. Then a concise description of the FMECA methodology is presented. After the introduction of the reengineered process (TO-BE), developed via introduction of RFID technology, the results of simulation will be presented. For each activity of the two configurations studied (AS-IS and TO-BE) some performance indicators were evaluated, then a sensitivity analysis has been carried out to investigate the consistency of FMECA analysis. Finally follows the comparison of results between the simulation of actual process and the reengineered one.

Keywords: FMECA, Blood Transfusion Chain, Sensitivity Analysis, Risk Priority Index

1. INTRODUCTION

Clinical Risk reduction, safety and quality improving of Italian Healthcare System (SSN) services, is nowadays a National priority and Transfusion medicine is one of the most interesting intervention areas. Due to high complexity of transfusion process, characterized by various checks, analysis and handlings of blood assets, probability of human errors is the most dangerous. Infectious exposure and mismatch between patient and assigned blood component group are the most serious transfusion risks.

Recent international studies reveal that pre analytical and clinical errors, which include incorrect ABO bedside testing and mistaken or missing patient identity check, represents about 80% of total adverse events (Ahrens, Pruss, et al. 2005). Particularly, "Acute Haemolytic Reaction" has deadly consequences in about 10% of cases (De Sanctis Lucentini, Marconi, et al. 2004). Statistical data of ABO-incompatible RBC transfusions incidence are relevant in different countries (rarely data are collected with standard procedures): Germany 1:36000; USA (New York) 1:38000; France 1:135207 (including autologous blood); Ireland 1:71428 (Ahrens, Pruss, et al. 2005).

Viral transmission has been reduced since the early '90, thanks to the introduction of compulsory tests based on sierology and Nucleic Acid Amplification Technique (NAT). Estimates of the risk per unit of blood in the post-NAT era are approximately 1:1,900,000 for HIV and 1:1,600,000 for HCV (Goodnough 2003).

Error rate reduction is the key factor for service quality and safety enhancing. Aims of the study are to devise a method to enhance patient safety and improve blood inventory management processes through an RFID-based process reengineering and also to estimate the potential clinical risk reduction (Orrù, Borelli, et al. 2010; Borelli, Pilloni, et al. 2010).

A key aspect for the success of the work consists in adopting the appropriate operational methodology for the analysis of the current and revised processes. In this field, the FMECA (Failure Modes and Effects Analysis Criticalities) is a valuable and tested tool, not only for the analysis of processes transfusion (Trucco, Cavallin 2010; Gianino, Finiguerra, et al. 2008) but also for the study of clinical risk in sensitive hospital areas (Coles 2006) and for the administration of drugs (Saizy-Callaert, Causse, et al. 2002).

The introduction of RFID technology in transfusion process, with the aim of improving the safety and quality of the processes involved, is nowadays under examination and it is the source of several application examples (Hohberger, Davis, et al. 2012; Sandler, Langberg, et al. 2006; Abarca, de la Fuente, et al. 2009; Van der Togt, Bakker, Jaspers 2011).

Although there are several problems associated with the use of this tracking technology in the hospital environment, such as privacy issues, the assessment of the effects of electromagnetic fields on biological materials (blood, platelets, plasma, etc.) (Otin 2011; Uysal, Hohberger, et al. 2012; Wang Q.L, Wang X.W, et al. 2013) and the economic feasibility of its use (Borelli, Orrù, Zedda 2012), the benefits achievable, especially in terms of patients safety, encourage the adoption of RFID in this field.

This study describes the experiences developed at Blood Transfusion Centre (BTC) of Brotzu Hospital (AOB) in Cagliari (Sardinia Island, Italy), where a new Blood Lab has been recently realized. Brotzu Hospital Blood Transfusion Centre operates in all standard transfusion processes: blood and platelet letting, therapeutic apheresis, blood-components separation, typing, analysis and assignment. About 50,000 blood units are treated every year, 60% of which are imported from other Italy regions in order to cover high Sardinian demand.

2. REVERSE ENGINEERING

In the first part of the study, a reverse engineering of present processes was performed, in order to map processes, to define information and material flows and to analyse infrastructure and technology status. Visits in Unit wards and in the Labs during working hours were scheduled and involved operators were interviewed. This study step involved BTC, the "Thalassemia adult patients day hospital ward of Thalassemia Hospital in Cagliari (MCT), and the "Cooley" BTC sub-department.

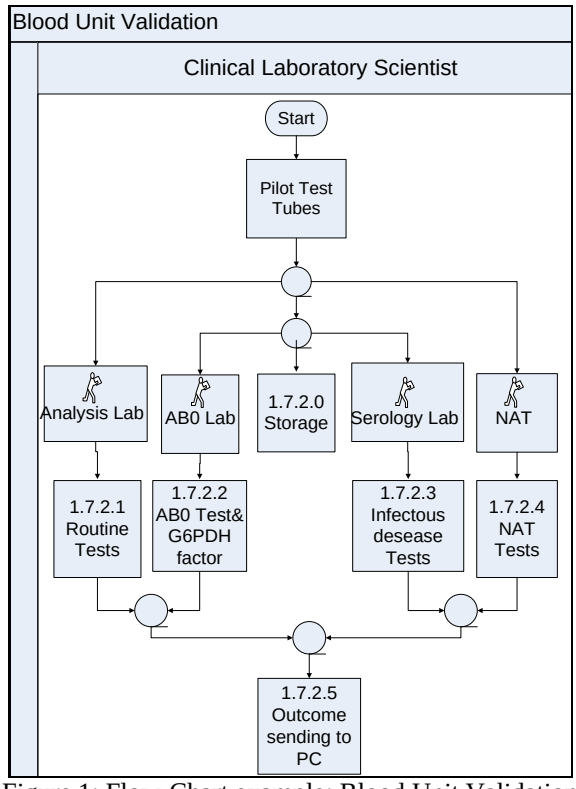

Figure 1: Flow-Chart example: Blood Unit Validation

Two main analysis tools were used: Flow Charts (figure 1) and Activity Forms. Flow chart is an algorithm graphical language. It allows to describe all process operations as a scheme. More than 20 Flow charts were designed, including both deep analysis charts and overall macro-process analysis charts. A specific form, which contains important data, was filled for each activity.

The whole Blood Chain has been conceptually split into two sub-systems in order to simplify and improve the analysis. The first one, called "Transfusion Loop", includes three macro-processes related to patient admission and blood component transfusion (Cooley; MCT Request; MCT Transfusion); the second one includes two process related to donation, blood components separation, validation and storage (Blood Donation; BTC). Analysis and synthesis study steps were independently performed for each sub-system; nevertheless they are mutually complementary (Orrù, Borelli, et al. 2010; Borelli, Pilloni, et al. 2010).

3. FMECA

Criticalities and process error sources were highlighted through a process FMECA, the improved evolution of FMEA (Failure Modes Effects Analysis), in order to suggest actions for process refinement. Since 2001 the Joint Commission on Accreditation of Healthcare Organizations (JCAHO) requires the incorporation of prospective process analysis methods as FMEA into organizational patient safety plans. FMEA approach is "bottom up": potential error modes were considered for each activity, causes were searched and potential consequences related to efficiency and effectiveness (patient safety) were evaluated.

While this step (FMEA) provided only a qualitative failure modes analysis (risk estimation), FMECA provided a criticality evaluation of each failure mode (risk evaluation): it was possible to pass from a qualitative to a quantitative analysis through the assignment of three numerical parameters (table 1), with values variable from 1 to 10, related to Detection Possibility (D), Severity (S) and error Frequency (F) and consequently by defining a Risk Priority Index (RPI):

$$RPI=D\cdot S\cdot F \quad (1)$$

Table 1: RPI's Factors and Their Values

INDEX	DETECTION POSSIBILITY
1	Always
2	Very High
3-4	High
5-6	Average
7-8	Low
9	Very Low
10	Impossible

INDEX	FREQUENCY
1	Impossible
2	Very Low (once a year)
3-4	Low (once a month)
5-6	Seldom (once a week)
7-8	Usually (more times a week)
9	Frequent (once a day)
10	Always (more times a day)
INDEX	**SEVERITY**
1	No harm for patient or cycle
2	Some consequences for the cycle
3-4	Some harm for the patient without further treatment
5-6	Moderate Haemolytic Reaction
7-8	Delaying of patient hospitalization
9	Acute Haemolytic Reaction
10	Possible deadly consequences

The FMECA analysis described was performed on the present blood transfusion chain (AS-IS) and on the reengineered process (TO-BE), the latter developed via introduction of RFID technology. The second sub-system of Blood Chain has not been the subject of process reengineering. Based on the FMECA analysis, for each activity of the two configuration, the following Key Performance Indicators (KPI) have been evaluated: average value of the RPI; RPI's peak; activity amount. After, we calculated the Normal Probability Density Function (2) (NPDF curves), parameterized in terms of mean value and standard deviation.

$$f(x,\mu,\sigma) = \frac{1}{\sigma\sqrt{2\pi}} e^{-\frac{1}{2}\left(\frac{x-\mu}{\sigma}\right)^2} \qquad (2)$$

The analysis of the Normal Probability Density Function curves is very important because it allows to visually establish the risk status of each activity examined. Less risky activities have curves with the peak of maximum moved towards the left part of the chart, corresponding to low values of RPI, and a contained tail, the right part of the curve. In contrast, riskier tasks will be characterized by the positioning of the maximum peak towards high values of RPI, and a very noticeable tail.

Aiming to investigate the degree of consistency of FMECA analysis method and the reliability of the results obtained, a sensitivity analysis has been carried out. Each and every factor (severity, detectability, frequency) that makes up the RPI was modified considering the variation of ±1 unit, outlining thus which are the factors that most influence the final result. In order to avoid the overstepping of the parameters outside their range (see table 1), the code has been programmed to saturate all the indexes to their boundary values (1-10). Finally, we compared the results of AS-IS and TO-BE, highlighting the differences for all individual activities and for the overall transfusion process.

All the analysis hitherto presented were carried out using a code, written with MATLAB, in which was implemented a numerical model of the FMECA.

4. RESULTS

4.1. AS-IS

The results reported in table 2 and figure 2 clearly show that blood transfusion (MCT Transfusion), although having the lowest activity amount (15), is the most "risky" of all the activities. This can be seen by analysing the values of the "Average RPI", 114 vs. an average of 30-45, which cause a shift of the NPDF (Normal probability Density Function) curve to the right side of the graph, corresponding to higher indices risk.

Table 2: KPI Results, AS-IS Process

ACTIVITY	Average RPI	Peak RPI	Activity Amount
Donation	33.9	80	16
BTC	31.2	108	17
Cooley	39.7	144	45
MCT Request	45.2	144	22
MCT Transfusion	114.0	162	15
Blood Chain	**56.31**	**162**	**115**

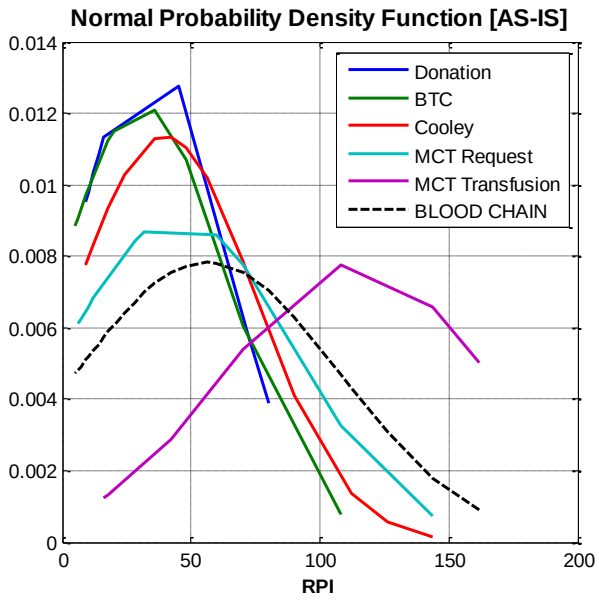

Figure 2: NPD Function associated with the activities of AS-IS configuration

Therefore all the efforts, through the reengineering procedure, must be focus on reducing the RPI of this particular process. Nevertheless, data suggest that even the other individual activities (especially those of the first level, such as Cooley, MCT Request, MCT Transfusion) are characterized by high values of KPIs that need to be controlled.

FMECA analysis highlights that the most critical activities are related to logistical assets recognition and manual operations, such as: patient identification; pilot test tubes and blood bags labelling; copying donation data from hand written papers to database management software; etc.

The results of AS-IS sensitivity analysis (table 3 and figures 3-4) show that the variation of the "frequency" factor entails greater changes in the KPI and NPDF curves, about 50%, while for the other two factors these changes are much smaller, about 10-20%.

During the collection of experimental data, via implementation of a pilot RFID system, will be therefore very important to quantify, with a low margin of error, the frequency of failure modes.

Table 3: AS-IS Sensitivity Analysis

Index Variation	**DETECTION**	
	Average RPI	*Peak RPI*
± 0	56.31	162
+ 1	68.56 (+21.8%)	180 (+11.1%)
- 1	45.74 (-18.8%)	144 (-11.1%)
Index Variation	**FREQUENCY**	
	Average RPI	*Peak RPI*
± 0	56.31	162
+ 1	86.77 (+54.1%)	243 (+50.0%)
- 1	31.92 (-43.3%)	81 (-50.0%)
Index Variation	**SEVERITY**	
	Average RPI	*Peak RPI*
± 0	56.31	162
+ 1	64.09 (+13.8%)	180 (+11.1%)
- 1	48.64 (-13.6%)	144 (-11.1%)

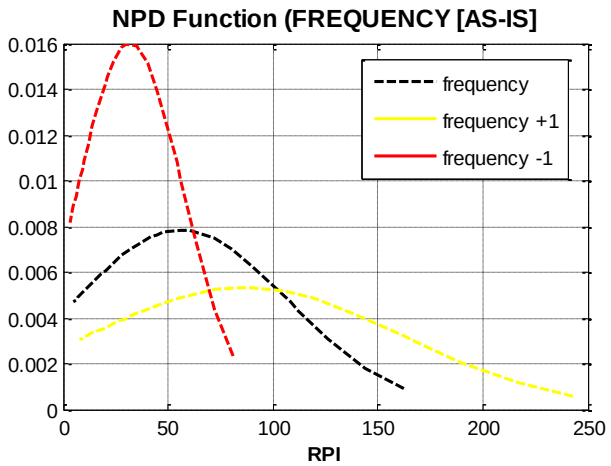

Figure 3: Sensitivity analysis of Frequency [AS-IS]

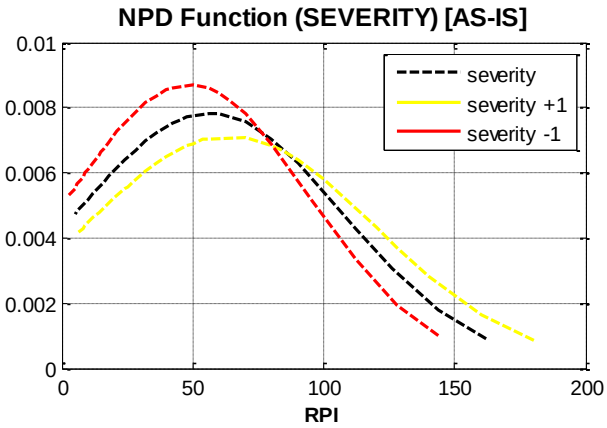

Figure 4: Sensitivity analysis of Severity [AS-IS]

4.2. TO-BE

The TO-BE configuration was analysed using the same methodology described for the AS-IS, both as regards the KPIs, both for sensitivity analysis.

Concerning KPI indices (table 4), the RFID technology implementation on processes of patient and logistic assets recognition, allowed us to obtain a significant reduction of the "Average RPI" and "Peak RPI" values of the following processes: MCT Request, MCT Transfusion.

Table 4: KPI Results, TO-BE Process

ACTIVITY	**Average RPI**	**Peak RPI**	**Activity Amount**
Donation	33.9	80	16
BTC	31.2	108	17
Cooley	24.8	70	48
MCT Request	16.9	36	23
MCT Transfusion	17.6	20	16
Blood Chain	**23.92**	**108**	**120**

Regarding the sensitivity analysis, it is possible to notice (Table 5, Figure 5) that results are quite similar to those of AS-IS configuration, with the frequency parameter able to lead to major deviations, about 30-60%, in case of overestimation or underestimation. The only exception to the AS IS model is represented by the factor "detection", whose changing involves a variation of 25-50% of the values of KPIs analysed.

Table 5: TO-BE Sensitivity Analysis

Index Variation	**DETECTION**	
	Average RPI	*Peak RPI*
± 0	23.92	108
+ 1	35.51 (+48.5%)	135 (+25.0%)
- 1	17.80 (-25.6%)	81 (-25.0%)

Index Variation	FREQUENCY	
	Average RPI	*Peak RPI*
± 0	23.92	108
+ 1	38.72 (+61.9%)	144 (+33.3%)
- 1	16.19 (-32.3%)	72 (-33.3%)
Index Variation	**SEVERITY**	
	Average RPI	*Peak RPI*
± 0	23.92	108
+ 1	27.83 (+16.3%)	120 (+11.1%)
- 1	20.15 (-15.8%)	96 (-11.1%)

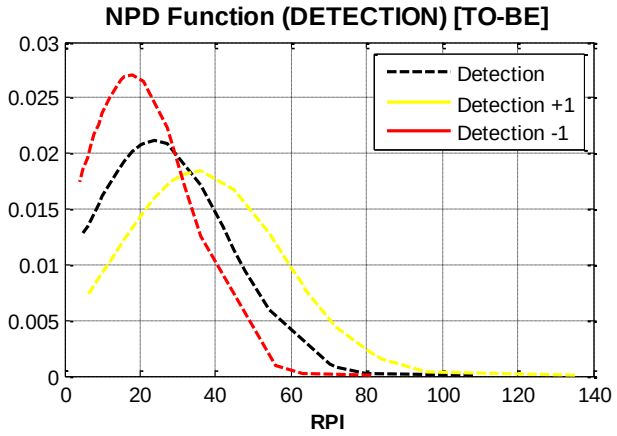

Figure 5: Sensitivity analysis of Detection [TO-BE]

4.3. Comparison AS-IS vs. TO-BE

The KPIs comparison of the two configurations analysed (table 6 and figure 6) shows that the average RPI of the TO-BE process (RPI = 23.9) is lower by about 57.5 % compared to the AS- IS (RPI = 56.3). This result was achieved mainly due to the significant reduction of clinical risk during the "MCT Transfusion" (-84.6 %) activity, obtained by the introduction of RFID technology in the processes of identification of patients and logistical assets (test tubes, blood bags, etc.). The introduction of the new technology, however, will result in a slight increase in the number of activities (+4.4 %) of the entire transfusion process.

Table 6: KPI Comparison, AS-IS vs. TO-BE Processes

ACTIVITY	Average RPI	Peak RPI	Activity Amount
Donation	0.0%	0.0%	0.0%
BTC	0.0%	0.0%	0.0%
Cooley	-37.7%	-51.4%	+6.7%
MCT Request	-62.6%	-75.0%	+4.6%
MCT Transfusion	-84.6%	-87.7%	+6.7%
Blood Chain	**-57.5%**	**-33.3%**	**+4.4%**

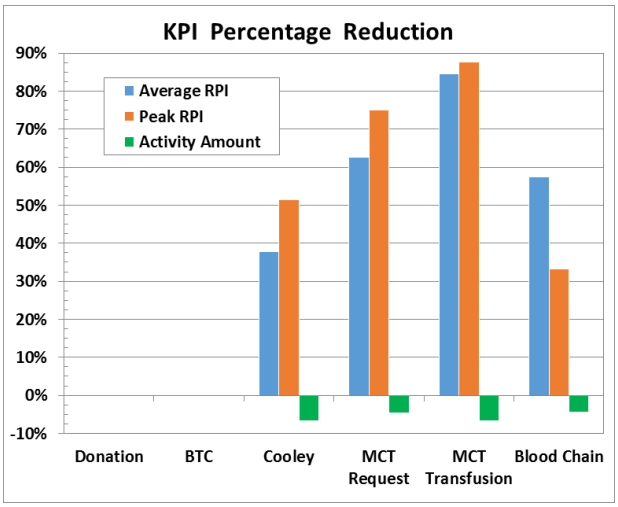

Figure 6: KPI Comparison, AS-IS vs. TO-BE

The difference between the current process and the reengineered one is clearly visible in figure 7. The graph shows both the improvement achieved in terms of reducing overall risk, shifting the mean value of the curve towards lower values of RPI, both the decrease of the peak values, the end of the curve at highest RPI. In the TO-BE process is also possible to appreciate the sharp decrease of the deviation of the values round the average, consequence of a widespread improvement on a large number of processes and activities.

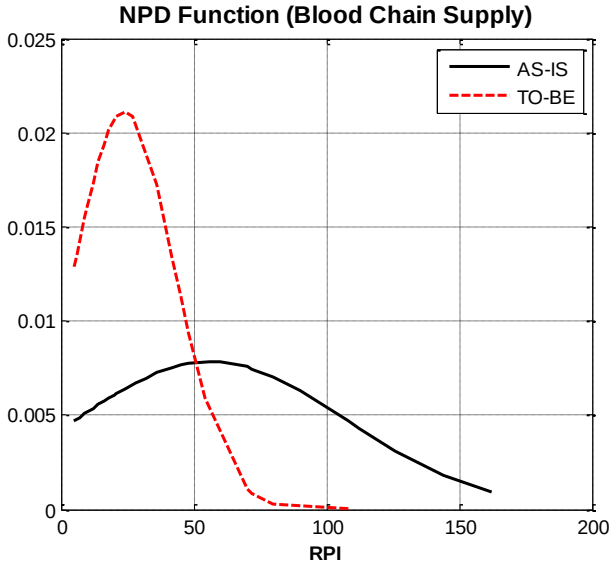

Figure 7: NPD Function comparison between AS-IS and TO-BE configuration

Despite the good results achieved, in terms of reducing the overall risk indicators (KPIs), it is possible to see in the TO-BE curve (figure 7) a queue corresponding to high RPI values and low NPD Function values. This is due to the lacking reengineering implementation of the second level of the Blood Chain, that is processes related to blood donation and the processing and storage of blood bags, both

performed in the Blood Transfusion Centre (BTC). Any future interventions on these two activities will improve the overall result, allowing a further reduction of the clinical risk. This result could be graphically evaluated through the shift of the peak of the curve to the left side of the graph, i.e. towards lower risk indices, and a consequent raising of the values of NPD function, which indicate an overall decrease of the probability of risk related to the fulfillment of the most adverse situations of an accident during the blood transfusion procedure.

5. CONCLUSIONS

A process reverse engineering was performed in order to identify and map the whole Blood Chain used in the BTC of AOB and in the "Thalassemia adult" ward of MCT, both located in Cagliari (Italy). Two configurations of the process were analysed: the first involving the actual blood chain (AS-IS), the other concerning the reengineered process (TO-BE), developed by introduction of RFID technology.

Using FMECA method, potentially error affected activities were founded and failure modes were classified by a risk priority index (RPI) which included detection possibility, severity and frequency factors.

Blood transfusion was identified as the process with foremost risk and FMECA analysis clearly pointed out that the most critical activities are related to logistical assets recognition and manual operations.

Results of the reengineered process have showed the improvement achieved in terms of reducing risk, not only of a large number of processes and activities, but of the overall Blood Transfusion Chain by about 57.5 % This result was achieved mainly by the introduction of RFID technology in the processes of identification of patients and logistical assets (test tubes, blood bags, etc.).

Regarding the sensitivity analysis, results showed us that the variation of the "frequency" factor leads to greater changes in the KPI and NPDF curves, implying therefore the need of a very thorough quantification of this parameter to avoid errors about the clinical risk assessment.

ACKNOWLEDGMENTS

Special thanks to "*Regione Autonoma della Sardegna*" (L.R. n.7-2007) and to "*Fondazione Banco di Sardegna*" for financing this research activity.

REFERENCES

Ahrens N, Pruss A, Kiesewetter H, et al, 2005. Failure of bedside ABO testing is still the most common cause of incorrect blood transfusion in the Barcode era. *Transfusion and Apheresis Science*; Volume 33, 25-29.

De Sanctis Lucentini E, Marconi M, Bevilacqua L, et al. 2004, *Risk Management in Sanità. Il problema degli errori.* Ministero della Salute Commissione tecnica sul rischio clinico, Roma. Available from: http://www.salute.gov.it/imgs/C_17_pubblicazioni_583_allegato.pdf [accessed 10 February 2012]

Goodnough LT, 2003, Risks of blood transfusion. *Crit Care Med*;31, S678–S686.

Orrù PF, Borelli G, Pilloni MT, et al. 2010, RFID System Project for Enhancing Blood Supply Chain Safety and Blood Transfusion Center Productivity. *Proceedings of Apms International Conference Advances in Production Management Systems*

Borelli G, Pilloni MT, Orrù PF, et al. 2010, Reduction of clinical risk in blood transfusion center with an RFId system. *Proceedings of The International Workshop on Applied Modelling & Simulation*. 218-223.

Trucco P, Cavallin M, 2010. Multidimensional FMECA for assessing the impact of RFId technology on blood transfusion risks. *Proceedings of European Safety and Reliability Annual Conference,* 70-78. 5-9 September 2010. Rhodes-Greece.

Gianino M.M, Finiguerra I, Maina L, et al, 2008. The risks in the blood transfusion: An application of the Failure Mode and Critical Effect Analysis (FMECA) technique. *Mecosan*; Volume 17, 85-103.

Coles G, 2006. A procedure for using fmeca to assess high-risk healthcare processes. *Proceedings of the 8th International Conference on Probabilistic Safety Assessment and Management,* 7p. 14-18 May 2006. New Orleans, LA-USA.

Saizy-Callaert S, Causse R, Thébault A, Chouaïd C, 2002. Failure Mode, Effects and Criticality Analysis (FMECA) as a means of improving the hospital drug prescribing. *International Journal of Risk and Safety in Medicine*; Volume 15, 193-202.

Hohberger C, Davis R, et al, 2012. Applying radio-frequency identification (RFID) technology in transfusion medicine. *Biologicals*; Volume 40, 209-213.

Sandler S.G, Langeberg A, et al, 2006. Bar code and radio-frequency technologies can increase safety and efficiency of blood transfusions. *Laboratory Medicine*; Volume 37, 436-439.

Abarca A, de la Fuente M, et al, 2009. Intelligent sensor for tracking and monitoring of blood temperature and hemoderivatives used for transfusions. *Sensors and Actuators, A: Physical*; Volume 152, 241-247.

Van der Togt R, Bakker P.J.M, Jaspers, M.W.M, 2011. Framework for performance and data quality assessment of Radio Frequency IDentification (RFID) systems in health care settings. *Journal of Biomedical Informatics*; Volume 44, 372-383A.

Otin R, 2011. Numerical study of the thermal effects induced by a RFID antenna in vials of blood plasma. *Progress In Electromagnetics Research Letters*; Volume 22, 129-138.

Uysal I, Hohberger C, et al. 2012. Effects of radio frequency identification-related radiation on in vitro biologics. *PDA Journal of Pharmaceutical Science and Technology*; Volume 66, 333-345.

Wang Q.L, Wang X.W, 2013. Impact on storage quality of red blood cells and platelets by ultrahigh-frequency radiofrequency identification tags. *Transfusion*; Volume 53, 868-871.

Borelli G, Orrù PF, Zedda F, 2012, Economic assessment for a RFId application in transfusion medicine. *14th International Conference on Harbor, Maritime & Multimodal Logistics Modelling and Simulation*, 134-139. 19-21 September 2012. Vienna-Austria.

AUTHORS BIOGRAPHY

Gianluca Borelli was born in Cagliari in 1967. Since 1997 he is Chief Engineer and Head of the Facility Operations at Brotzu Hospital in Cagliari. He developed several Healthcare projects for Italian Hospitals. He is member of the board of S.I.A.I.S. (Società Italiana dell'Architettura e dell'Ingegneria per la Sanità).

Francesco Valentino Caredda was born in Cagliari in 1983. He obtained Bachelor's Degree in Mechanical Engineering on December 2006 and Master's Degree in Mechanical Engineering on April 2010 at the University of Cagliari (Italy). In June 2013, at the same University, he obtained the PhD in Mechanical Design, with a dissertation about "Energy Audit of Brotzu Hospital". He is currently a research fellow at CINSA (Interdepartmental Centre of Engineering and Environmental Sciences) in Cagliari. His main research activities concern Logistics and RFID application in Health care facilities, Energy Audit.

Alessandro Fanti received the Master degree in electronic engineering and Ph.D. degree in electronic engineering and computer science from the University of Cagliari, Cagliari, Italy, in 2006 and 2012, respectively. He currently holds a post-doc scholarship for design of microwave components. His research activity is numerical methods in electromagnetics.

Gianluca Gatto is Assistant Professor at DIEE (Department of Electrical and Electronic Engineering) in Cagliari. His research interests concern design and implementation of predictive control algorithms for switching power converters and electrical drives, modelling of power electronics converters, electromagnetic compatibility interference issues.

Giuseppe Mazzarella was born in 1959. From 1990 to 1992 he was Assistant Professor of "Electromagnetic Fields" at Federico II University in Napoli. From 1992 to 2000 he was Associate Professor at DIEE – Cagliari. He is currently Professor of "Electromagnetic Fields" at DIEE in Cagliari.

Pier Francesco Orrù was born in Cagliari, May 5, 1973. Since June 2006 he works in the Scientific Area "Industrial Plant Mechanics", at the DIMCM (Mechanical, Chemical and Material Engineering), University of Cagliari. The main research areas concern the optimization of industrial processes, the design of automated systems for the food industry and numerical applications (FEA and CFD) in plants.

Andrea Volpi was born in Parma, April 8, 1979. Since November 2008 he works in the Scientific Area "Industrial Plant Mechanics", at the Department of Industrial Engineering, University of Parma (Italy). Since 2006 he is research manager and coordinator of activities of the RFID Lab, at the Department of Industrial Engineering of the University of Parma.

Francesco Zedda was born in Cagliari, October 29, 1983. He obtained Bachelor's Degree in Biomedical Engineering on February 2008 and Master Degree in Mechanical Engineering on October 2010 at the University of Cagliari (Italy). Nowadays he is attending the third year of Mechanic Design PhD course at the same University. His main research areas concern Logistics and RFID application in Health care facilities.

LEAN MANAGEMENT TOOLS APPLIED TO HOSPITAL FACILITIES: THE CASE OF AN OPERATIVE UNIT OF INTENSIVE CARE

Francesco Longo [(b)], Antonio Calogero [(b)], Letizia Nicoletti[(c)], Marina Massei[(d)], Fabio De Felice[(e)], Antonella Petrillo[(f)]

[(a)(b)(c)] DIMEG, University of Calabria, Italy
[(d)]DIME University of Genoa, Italy
[(e)] University of Cassino, Italy
[(f)] Department of Engineering - University of Naples "Parthenope", Italy

[(a)] f.longo@unical.it, [(b)] antonio.calogero@unical.it, [(c)]letizia.nicoletti@unical.it
[(d)]massei@itim.unige.it, [(e)]defelice@unicas.it, [(f)] antonella.petrillo@uniparthenope.it

ABSTRACT

This paper presents the results of a simulation study that has involved a public Facility Healthcare, in particular an operative unit of intensive care. This unit represents the core of a healthcare facility where patients with abnormal vital signs as a result of diseases of the medical or surgical treatment of trauma are greeted. The approach proposed in this research work begins with the study and analysis of the processes that take place within the unit of intensive care; after that tools and methods of lean management are applied by using a Modeling & Simulation based approach. The work illustrates the improvement obtained with the application of Kanban technique and the 5S method. To this end, a simulation model of the intensive care unit considering the main processes and activities has been developed. Main goal of simulation was to see to which extent the operative unit is improved after the changes implemented through lean management tools and methods. The simulation model highlights the delays due to poor internal organization and the improvements achieved by redesigning the flows, minimizing the pathways and reengineering the layout of the operative unit. The results obtained by using the simulation model have been transferred to the real system with a relevant increase of the intensive care unit performances (giving a quantitative measure of the value added to care and wellness of patients).

Keywords: Health care facilities, Lean Management, Modeling & Simulation, Kanban

1. INTRODUCTION

Many manufacturing companies, sought to master the principles of lean thinking, other industries were also struggling with process improvement and health care was one of these industries. The core idea of the Lean approach is to maximize value for customers while using fewer resources and minimizing waste. Lean management theory has a long history of success in manufacturing. As matter of fact, the same Lean principles and tools that are applied in manufacturing plants are directly applicable to the health care facilities (Ross and Simon., 2012). Indeed, the root cause for failures is often the same both for manufacturing and health care systems, e.g. breakdowns in communications and misunderstanding the needs of customers. In the literature, there are many articles that focus on the use of Lean management techniques in health care and give descriptions of Lean theories, tools, empirical studies and applications about improvement of processes and service delivery; as mentioned by Machado et al. (2010), the Lean approach is a tested methodology for improving the way work gets done. Lean has been spreading slowly and inexorably from industry to industry for over half a century as its principles have been fine tuned, tested, demonstrated and proved.

Another important aspect to consider is the improvement of processes through modeling and simulation based approaches. Indeed, there is a large availability of discrete event simulation models that have been used in different domains: from industry to supply chain (consider for instance Rego Monteil et al. 2013), from healthcare to business management, from training to complex systems design (i.e. Bruzzone and Longo 2013). Simulation modeling is a way to test changes and give ideas for improvements before the implementation or tests in the real system. The focus of this work is oriented on the use of simulation as decision support in health care facility management. Indeed Lean management and discrete-event simulation (DES) can be jointly used for improvement of processes and service delivery (Robinson et al., 2012). Rarely they are used together. Different examples of simulation applications in health care can be found in research literature, to mention a few: Holm et al. (2013) deal with the improvement of hospital beds utilization through simulation and optimization; Weerawat et al. (2013) presents a generic discrete-event simulation model for outpatient clinics in a large public hospital.
Bruzzone et al. (2011) use simulation to analyze obesity epidemics.
Bruzzone et al. (2013) propose a simulation model to improve the overall efficiency of a healthcare facility showing how discrete event simulation can be

profitably used to design correctly doctors and nurses workloads as well as resources utilization.

Simulation offers immediate feedback about proposed changes, allows analysis of scenarios and promotes communication on building a shared system view and understanding of how a complex system works (Longo et al., 2013; Forsberg et al., 2011). As for mathematical models for medical parameters that can be easily embedded in simulation models, meaningful applications and case studies can be found in Winkler et al. (2013) and Winkler et al. (2011).

Case studies of Lean improvement simulation-based are oriented primarily on Emergency Department (Zeltyn at al., 2011) where there is a continuous flow of patients, leading to the medical personnel overload and to excessive waiting times to receive proper care. These adverse effects directly affect the patient satisfaction levels, the ability of the medical professionals to attend promptly to patients' health issues and generate unnecessary costs. Identifying the sources of waste and improving all the processes involved is the most suitable way to provide a better care and higher patient satisfaction and to increase the operational efficiency and the ability of the medical professionals to intervene on time (Khurma et al., 2008).

This research work begins with an experimental approach in a healthcare facility that includes the operative unit of intensive therapy and resuscitation, where we have addressed our studies. The experimental approach begins with the study and analysis of the operative unit, carrying out interview, data collection, processes and activities mapping. An important premise is that the production and delivery of health services in this operative unit is a complex task, where human and material resources should be planned and synchronized to ensure the effectiveness of the action and the expected result. The fundamental phases of this research work were:

- Interview and data collection in the intensive care unit;
- Conceptual models and simulation model development;
- Simulation analysis of the current system;
- Identification of strengths, weaknesses and actions to improve.
- redesign of the processes by using the simulation model jointly with all the technical and legislative references
- Simulation results transfer in the real system;
- Implementation of pilot projects with continuous support and methodological advice;
- Training of the operators involved to the new processes

Building the simulation model has revealed quite a difficult task due to the complexity of the processes, activities and procedures of the operative unit. There are many variables to consider and different entities flows. The simulation model was built on the real layout of the operative unit, identifying the location of patients' rooms, the beds, medicines and materials, equipment, paths followed by the staff and patients, entry rooms, doctors and nurses locations. The simulation model has been developed by using the simulation software Anylogic. The main goal of the simulation model was to see to which extent the operative unit can be improved by implementing lean tools and methods. The simulation model and the use of lean tools and methods have highlighted the delays due to poor internal organization and the improvements achieved by redesigning the flows, minimizing the pathways and reengineering the layout of the operative unit. The results obtained by using the simulation model and the lean tools and methods were both qualitatively and quantitatively relevant.

2. LEAN MANAGEMENT APPROACHES APPLIED TO HEALTHCARE FACILITIES

The basic idea of Lean Management is fundamentally that the healthcare organisation should be obsessively focussed on the most effective means of producing value for their patients. The Lean management contributes with a set of principles and tools to disentangle the various forms of waste and tackle their root causes. Used separately, these tools are helpful. Used together, in a planned, disciplined and co-ordinated way, they can chip away at accumulated layers of waste to release the organisation's real potential (Jones et al., 2006). To better clarify this concept we denote some possible approaches as explained in Jones et al. (2006):

- focus on improving the end-to-end process;
- where things are hard to see, make them as visible as possible so that everyone can see when and if there is a problem;
- where responsibilities are not clear, create detailed, standardised processes to avoid error, ambiguity and confusion – and as a springboard for improvement;
- where there is unnecessary work or waste, whether it is in the form of excess inventory, excess processing, excess movement of people or things, waiting and queuing, redesign the work;
- where problems are not resolved, ferret out their root cause.

Furthermore, targets must be clearly defined and achieved on regular basis. Targets can be achieved by using a Patients' perspective (everything is done to create a value-added for the patient), by pulling resources and work where needed in order to reduce queuing, bottleneck and waste, by analyzing all the processes steps by steps to understand how processes activities affect each other.

Lean also means a correct understanding and elimination of waste. The elimination of waste passes

through the involvement of all the people working in the same unit. Indeed, most of the people are usually reluctant to changes; they must be opportunely convinced that changes are needed to improve the overall system performances as part of a continuous improvement process. Workers need also to be fully involved in the change, so they can promote it, discover and eliminate all the sources of waste.

2.1 Lean Tools applied in operative care unit

The application of Lean tools to an operative care unit encompasses a combination of the following steps:

1. Observe a problem, phenomenon, practice, activity;
2. Formulate a hypothesis to explain why the issue and how the process might be modified to yield an improvement;
3. Predict the result of the improvements;
4. Test the prediction by implementing the changes;
5. Reassess the hypothesis and prediction, based on the test results;

The first method that has been applied was the process mapping. Mapping the process of the operative unit has required the involvement of all the staff. For each work shift, physicians, nurses, technicians have used and filled ad-hoc forms to capture specific information about activities carried out, starting and ending time, type of activity, problems encountered and notes about how to improve the activity considered.

Particular emphasis was given to the administration of the therapy process. Indeed, the activities that characterize this process have many inefficiencies in different areas including external supply, internal organization, optimal arrangement of resources and medicines, control methods. For this reason it was useful to use the 5S method that is a specific method for organizing a workspace. The goal of the 5S method is to organize the work area in the way that needed objects are found easily and quickly and the work can be done more efficiently by creating smooth workflow. 5S refers to the five Japanese words “seiri, seiton, seiso, seiketsu, shitsuke”. In English these words mean “organize, orderliness, cleanliness, standardize, discipline”. In order to maintain the 5S acronym, five related English words beginning with the letter S have been adopted: “sort, straighten, scrub, standardize and sustain” (Zidel, 2006). Every word describes a step in the 5S work space transformation process. The first step “Sort” is the elimination of all the unneeded items from the work area. There is no space for useless things so storage of not needed items is absolutely unnecessary.
The second step “Straighten” means that items must be placed in well defined positions in order to reduce or eliminate time for searching. Items should be easily found and used. Those items that are frequently used should be placed closer to the workplace compared to rarely used items. A better overview of storage areas can simply be achieved by implementing a labeling system. The third step “Scrub” describes the need of a clean environment. Everything should be well cleaned and bright to provide a more comfortable workspace and subsequently increase efficiency and quality. Keep clean and orderly helps to the discovery of problems. The fourth step “Standardize” helps to define and formalize new standards of accommodation, order and clean achieved by the implementation of the first three S’s. The fifth step “Sustain” is about maintaining and improvement standards and results achieved. Everyone is responsible for maintaining goals. Accordingly, communication is fundamental during this phase. Staff must be instructed to this new kind of system and educated on how to implement, use and, most importantly, maintain it (Machado V. et al., 2010). In the Table 2, attached to the paper, the actions to be undertaken during the implementation of the method 5S are shown.

Another method is the Visual Management that is closely linked to the 5S method and helps in arranging a well-ordered and organized workplace. The use of signs, lines, labels, lists and colour coding facilitates materials searching and picking. Visual management can help in pointing out whether the process was operating correctly or not and what kinds of quality problems and errors were occurring (Fillingham, 2007). Finally, a way to handle a system of planning and control is the Kanban. In Japanese it means card, and it is used in the stages of production or services by operators to notify the warehouse that a stock-out is going to occur. We can distinguish three different types of kanban:

- kanban movement that is used to signal to the upstream stage that the material can be taken from the warehouse and transferred to a specified destination;
- kanban production which signals to the manufacturing process to enable the machining of a certain component that will be then deposited in a small warehouse;
- kanban sales used to signal the necessity of material to an external supplier.

In our work, we used the kanban movement which provides information on the category of material, the amount of material required, warehouse picking and delivery destination. By creating a Kanban, the operative unit will avoid stock-out occurrences as well as calls to the hospital pharmacy for an emergency delivery.

3. THE OPERATIVE UNIT OF INTENSIVE CARE AND RESUSCITATION

The Intensive Care Unit and Resuscitation (ICUR) analyzed in this paper is located in a public healthcare facility in Southern Italy and it is operating since 70s’. The ICUR activities take place without interruption H24, 7 days a week and 365 days per year. The organization aims at responding to emergencies and to "critical events" immediately when patients are in danger of life. For this reason, it is necessary to have a

well trained staff, always ready to react and understand what is happening both inside and outside the hospital. The ICUR consists of four major zones:

- The Patient's Care Zone and the Clinical Support Zone are two zones that include the patients' rooms and adjacent areas; their primary functions are the direct patients' care.
- The Unit Support Zone refers to areas of the unit where administrative, materials management, and staff support functions take place.
- The Family Support Zone refers to areas designed to support families and visitors.

The Patient's Care Zone includes two rooms with seven beds, called "open space", and a room with two beds. Each bedroom is connected to a sophisticated monitoring system that ensures the constant monitoring of patient's vital functions and it is equipped with all the necessary equipment to provide respiratory care and infuse fluids, foods and medications.

The operative unit includes the following key-personnel:

- The Head Physician is a medical specialist in anesthesia and intensive care and he/she assumes the ultimate responsibility for clinical and organizational choices. He/she coordinates the work of physicians and nurses. He/she also establishes operational objectives and, in collaboration with the nursing coordinator, helps to achieve them through leadership and correct stimulation of all the operators involved. The Head Physician responds directly to the Director of the Hospital.
- The Senior Physician can replace the Head Physician taking the same tasks and responsibilities in case of Head Physician absence. He/she is a medical specialist in anesthesia and intensive care, which follows the day by day clinical course of hospitalized patients. He/she guides and coordinates the work of physicians, ensuring the continuity and adequacy of treatment choices. He/she draws up internal guidelines in agreement with other physicians and supervises their correct application. Coordination capabilities and high clinical skills are required.
- The Medical Assistant that supports both the Head and the Senior Physicians. He/she has the fundamental task to execute immediately the necessary life-saving procedures, safeguarding the well-being of patients admitted to the ICUR in cases of serious alteration of vital functions (e.g., cardiac, respiratory, neurological, metabolic problems). He/she also deals with emergencies arising outside the hospital (helicopter and ambulance).
- The Head Nurse is responsible for the care and clinical decisions laid down by the head physician and his staff; the Hear Nurse is also responsible for the organization of resources and materials and coordinates all nurses and support workers. The Head Nurse contributes to achieve organizational and clinical goals and spurs of all the involved nurses. He/She collaborates to guidelines drafting for procedures and protocols. The Head Nurse is also in charge of medicines and medical products logistics management.
- The Professional Nurse belongs to the paramedical personnel administering therapies to the patients. The Professional Nurse carries out the activities for health prevention, care and preservation autonomously, based on laws, ethics and professional practice. Professional Nurses perform also several essential tasks, such as continuous monitoring of the patient, administration of the therapy prescribed by physicians, the hygienic care and the patient transport (if needed).
- The Technical Operator supports the operative unit by carrying out tasks for the nursing care, such as delivery of biological materials for laboratory tests, disinfection / sterilization of medical equipment, warehouse management materials. The Technical Operator works directly with nurses in the hygienic care and transport of patients.
    - The ICUR is also characterized by the presence of machineries and equipment that surround the patient: mechanical ventilators that help respiratory muscles in case of respiratory failure;
    - infusion pumps that ensure fluid administration (drugs, food, etc.);
    - aspirations systems needed to remove bronchial secretions from lungs;
    - monitors used to display continuously the patient's vital signs (heart rate, pressure, temperature, etc.). Monitors emit many types of alarms, each with its own meaning, than can be heard anywhere in the operative unit. Each monitor is also connected to a central screen that allows the simultaneous observation of all hospitalized patients.

4. INTERVIEW AND DATA COLLECTION IN THE ICUR

At the beginning, the ICUR team thought there was too much variation in their work to apply any method, concept or tool that would help them. To this end, the very first action was to create a Current Value Stream map. The map included all processing steps from the moment the patients enter in operative unit until they are discharged. In order to map all the processes and activities correctly, we spent a 6 months period in the ICUR. Data collection for processes mapping has been done by using an ad-hoc template (see figure 1), where for each task (activity) of a specific process a number of information, including criticalities, were reported. The survey was carried out by professional nurses, for a period of thirty days and for all three daily shifts. In

addition, the processes were extensively analysed, observing all the activities, the operators' paths and the layout of the operative unit. All the information collected revealed a clear situation of non-organization. Each process presented problems mostly dependent on the hospital management policies (e.g. underpowered staff, too stressful shifts, etc.), on motivational factors (e.g., lack of professional recognition, lack of interest, lack of autonomy, lack of professional involvement), on poor communications and internal organization (lack of rules and procedures, inhomogeneous working groups, disorganized supply of medicines, non-optimal layout, etc.). To this end, table 1 shows different types of criticalities and their occurrence percentage over 90 observations collected during a 3 months period. In percentage terms, we can see that the most critical process refers to materials management. This process has a direct impact on the medical treatment of patients, because the time used to search for a medication or medical material in the warehouse (or in the worst case of missing material), decreases the time devoted to patients care.

In addition, there were other inefficiencies:

- medicines and medical equipment was positioned in the ward based on experience;
- Medicines and products could not be found immediately due to poor containers organization.
- The medicines and products inventory position were not updated according to medicines and products, consumed and ordered
- Quantity ordered for each medicine and product was often based on experience with consequent stock-out occurrences or excessive inventories (the latter may cause problems in other hospital department)
- Stock-out occurrences in case of emergency situations, force the staff to require medicines and products to the hospital pharmacy or in other operative units;
- the hospital pharmacy provides products based on historical data that are not in line with real demand;

DATE :	**Start Time :**	**Name:**	**Surname:**
No. Observation:	**End Time :**	**SHIFT** Morning ☐ Afternoon ☐ Night ☐	
Key-Personal :	Physician ☐	Nurse ☐	Technical Operator ☐

DATA COLLECTION

PROCESS	ACTIVITY	START TIME [hh:mm]	END TIME [hh:mm]	CRITICALITY

Figure 1: Form for data Collection within the ICUR

Table 1: Criticalities description and frequencies

Criticality description	Frequency measuring in 12 weeks	Percent on 90 observations
Interruption of the therapy administration for physician assistance	16	18%
Interruption of the therapy administration due to urgency intervention on broken machinery (absence of preventive maintenance)	36	40%
Patients waiting for CAT	10	11%
Picking material in the operative unit warehouse	44	49%
Missing material in the ICUR	64	71%
Presence of only two nurses during the shift (under sizing)	8	9%
Lack of information	20	22%
Lack of materials on dressing carts	28	31%
Work overload (reduced time for each patient)	20	22%
Poor knowledge of medical electrical equipment	32	36%

- the warehouse of the ICUR contained many low rotating products;
- optimal locations for medications and medical materials within the ward had not been identified;
- medical electrical equipment had not been controlled after use (absence of preventive maintenance);
- Personnel was not perfectly trained to use new medical electrical equipment;

All the anomalies described above represent a waste which substantially decreases the time devoted to patients and the vision of value-added activities.
A significant problem within their Value Stream was the lack of standardization in terms of how different team members carry out their assessment, testing, care and treatment. Therefore, many meetings were planned and organized with the goal of developing standard practices to increase the time for patient care and provide the optimum care (improve quality and service).
In the following, we will describe some improvement actions implemented in the ICU. In particular, we will refer to the logistics management of medicines and medical materials.

5. THE ICUR SIMULATION MODEL

The main idea behind our research work was to develop a discrete event simulation model able to recreate the complexity of the ICUR (as described in the previous sections). The proposed simulation model has been used as test bed to show how Lean tools and methods can be profitably used to improve the ICUR performances. The following section describes all the steps of the simulation model development.

1st Step - Environment representation

A 2D layout of the ICUR has been imported in AnyLogic and has been referred to create a transportation network defining the paths of the staff and patients, rooms and bed's location, medicines, materials and equipment storages, entry rooms. Within the network, a rectangle represents an entry or exit point, the idle position of some resources, a destination point in the facility. A line is the path followed by the entities moving among rectangles. This way, we define a network topology where entities and resources are directly traceable.

2nd Step – Defining the network resources pool

According to the AnyLogic Library, the resources network can be of three types: moving, portable and static. In our model, physicians and nurses are moving resources. Stretchers, tools, equipment, medicines medical material are portable resources. Procedures rooms, therapy, beds assignment, placement of patient records are the static ones.

3rd Step – Animating Patients and Resources

The third step was to draw animations to depict patients, doctors, nurses, stretchers, equipment, medicines.

4th Step – Creating a Flowchart for each process

This model has been built considering five fundamental processes.

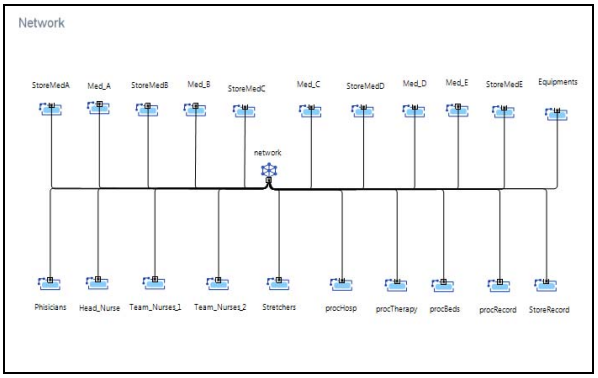

Figure 2: Simulation Model network and resources objects

Patients' Arrival process:
Only serious patients with disease that involve vital organs are admitted into the ICUR. Critical patients may arrive from two different sources: from the Emergency Room or from other operative units. During the six months period spent at the ICUR we observed 276 incoming patients, 57% coming from other operative units and 43% from the emergency room. The average hospitalization time is 20 days. When patients arrive, nurses are required to take the incoming stretcher, attach the patient to different machineries (to monitor vital parameters) and then to move the patient to the bed location. The figure 3 depicts the flow chart of the Patients' arrival process.

Patient record creation process
For each patient arrived into the ICUR, the physician creates a medical record, where all the information about the patient and the therapy are stored (the figure 3 also shows the Patient record creation process).

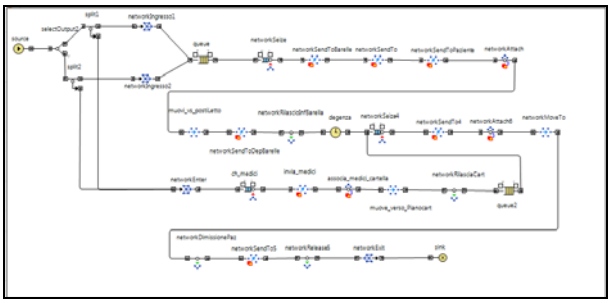

Figure 3: Simulation model Flow Chart: Patient Arrival Process and Patient record creation process

Hygienic care process
The process is repeated three times per day. For each patient and every 8 hours, two nurses perform the hygienic care process. The figure 4 depicts the flow chart of the hygienic care process.

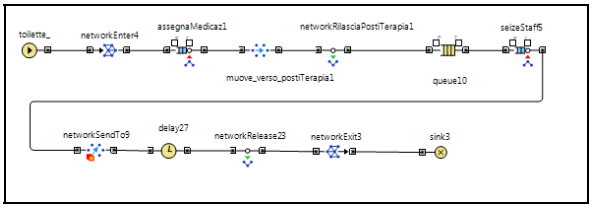

Figure 4: Simulation model Flow Chart: Hygienic care process

Medication and monitoring process:
Patients in the ICUR require continuous monitoring, vital functions stabilization and / or invasive procedures. "Intensive care" is the highest available level of continuous treatment of the patient. In this process, each patient represents a static entity that requires the intervention of nurses several times a day. The figure 5 depicts the flow chart of the Medication and Monitoring Process.

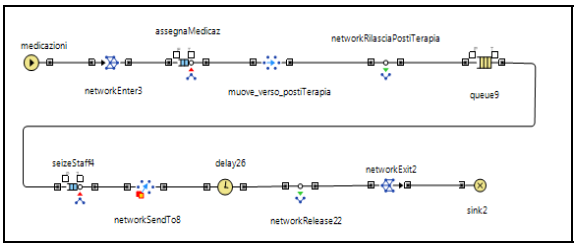

Figure 5: Simulation model Flow Chart: Medication and monitoring process

Therapy administration process:
This process is the core of our analysis. Here, wastes entail less time for patients care. Based on the data analysis, the simulation model allows distinguishing five types of medications necessary to maintain life and nutrition of patients. These medications (each one made up of specific products) are stored in different points inside the operative unit, causing inconvenient and delays in picking operations and therapy administration. The simulation model demonstrates the benefits achieved applying lean methods that lead to the design of a new layout and to the definition of new logics for storage and inventory management. The process is trigged three times/day according to a well-defined schedule and all nurses are required to read the medical record, to pick medications in the storage location, to prepare products, medicines and medical devices and finally to perform therapy administration at bed position. The figure 6 depicts the flow chart of the therapy administration process.

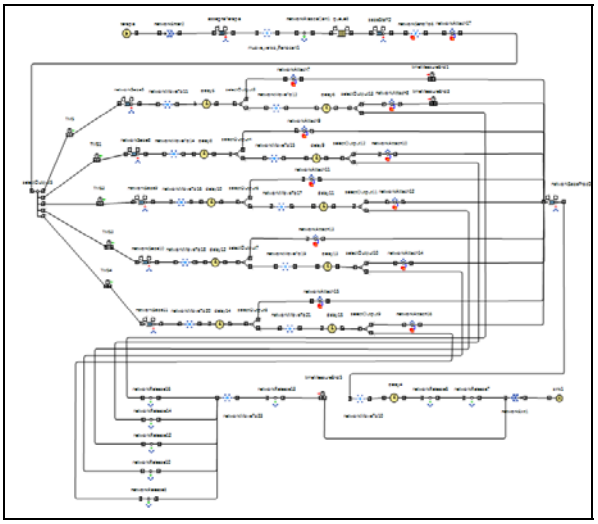

Figure 6: Simulation model Flow Chart: Therapy administration process

The five processes described above have been implemented as part of the simulation model that seeks to recreate the ICUR complexity. During the simulation runs it is possible to assess time savings (that can be devoted to patients), if the labor organization is optimized and if it is grounded on clear operational methodology with a smooth flow of activities. The last step of our simulation study is the simulation experimentations and results analysis.

6. ANALYSIS AND SIMULATION RESULTS

The main goal of the simulation model is to assess if the performances of the operative unit are improved after the changes implemented as a result of the lean methods application. Indeed the simulation model is able to highlight the delays due to poor internal organization and the improvements achieved by redesigning the flows, minimizing the pathways and reengineering the layout of the operative unit.
Simulation experiments were carried out considering three different scenarios. The first scenario simulates the ICUR as it is; indeed it happens frequently (as shown in table 1) that when nurses prepare the therapy, because of the lack of medicines in the ward, they are obliged to reach the warehouse and look for medicines, materials and machineries into warehouse shelves. This operation, when repeated many times during the same day for multiple patients, inevitably generates a waste of time. The figure 7 shows the simulation results of the therapy administration in the scenario 1. The process begins with the medical record reading, then the nurse, according to the ward situation may be required to move into the storage and search for medicines, materials and machineries. The simulation model evaluates and average time of about 17.8 minutes between medical record reading and the therapy administration.

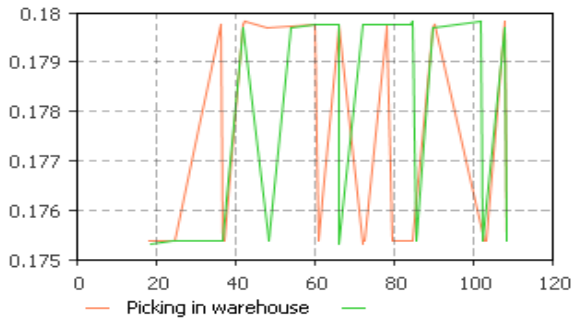

Figure 7: average therapy administration time for scenario 1

On average, only 50% of the total therapy administration time is dedicated to the patient, while the remaining 50% of the time is wasted by walking, searching for medicines, materials and machineries.
As additional results for scenario 1, the simulation model has evaluated a 57% average utilization level of the nurses team. While this value can be regarded as a good utilization level, it is worth mentioning that on average, only 50% of the nurse busy time is dedicated to the patient.
As far as the second scenario is concerned, this can be regarded as the worst scenario. Indeed, in this case nurses search for medicine in the ward, but it can happen that the nurses is redirected to the warehouse where a stock-out occurs (some medicines or materials are missing or a machineries is unavailable due maintenance operations). As matter of facts, in the scenario 2 the waste of time increases even more. The stock-out occurrence is communicated to the Head Nurse that, in turn, sends a new order to the hospital pharmacy. Only when the materials and medicine will be available, the therapy will be administered. The average time between the medical record reading and the therapy administration in scenario 2 is about 22.6 minutes (see figure 8).

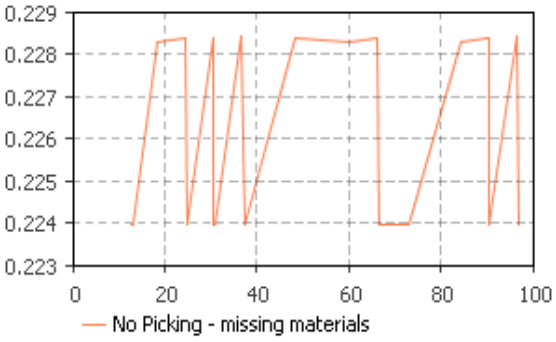

Figure 8: average therapy administration time for scenario 2

The scenario 2 is the worst situation in terms of value added for the wellness of the patient. Indeed in this case the nurse wastes additional time to communicate with the Head Nurse and, in turn, the Head Nurse must place the order to the Hospital Pharmacy. The simulation model evaluates that in this case only 14% of the total nurses busy time is dedicated to the patient. As far as the nurses utilization level is concerned, the simulation model evaluates an average value of 63%. While this result seems to be even better compared to scenario 1, conversely the nurses spend more time for materials and medicine searching as well as for communications without a real value added for the patient.
As far as the third scenario is concerned, this case considers the use of lean methods and tools described in the previous sections (e.g. the 5S method, the kanban method, layout optimization, etc.). In this case, medications, medical materials and machineries are always available in the department. Thanks to Kanban the replenishment is performed on time and a safety stock has also been added. In figure 9 we can note that the average time that elapses between the medical record reading and the therapy administration is about 9.9 minutes.

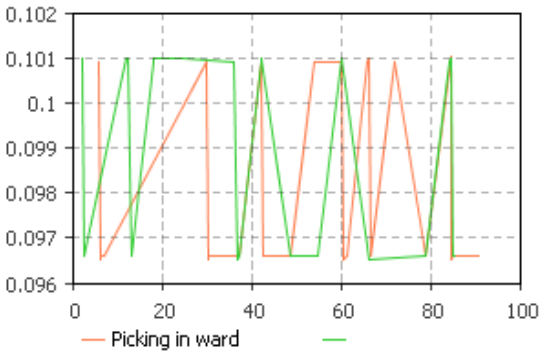

Figure 9: average therapy administration time for scenario 3

The simulation results for the scenario 3 clearly shows that most of the nurses busy time is dedicated to the patient, passive times that do not provide value added to the patient cannot be further reduced, therefore we can assert that the value added for the patient is 100%. The average nurses utilization level is about 30%; while this value may appear as very low, on the contrary it gives the possibility to carry out other patients care therefore assigning more patients to one nurse (workload optimization).

To summarize the simulation results, we can assert that in scenario 1, on the average one hour is wasted over 8-hours shift; in scenario 2, on the average one hour and half is wasted, while scenario 3 represents the best situation with no waste of time

The table 2 summarizes the simulation results for the three scenarios.

Table 2: Simulation results for the three scenarios

Scenario	Time to picking [minutes]	Value added to the patient (Wellness)	Cumulated time waste (on 100 picking) [minutes]	Average time wasted in one work shift [hours]
Scenario 1	17.8	50 %	800	1
Scenario 2	22.6	14 %	1200	1.5
Scenario 3	9.9	100 %	0	0

7. CONCLUSIONS

Like in all operative units of intensive care, the staff works under enormous stress and the workload has continued to increase during the last years. Usually this type of environment creates an atmosphere of frustration and anxiety for all staff due to particulars conditions of patients. In this particular scenario, the Intensive Care Unit team that we presented in this research work was introduced to the results of the simulation and to the Lean concepts through dedicated training courses. The period of training and information lasted for a week involving 15 physicians, 25 nurses and 1 technician. The Lean methods and tools as well as simulation results were successfully transferred to the real system with a relevant increase of the overall performances.

The implementation of Lean methods and tools can help any organization to launch its Lean transformation and improvement. This is even more important for Hospitals that cannot continue to operate as they have done in the past. Even considering the ongoing financial crises (at least in Italy) hospitals need to ensure their processes with much more value added work and such work must be totally directed on patients.

REFERENCES

Bruzzone, A. G., Longo, F. (2013). 3D simulation as training tool in container terminals: The TRAINPORTS simulator. *Journal of Manufacturing Systems*,*32*(1), 85-98.

Bruzzone, A., Longo, F., Nicoletti, L., Spadafora, F., Diaz, R., Behr, J. (2013). Health care facility improvement through simulation. *2nd International Workshop on Innovative Simulation for Health Innovative Simulation for Health, IWISH 2013*, Held at the Int. Multidisciplinary Modeling and Simulation Multiconference, I3M 2012, pp. 115-123.

Bruzzone, A.G., Novak, V., Madeo, F., Cereda, C. (2011) Modeling of obesity epidemics by intelligent agents. *23rd European Modeling and Simulation Symposium, EMSS 2011*, pp. 768-774. Cited 2 times.

Dickson E.W., S. Singh, D.S. Cheung, C.C. Wyatt, A.S. Nugent (2009), Application of Lean Manufacturing Techniques in Emergency Department. *The Journal of Emergency Medicine, Vol. 37, No. 2, pp. 177–182.*

Fillingham, D. (2007). Can lean save lives? *Leadership in Health Services, 20(4):231–241.*

Forsberg H.H., H. Aronsson, C. Keller, S. Lindblad, (2011), Managing Health Care Decisions and Improvement Through Simulation Modeling. *Quality Management in Health Care, January/March 2011, Vol.20, Issue 1, pp. 15–29.*

Hiroyuki H., (1989). JIT implementation manual: The guide to just in time manufacturing. *Tokyo, Japan: JIT Management Laboratory Company, Ltd. ISBN-13: 978-1-4200-9016-1*

Holm L.B., Luras H., Dahl F.A., (2013), Improving hospital bed utilization through simulation and optimization: With application to a 40% increase in patient volume in a Norwegian general hospital. *International Journal of Medical Informatics*, 82(2), 80–89.

Jones D., A. Mitchell (2006), Lean thinking for the NHS. *Book published by the NHS Confederation, 2006, ISBN 1859471277.*

Khurma N., G.M. Baciou, Z.J. Pasek, (2008), Simulation-based verification of Lean improvement for emergency room process. *Simulation Conference, 2008. WSC 2008. Winter,7-10 Dec.2008, Austin- Texas, pp.1490-1499.*

Longo, F., Huerta, A., Nicoletti, L., (2013). Performance analysis of a Southern Mediterranean seaport via discrete-event simulation. *Strojniski Vestnik/Journal of Mechanical Engineering*, 59 (9), pp. 517-525.

Machado V., U. Leitner (2010), Lean tools and lean transformation process in health care. *International Journal of Management Science and Engineering Management, 5(5): 383-392.*

Rego Monteil, N., Crespo Pereira, D., del Rio Vilas, D., & Rios Prado, R. (2013). A Simulation-Based Ergonomic and Operational Analysis for the Improvement of a Fish Processing Factory Ship. *International Journal of Food Engineering, 9(3), 279-295.*

Robinson S., Z. J. Radnor, N. Burgess, C.

Worthington (2012), Utilising Simulation in the implementation of Lean in Healthcare. *European Journal of Operational Research, vol.219, Issue 1,16 may 2012, pp. 188-197.*

Ross W. Simon, Elena G. Canacari (2012), A Practical Guide to Applying Lean Tools and Management Principles to Health Care Improvement Projects. *AORN Journal vol. 95 N.1(January 2012) pp.85-100.*

Weerawat, W., Pichitlamken, J., Subsombat, P., (2013), A Generic Discrete-Event Simulation Model for Outpatient Clinics in a Large Public Hospital. *Journal of Healthcare Engineering, 4(2), vol.4, N.2,June 2013, pp.285-306.*

Winkler, S. M., Affenzeller, M., Jacak, W., & Stekel, H. (2011). Identification of cancer diagnosis estimation models using evolutionary algorithms: a case study for breast cancer, melanoma, and cancer in the respiratory system. *In Proceedings of the 13th annual conference companion on Genetic and evolutionary computation (pp. 503-510). ACM.*

Winkler, S. M., Kronberger, G., Affenzeller, M., & Stekel, H. (2013). Variable Interaction Networks in Medical Data. *International Journal of Privacy and Health Information Management (IJPHIM), 1(2), 1-16.*

Zeltyn S., B. Carmeli, O. Greenshpan, Y.Mesika, S. Wasserkrug, P. Vortman, Y.N. Marmor, A. Mandelbaum, A. Shtub, T. Lauterman, D. Schwartz, K. Moskovitch, S. Tzafrir, F. Basis, (2011), Simulation-Based Models of Emergency Departments: operational, tactical, and strategic staffing. *ACM Transactions on Modeling and Computer Simulation, vol.21, Issue 4, August 2011, Article N.24.*

Zidel T., (2006). A lean guide to transforming healthcare: how to implement lean principles in hospitals, medical offices, clinics, and other healthcare organizations. *American Society for Quality, Quality Press, Milwaukee, WI 532.*

Author's Index